A Review of Particle Transport Theory in a Binary Stochastic Medium

por

Richard Vasques

Prof. Dr. Marco Túllio Menna Barreto de Vilhena
Orientador

Prof. Dr. Edward William Larsen
Co-orientador

Porto Alegre, Janeiro de 2005.

Livros Grátis

http://www.livrosgratis.com.br

Milhares de livros grátis para download.

CIP - CATALOGAÇÃO NA PUBLICAÇÃO

A Review of Particle Transport Theory in a Binary Stochastic Medium

por

Richard Vasques

Dissertação submetida ao Programa de Pós-Graduação em Matemática Aplicada do Instituto de Matemática da Universidade Federal do Rio Grande do Sul, como requisito parcial para a obtenção do grau de

Mestre em Matemática Aplicada

Linha de Pesquisa: Teoria do Transporte e Transformadas Integrais

Orientador: Prof. Dr. Marco Túllio Menna Barreto de Vilhena

Co-orientador: Prof. Dr. Edward William Larsen

Banca examinadora:

Prof. Dr. Roberto David Martinez Garcia
CTA/IEAV

Prof. Dr. Fernando Carvalho da Silva
COPPE/UFRJ

Prof. Dr. Mark Thompson
PPGMAp/UFRGS

Prof^a. Dr^a. Cynthia Feijó Segatto
PPGMAp/UFRGS

Dissertação apresentada e aprovada em
13 de Janeiro de 2005.

Prof^a. Dr^a. Maria Cristina Varriale
Coordenadora

RESUMO

A finalidade deste trabalho é apresentar uma revisão da teoria do transporte de partículas em meios compostos por uma mistura aleatória binária. Para atingir este objetivo nós apresentamos brevemente alguns conceitos básicos de teoria do transporte, e então discutimos em detalhes a derivação de duas abordagens desenvolvidas para a solução de tais problemas: os modelos de mistura atômica e de Levermore-Pomraning. Providenciamos ainda, com o uso da formulação LTS_N, comparações numéricas destes modelos com resultados de benchmark gerados através de um processo de Monte Carlo.

ABSTRACT

The aim of this work is to present a review of particle transport theory in randomly mixed binary media. To accomplish this objective we briefly report some basic concepts of transport theory, and then we discuss in detail the derivation of two approaches developed to predict the solutions of such problems: the atomic mix and the Levermore-Pomraning models. Also, using the LTS_N formulation, we provide numerical comparisons of these models with benchmark calculations generated through the use of a Monte Carlo procedure.

AGRADECIMENTOS

Este trabalho é dedicado a Laís Cristina. Eu não conseguiria sem ti.

ACKNOWLEDGEMENTS

I wish to thank

This work is dedicated to Laís Cristina. I would not succeed without you.

SUMMARY

LIST OF FIGURES

LIST OF TABLES

LIST OF SYMBOLS

c_i	single scatter albedo of material i
E	kinetic energy
$i,\ j$	labels of materials ($i,\ j \in \{1,2\}$, $i \neq j$)
ℓ	mean free path
n	unit outward normal vector
p_i	probability of finding material i
Q	internal source of particles
r	spatial vector
S_i	scattering operator for material i
t	time
v	particle speed (nonrelativistic case)
v	velocity vector
$x,\ y,\ z$	Cartesian coordinates
w	"fast" spatial variable (scaling)
α	specified function (initial condition)
Γ	specified function (boundary condition)
γ	variation coefficient
θ	polar angle (measured with respect to the z-axis)
φ	azimuthal angle
λ	Markov transition length
λ_c	correlation length
Λ	mean chord length
μ	$\cos\theta$
σ	standard deviation
$\Sigma_a,\ \Sigma_s,\ \Sigma_t$	macroscopic absorption, scattering and total cross sections
ϕ	scalar flux
ψ	angular flux
$\sigma_t,\ \sigma_s,\ q,\ \hat{\psi},\ \hat{\phi}$	"fast" spatial functions
χ	characteristic function
Ω	angular unit vector

1 INTRODUCTION

1.1 English Version

The mathematical description of the transport of particles such as neutrons, electrons, photons and molecules through a background material is commonly called *Transport Theory*. The so-called transport equations can be described as the mathematical statement of particle conservation in phase space. These equations play a fundamental role in many different physical situations, such as nuclear reactor physics, astrophysics, rarefied gas dynamics, charged particle transport, electromagnetic radiation, plasma physics, etc. A vast range of literature exists for the cases when the properties of the background material (as functions of space and time) are specified. However, all materials in nature have a stochastic character to some extent, and sometimes this stochasticity cannot be ignored.

The last several years have seen an increasing interest in formulating particle transport descriptions in stochastic mixtures. By stochastic mixtures, we mean that the properties of the background material are known only in a statistical sense. This research area is known as *Stochastic Transport Theory*. The goal of this theory is to find the ensemble average (expected value) of the particle intensity in phase space, as well as higher moments, such as the variance.

A direct way to do this is to generate a large number of physical realizations of the problem, solve each realization deterministically, and then average the solutions [1, 12, 38, 78, 90, 94]. However, one must keep in mind that the total number of possible physical realizations is infinite, and conceptually one must perform these calculations an infinite number of times in order to obtain a zero statistical error of the solution. In practice, a large number of such calculations is necessary to get an accurate estimate of the ensemble-averaged intensity. For these reasons, the task of developing improved models to predict the solution is the objective of recent research (as neutron transport in pebble bed reactors [12], for example). In

this work we will discuss the two most important models available: the *Atomic Mix* and the *Levermore-Pomraning* models.

The term atomic mix applies to mixtures of two or more materials in which the "chunks" of the materials are so small that we can assume mixing at atomic level. Then the volume fraction of each material is used to calculate homogenized cross sections for the mixture. This notion appears to have been used in chemistry over 200 years ago, to find rules for adding partial pressures of mixtures. Maxwell [34], in his attempt to treat molecular diffusion coefficients, modeled atomic mixtures of certain ideal gases in order to compute transport coefficients.

Nuclear engineering (as a distinct discipline of engineering) began in the 1940's. It is reasonable to assume that physicists who knew the concept of atomic mix adopted it to model neutron transport problems. In fact, much of the work that was done from the 1940's to the 1960's regarding transport in mixtures used the atomic mix approximation. The atomic mix model [12, 43, 90] is a widely-used homogenization technique, which is valid when the system's spatial heterogeneities occur on a length scale which is small compared to a typical mean free path. This assumption, however, is physically very restrictive.

These limitations leaded to the development of different approaches to solve problems where the atomic mix assumptions were not valid. Under this motivation, a formulation of a particle transport formalism in binary random media arose in the mid-1980's, providing the foundations for the so-called Levermore-Pomraning method.

The first derivation of the Levermore-Pomraning method [25, 44] considered time independent transport in a purely absorbing medium. The mixture was taken as Markovian, and using a projection operator technique known as the method of smoothing [15, 17], an exact solution was obtained for the ensemble-averaged angular flux. However, this derivation becomes algebraically too cumbersome to lead to useful results when the scattering interaction is involved [43]. In fact, in scattering

problems, the task of reducing this exact expression to an useable one is exceedingly complex.

Later, Vanderhaegen [86] pointed out that the time independent, non-scattering case can be treated exactly under the assumption of Markovian statistics. He observed that in this case the stochastic problem is a joint Markov process, and thus the Liouville master equation applies [18, 89]. Although this approach is not valid when scattering is present [88], it was suggested [43, 49, 53] that the use of the master equation might produce a useful approximate model for problems with time dependence and scattering. In 1989, Adams, Larsen and Pomraning [1] introduced a new derivation using the idea of stochastic balance, and Sahni obtained the same results using techniques of nuclear reactor noise analysis [67] and by assuming that each photon track is independent of prior tracks [68].

Since then, a vast literature has arisen on formulation and solution methods, both analytical and numerical, for this model. Among these contributions we underline the following: the development of a monoenergetic particle transport model in a binary Markovian mixture within the framework of integral transport theory [84, 95]; the development of several important asymptotic limits [28, 29, 31, 54, 58, 59, 60, 70, 83]; the development of P_1 and P_2 diffusive descriptions [82]; the development of flux-limiting algorithms [56, 69]; the development of alternate closures and higher-order models [51, 55, 80, 81]; the treatment of anisotropic scattering [36, 54, 76] and eigenvalue problems [65, 93]; and the use of renewal theory to describe stochastic transport in non-Markovian mixtures [16, 26, 48, 50, 63, 78, 87, 94]. There is also a great number of papers dealing with important applications for this kind of problem: atmospheric applications [32, 33, 59, 77, 79, 84, 85, 95]; applications in astrophysics [3, 4, 10]; applications in criticality problems [52, 91, 92]; applications in nuclear medicine [36, 57, 58, 60, 66, 83]; etc.

The aim of the present work is to provide a detailed discussion regarding the subject of Stochastic Transport Theory, focusing on the two models already

mentioned. We report in detail the derivation steps and physical assumptions, and we discuss the particularities encountered. We also present some new ideas regarding the derivation of the Levermore-Pomraning method, and we perform numerical calculations comparing both models with benchmark solutions. We are aware of very few papers in which a systematic comparison of atomic mix, Levermore-Pomraning, and benchmark calculations is done [12, 90], which leads us to believe in the importance of this contribution.

It is important to underline that all numerical simulations were performed using the LTS_N method [73, 74, 75], which analytically solves the discrete ordinate (S_N) approximation of the neutron transport equation in a slab for a wide class of problems. To our knowledge, the work of Vasques et al. [90] is the first in which the LTS_N method is applied in the calculation of benchmark results for this class of stochastic problems, as well as in the calculation of the atomic mix and Levermore-Pomraning predictions. The power of the LTS_N method makes it well-suited to perform benchmark results for problems where solutions for a large number of physical realizations are required. Therefore we improved the algorithms used in [90] to include problems with internal sources, and we performed all numerical calculations in such way that the statistical relative error is less than 1% with 95% confidence. A total of 117 problems are presented in this work.

The outline of this work is as follows:

• In Chapter 2, we first introduce the basic concepts needed to describe the interaction of particles with matter (section 2.1). We then use particle conservation to formulate the integro-differential transport equation in a nonstochastic medium (section 2.2). We finish the chapter by deriving some important statistical results that will be used often along the rest of the work, regarding the infinite line populated statistically with alternating segments of two different materials (section 2.3).

• We start Chapter 3 presenting an empirical derivation of the atomic mix equation (section 3.1). In section 3.2 we derive the atomic mix equation using the

formal procedure of multiscale expansion technique [14]. We close the chapter with a discussion regarding the limitations of the atomic mix model for the cases in which its assumptions are not satisfied, and we show why the multiscale expansion technique can be performed only as a formal procedure when deriving the atomic mix equations (section 3.3).

- Chapter 4 presents a detailed discussion regarding the Levermore-Pomraning method. We present two different derivations of this method in section 4.1: one using the master equation approach [43, 49, 53, 86, 88]; and one using the idea introduced by Adams, Larsen and Pomraning [1]. Here, however, the details of the derivation are done following Vasques et al. [90], in such a manner that the reader may find it more illuminating in terms of the physics of the problem. We go still further and present a discussion whose main point is that the Levermore-Pomraning equations, in their traditional form, are incorrect for random three dimensional geometries. In section 4.2, we present a physical interpretation of the model developed by Sahni [68] and discuss a possible flaw of the model for isotropic scattering. We also report a new idea proposed by Larsen [20, 24] for a corrected model with a Sahni-like interpretation. Section 4.3 discusses some of the important developments regarding this research: the derivation of some asymptotic limits is treated in section 4.3.1; and alternate closures, as well as higher order models, in section 4.3.2.

- Numerical results for time independent transport problems in planar geometry are presented in Chapter 5. The numerical procedure to obtain the solutions is described in section 5.1. In section 5.2, results for Reflection/Transmission problems are reported. Simulations for source problems within a medium containing slabs of two different densities of the same material are shown in section 5.3.

- Chapter 6 present our conclusions regarding the work developed, as well as ideas for future work in this research line.

1.2 Portuguese Version

A descrição matemática do transporte de partículas tais como nêutrons, elétrons, fótons e moléculas através de um determinado material é normalmente denominada *Teoria do Transporte*. As chamadas equações do transporte podem ser descritas como sendo a representação matemática da conservação de partículas em um espaço de fase. Estas equações têm um papel fundamental em um grande número de situações físicas, tais como física de reatores nucleares, astrofísica, dinâmica de gases rarefeitos, transporte de partículas carregadas, radiação eletromagnética, física do plasma, etc. Existe uma vasta literatura para os casos em que as propriedades do meio estão especificadas (como funções do espaço e do tempo). No entanto, todo material na natureza possui um caráter aleatório até um certo ponto, e às vezes esta aleatoriedade não pode ser ignorada.

Nos últimos anos, um interesse crescente na formulação de descrições do transporte de partículas em misturas estocásticas pode ser observado. Por misturas estocásticas nos referimos aos casos nos quais as propriedades do meio são conhecidas apenas de um modo estatístico. Esta linha de pesquisa é conhecida como *Teoria do Transporte Estocástico*. O objetivo desta teoria é encontrar a média (valor esperado) do fluxo de partículas em um espaço de fase, assim como momentos de ordem superior, tais como a variância.

Um modo direto de se fazer isso é gerar um grande número de realizações físicas do problema, resolver cada realização deterministicamente, e então calcular a média das soluções [1, 12, 38, 78, 90, 94]. Entretanto, deve-se ter em mente que o número total de realizações físicas possíveis é infinito, e conceitualmente estes cálculos deveriam ser realizados um número infinito de vezes para que o erro estatístico da solução fosse nulo. Na prática, é necessário que se resolva um grande número destas realizações físicas para se obter uma estimativa precisa da solução média. Por estas razões, o desenvolvimento de modelos aperfeiçoados que predigam esta solução média tem sido objeto de recentes pesquisas (como, por

exemplo, no transporte de nêutrons em reatores "pebble bed" [12]). No presente trabalho discutiremos os dois modelos mais importantes atualmente disponíveis: os modelos de *Mistura Atômica* (*Atomic Mix*) e de *Levermore-Pomraning*.

O termo mistura atômica se aplica a misturas de dois ou mais materiais onde os "pedaços" destes materiais são tão pequenos que podemos assumir que a mistura se dá em nível atômico. Isto nos permite utilizar a fração do volume de cada material para calcular seções de choque homogeneizadas para a mistura. Esta noção parece ter sido empregada em química há mais de 200 anos, com o intuito de se encontrar regras para a adição de pressões parciais de misturas. Maxwell [34], na sua tentativa de lidar com coeficientes de difusão moleculares, modelou misturas atômicas de certos gases ideais com a finalidade de computar os coeficientes de transporte.

A engenharia nuclear, como uma área distinta da engenharia, teve seu início na década de 1940. É razoável admitir que físicos familiarizados com o conceito de mistura atômica adotaram este conceito para modelar problemas de transporte de nêutrons. De fato, grande parte do trabalho relacionado com transporte em misturas realizado entre as décadas de 1940 e 1960 faz uso desta aproximação. O modelo de mistura atômica [12, 43, 90] é uma técnica de homogeneização largamente difundida, e é válido quando as heterogeneidades espaciais do sistema ocorrem em um comprimento de escala pequeno em comparação com um livre caminho médio. Contudo, esta hipótese é fisicamente muito restritiva.

Estas limitações levaram à busca de abordagens diferentes para a resolução de problemas onde as hipóteses de mistura atômica não fossem válidas. Com esta motivação, uma formulação para o transporte de partículas em um meio estocástico binário surgiu em meados da década de 1980, fornecendo o alicerce para o chamado método de Levermore-Pomraning.

A primeira derivação do método de Levermore-Pomraning [25, 44] tratava do transporte em um meio puramente absorvente sem dependência no tempo.

Assumiu-se a estatística da mistura como sendo Markoviana, e uma solução exata foi obtida para o fluxo angular médio através do uso de uma técnica de operadores de projeção [15, 17]. No entanto, quando há espalhamento envolvido, esta derivação se torna por demais complicada algebricamente para levar a resultados úteis [43]. De fato, em problemas com espalhamento, a tarefa de reduzir esta expressão exata para uma expressão utilizável é excessivamente complexa.

Mais tarde, Vanderhaegen [86] fez notar que o caso sem dependência no tempo e sem espalhamento poderia ser tratado de forma exata sob a hipótese de estatística Markoviana. Ele observou que, neste caso, o problema estocástico é um processo de Markov associado, e portanto a equação master de Liouville se aplica [18, 89]. Embora esta abordagem não seja válida quando há espalhamento envolvido [88], foi sugerido [43, 49, 53] que o uso da equação master poderia produzir um modelo aproximado útil para problemas com dependência no tempo e espalhamento. Em 1989, Adams, Larsen e Pomraning [1] apresentaram uma nova derivação utilizando a idéia de balanço estocástico, e Sahni obteve os mesmos resultados através de técnicas de análise de ruído de reatores nucleares [67] e assumindo que a trajetória de cada fóton é independente das trajetórias anteriores [68].

Desde então, inúmeros trabalhos lidando com métodos analíticos e numéricos de formulação e solução para este modelo vêm sendo apresentados. Entre estas contribuições nós destacamos as seguintes: o desenvolvimento de um modelo de transporte de partículas monoenergético em uma mistura Markoviana binária sob a ótica da teoria do transporte integral [84, 95]; o desenvolvimento de diversos limites assintóticos importantes [28, 29, 31, 54, 58, 59, 60, 70, 83]; o desenvolvimento de descrições difusivas P_1 e P_2 [82]; o desenvolvimento de algoritmos "flux-limiting" [56, 69]; o desenvolvimento de fechamentos alternativos e modelos de ordem superior [51, 55, 80, 81]; o tratamento de espalhamento anisotrópico [36, 54, 76] e problemas de autovalores [65, 93]; e o uso da chamada "renewal theory" para descrever o transporte estocástico em misturas não-Markovianas [16, 26, 48, 50, 63, 78, 87, 94]. Existe também um grande número de artigos que lidam com importantes aplicações

para este tipo de problema: aplicações atmosféricas [32, 33, 59, 77, 79, 84, 85, 95]; aplicações em astrofísica [3, 4, 10]; aplicações em problemas de criticalidade [52, 91, 92]; aplicações em medicina nuclear [36, 57, 58, 60, 66, 83]; etc.

O presente trabalho tem por meta apresentar uma discussão detalhada no que se refere à Teoria do Transporte Estocástico, com ênfase nos dois modelos já mencionados. As derivações e as hipóteses físicas são apresentadas em detalhes, e as particularidades encontradas são cuidadosamente discutidas. Apresentamos também algumas novas idéias relacionadas com a derivação do método de Levermore-Pomraning, assim como cálculos numéricos comparando ambos os modelos com soluções de benchmark. Existem poucos trabalhos onde uma comparação sistemática entre os resultados de benchmark e os modelos de mistura atômica e de Levermore-Pomraning é feita [12, 90], o que nos leva a crer na importância desta contribuição.

É importante salientar que todas as simulações numéricas foram realizadas usando o método LTS_N [73, 74, 75], que resolve analiticamente a aproximação de ordenadas discretas (S_N) da equação do transporte de nêutrons em uma placa. Até onde sabemos, o trabalho de Vasques et al. [90] é o primeiro onde o método LTS_N é aplicado no cálculo de resultados de benchmark para esta classe de problemas estocásticos, bem como no cálculo das estimativas dos modelos de mistura atômica e de Levermore-Pomraning. O poder do método LTS_N o faz se adaptar muito bem no cálculo dos resultados de benchmark para problemas que requerem soluções para um grande número de realizações físicas. Portanto, os algoritmos usados em [90] foram aperfeiçoados com a finalidade de incluir problemas com fonte interna, e todos os cálculos numéricos foram realizados de modo que o erro estatístico relativo é menor que 1% com 95% de confiança. Um total de 117 problemas é apresentado neste trabalho.

O trabalho é delineado da seguinte forma:

• No Capítulo 2, os conceitos básicos necessários para descrever a interação de partículas com a matéria são introduzidos (seção 2.1). Após, faz-se uso do

princípio de conservação de partículas para formular a equação do transporte íntegro-diferencial em um meio não-estocástico (seção 2.2). O capítulo se encerra com a derivação de alguns resultados estatísticos importantes que serão usados ao longo do trabalho, relacionados à linha infinita estatisticamente preenchida com segmentos alternados de dois materiais diferentes (seção 2.3).

- O Capítulo 3 começa com a apresentação de uma derivação empírica da equação de mistura atômica (seção 3.1). Na seção 3.2, a equação de mistura atômica é derivada utilizando um procedimento formal de expansão multiscale [14]. O capítulo é encerrado com uma discussão relacionada às limitações do modelo de mistura atômica para os casos nos quais suas hipóteses não são satisfeitas, e o motivo pelo qual a técnica de expansão multiscale só poder ser utilizada como um procedimento formal é apresentado (seção 3.3).

- O Capítulo 4 fornece uma discussão detalhada sobre o método de Levermore-Pomraning. Duas derivações diferentes deste método aparecem na seção 4.1: uma utilizando a abordagem da equação master [43, 49, 53, 86, 88]; e uma usando a idéia introduzida por Adams, Larsen e Pomraning [1]. Aqui, no entanto, os detalhes da derivação são feitos de acordo com Vasques et al. [90], de maneira que o leitor pode achá-la mais esclarecedora em termos da física do problema. Segue-se uma discussão cujo ponto principal é o fato das equações de Levermore-Pomraning, na sua forma tradicional, serem incorretas para geometrias tridimensionais aleatórias. Na seção 4.2 é apresentada uma interpretação física do modelo desenvolvida por Sahni [68], e uma possível falha do modelo para espalhamento isotrópico é discutida. Em seguida, relata-se uma nova idéia proposta por Larsen [20, 24] para um modelo corrigido. A seção 4.3 discute alguns importantes progressos relacionados a esta pesquisa: a derivação de alguns limites assintóticos é tratada na seção 4.3.1; e fechamentos alternativos, assim como modelos de ordem superior, na seção 4.3.2.

- Resultados numéricos para problemas de transporte em geometria planar sem dependência no tempo são apresentados no Capítulo 5. O procedimento numérico para a obtenção destas soluções é descrito na seção 5.1. Na seção 5.2, re-

sultados para problemas de Reflexão/Transmissão são mostrados. Simulações para problemas com fonte em um meio contendo placas de duas densidades diferentes de um mesmo material são apresentadas na seção 5.3.

• O Capítulo 6 apresenta as conclusões relacionadas ao trabalho desenvolvido, assim como novas idéias para trabalhos futuros nesta linha de pesquisa.

2 TRANSPORT IN A KNOWN MEDIUM AND STATISTICAL CONSIDERATIONS

2.1 Basic Concepts

In this section, we introduce some basic concepts needed to describe the interaction of particles with matter. (We refer the interested reader to [8, 9, 13, 19] for a more detailed description of these concepts.) Let us consider neutral particles flowing through a background material and interacting with it. Assuming that no forces act on these particles, between collisions they will travel in a straight line at a constant speed. At any time t, we use six variables to specify the position of any particle in phase space: three position variables denoted by the vector r, the kinetic energy E, and a unit vector Ω, which indicates the direction in which the particle is traveling. With these variables we can define the distribution function

$$n = n(r, E, \Omega, t), \tag{2.1}$$

such that

$$n(r, E, \Omega, t) dr dE d\Omega \tag{2.2}$$

is the number of particles in a differential volume element dr at a spatial point r, with energy in dE about E, traveling in a solid angle element $d\Omega$ about direction Ω, at time t.

Let the vector r be described by the Cartesian coordinates x, y, z, and the vector Ω be described by a polar angle θ measured with respect to the z-axis and a corresponding azimuthal angle φ (Figure 2.1).

If we introduce $\mu = \cos\theta$, then

$$dr = dx dy dz, \tag{2.3}$$

$$d\Omega = \sin\theta d\theta d\varphi = d\mu d\varphi. \tag{2.4}$$
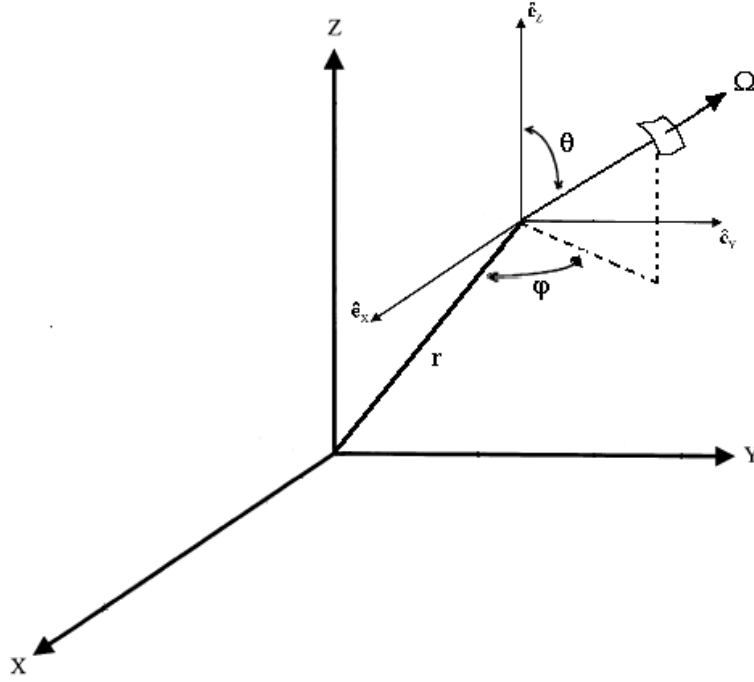
Figure 2.1: State of a particle in a coordinate system

Here, a minus sign was omitted from Eq. (2.4), since μ runs from 1 to -1 when θ runs from 0 to π. If v is the velocity vector, then $\Omega = \mathrm{v}/|\mathrm{v}|$, and it is easy to see that the components of the particle velocity in the Cartesian coordinates are given by

$$\dot{x} = v\Omega_x, \tag{2.5}$$

$$\dot{y} = v\Omega_y, \tag{2.6}$$

$$\dot{z} = v\Omega_z, \tag{2.7}$$

where v is the particle speed in the nonrelativistic case, that is $v = \sqrt{2E/m_p}$, with m_p denoting the particle mass. In fact, we can express the distribution function in terms of the vector v:

$$n(r, E, \Omega, t) = \left(\frac{v}{m_p}\right) n(r, \mathrm{v}, t), \tag{2.8}$$

and integrating over these velocity space variables, we find the particle density

$$N(r, t) = \int_0^\infty n(r, \mathrm{v}, t) d\mathrm{v} = \int_0^\infty \int_{4\pi} n(r, E, \Omega, t) d\Omega dE. \tag{2.9}$$
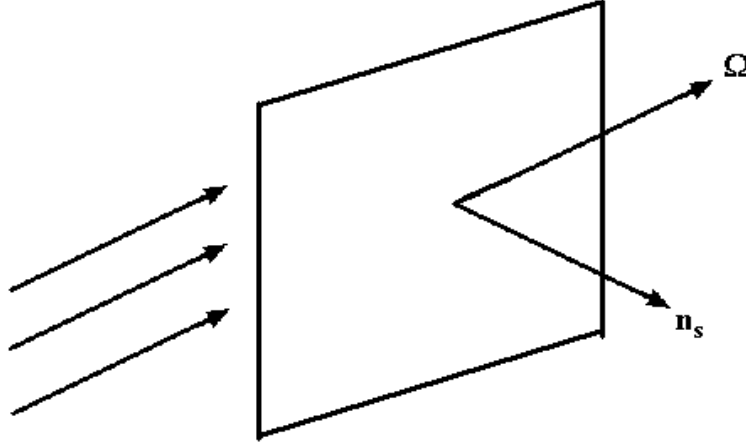
Figure 2.2: Particles incident on an incremental surface area dA

It is conventional in linear transport theory to introduce a new function, the angular flux, given by

$$\psi(r, E, \Omega, t) = vn(r, E, \Omega, t). \tag{2.10}$$

Integrating ψ over E and Ω, we obtain the scalar flux ϕ:

$$\phi(r, t) = \int_0^\infty \int_{4\pi} \psi(r, E, \Omega, t) d\Omega dE. \tag{2.11}$$

Another important concept is the angular current density $j(r, E, \Omega, t)$, defined by

$$j(r, E, \Omega, t) = \Omega \psi(r, E, \Omega, t), \tag{2.12}$$

such that

$$j(r, E, \Omega, t) \cdot n_s dA dE d\Omega = \Omega \psi(r, E, \Omega, t) \cdot n_s dA dE d\Omega \tag{2.13}$$

is the rate at which particles, with energy in dE about E, with direction of flight in $d\Omega$ about Ω, cross an incremental surface area dA (with unit outward normal n_s) at r, at time t (Figure 2.2). In a similar sense, we can introduce the scalar current density $J(r, t)$ given by

$$J(r, t) = \int_0^\infty \int_{4\pi} j(r, E, \Omega, t) d\Omega dE. \tag{2.14}$$

One should notice that, while the angular flux ψ and the scalar flux ϕ are scalars, both current densities defined by equations (2.12) and (2.14) are vectors.

Since particles are expected to interact with the background material through which they are flowing, we will introduce the concepts of the two basic interactions between particles and matter: absorption and scattering. As a particle travels through matter, there is a probability that it will not scatter when undergoing an interaction. In this case, the particle is said to have been absorbed. As examples of absorption, we can mention radiative capture and nuclear fission, common processes in reactor theory.

A basic assumption in absorption processes is that, in traveling a distance ds, the probability of absorption is proportional to ds, independent of the past history of the particle. The proportionality constant between the probability of absorption and the distance ds is called the macroscopic absorption cross section, denoted by $\Sigma_a(r, E, \Omega, t)$. In general, the absorption cross section depends upon the energy E of the particle as well as both space and time, since the background material properties are (in general) functions of r and t. Assuming that the matter is isotropic, the probability of absorption is independent of the direction of travel of the particle:

$$\Sigma_a(r, E, t)ds = \text{probability of absorption.} \tag{2.15}$$

Similar to absorption, a particle can scatter when interacting with matter. In this case, the particle does not disappear as in absorption, but continues to exist with, in general, a different energy and direction of travel. If there is no energy change upon scattering, the scattering is said to be coherent. We define the macroscopic scattering cross section $\Sigma_s(r, E, t)$ in analogy to the absorption cross section such that, for a particle travelling a distance ds,

$$\Sigma_s(r, E, t)ds = \text{probability of scattering.} \tag{2.16}$$

The changing of the particle's energy and direction E' and Ω' to a new energy and direction E and Ω leads to the definition of the macroscopic differential scattering cross section $\Sigma_s(r, E' \rightarrow E, \Omega' \rightarrow \Omega, t)$, such that the probability that a particle travelling a distance ds will scatter from E' to dE at E and from Ω' to $d\Omega$ at Ω is

given by

$$\Sigma_s(r, E' \to E, \Omega' \to \Omega, t)dEd\Omega ds. \tag{2.17}$$

When the scattering process is rotationally invariant, the probability that a particle will scatter from direction Ω' to direction Ω depends only on the scattering angle (the angle between Ω' and Ω), or, on $\mu_0 = \Omega' \cdot \Omega =$ the cosine of this angle. In this case, Eq. (2.17) becomes

$$\Sigma_s(r, E' \to E, \Omega' \cdot \Omega, t)dEd\Omega ds, \tag{2.18}$$

and integrating this equation over all final energies and angles, we obtain the macroscopic scattering cross section at the initial energy, as defined by Eq. (2.16) [13]:

$$\Sigma_s(r, E, t) = \int_0^\infty \int_{4\pi} \Sigma_s(r, E \to E', \Omega \cdot \Omega', t)d\Omega' dE'. \tag{2.19}$$

If in Eq. (2.18) the differential scattering cross section is independent of $\Omega' \cdot \Omega$, the scattering process is said to be isotropic. In this case, when a particle with direction Ω' scatters, all outgoing directions Ω are equally probable.

Finally, the macroscopic total cross section is defined as

$$\Sigma_t(r, E, t) = \Sigma_a(r, E, t) + \Sigma_s(r, E, t), \tag{2.20}$$

such that for a particle travelling a distance ds

$$\Sigma_t(r, E, t)ds = \text{probability of undergoing an interaction.} \tag{2.21}$$

Consider a homogeneous medium, and let $K(s)$ be the number of particles at position s in a directed beam of radiation. In traversing an additional element of path length ds along this beam, the value of $K(s)$ will be decreased by the number of particles that have interacted during this process. From the definition of the total cross section we have

$$-dK(s) = K(s)\Sigma_t ds. \tag{2.22}$$

Equation (2.22) can be integrated with the result

$$K(s) = K_0 e^{-\Sigma_t s}, \tag{2.23}$$

which means that K_0 particles initially in the beam will decrease exponentialy with distance. It should be noted that, since $K(s)$ refers to those particles that have not interacted in travelling the distance s, the ratio

$$\frac{K(s)}{K_0} = e^{-\Sigma_t s} \tag{2.24}$$

is the probability that a particle will move through this distance without interacting. Now let us define $\tilde{p}(s)ds$ as the probability that a particle will have its first interaction in ds in the neighborhood of s. This is equal to the probability that the particle reaches s without interacting *times* the probability that it does interact in the additional distance ds, i.e.,

$$\tilde{p}(s)ds = e^{-\Sigma_t s} \times \Sigma_t ds = \Sigma_t e^{-\Sigma_t s} ds. \tag{2.25}$$

The average distance between interactions is known as the mean free path, denoted by ℓ. This quantity is equal to the average value of s, the distance traversed by a particle without interaction, over the interaction probability distribution $\tilde{p}(s)$. That is,

$$\ell = \frac{\int_0^\infty s\tilde{p}(s)ds}{\int_0^\infty \tilde{p}(s)ds} = \Sigma_t \int_0^\infty s e^{-\Sigma_t s} ds = \frac{1}{\Sigma_t}. \tag{2.26}$$

Therefore, in a homogeneous medium the mean free path is just the inverse of the total cross section $\left(\ell(E) = \Sigma_t^{-1}(E)\right)$. If the material properties are functions of space and time, the mean free path will depend upon these variables. In this situation, Eq. (2.26) is taken as a definition of the mean free path:

$$\ell = \ell(r, E, t) = \frac{1}{\Sigma_t(r, E, t)}. \tag{2.27}$$

By analogy, we can define absorption and scattering mean free paths as

$$\ell_a(r, E, t) = \frac{1}{\Sigma_a(r, E, t)}, \tag{2.28}$$

$$\ell_s(r, E, t) = \frac{1}{\Sigma_s(r, E, t)}, \tag{2.29}$$

and by Eq. (2.20), the inverse addition rule is satisfied:

$$\frac{1}{\ell} = \frac{1}{\ell_a} + \frac{1}{\ell_s}. \tag{2.30}$$

2.2   The Integro-Differential Transport Equation

The transport equation was first introduced by Boltzmann in 1872, in the kinetic theory of gases [5]. This equation describes the relationship between the mechanisms of loss and gain of particles in any given volume of a phase space. Much neutral particle transport work is based on this equation, or equations derived from it.

Let the vectors r and Ω be described by the representation introduced earlier, in such way that Eqs. (2.3-2.4) and Figure 2.1 are satisfied. We consider a six dimensional volume (as a six dimensional cube) fixed in space, of dimensions $\triangle x$, $\triangle y$, $\triangle z$, $\triangle E$, $\triangle \mu$, $\triangle \varphi$. Then, by Eq. (2.2), the number of particles within this volume at time t is

$$n(r, E, \Omega, t)\triangle x\triangle y\triangle z\triangle E\triangle\mu\triangle\varphi = n(r, E, \Omega, t)\triangle P, \qquad (2.31)$$

where all arguments of n are "average" arguments in the increment of six dimensional phase space $\triangle P$. The number of particles in this cube changes with time, and the time rate of change is given by

$$\triangle P\frac{\partial}{\partial t}n(r, E, \Omega, t). \qquad (2.32)$$

This time rate of change is due to five separate processes. One is the rate of streaming of particles out of the volume through the boundaries. The others occur within the six dimensional "cube": the rate of absorption; the rate of scattering from E, Ω to all other energies and directions, known as outscattering; the rate of scattering into E, Ω from all other energies and directions, known as inscattering; and the rate of production of particles due to an internal source.

Now, let us consider the surfaces of the cube perpendicular to the x axis. For the net rate of particles leaving the cube through these two surfaces we have

$$(\text{Streaming})_x = \dot{x}n(r, E, \Omega, t)\mid_x^{x+\triangle x}\triangle y\triangle z\triangle E\triangle\mu\triangle\varphi, \qquad (2.33)$$

where $\dot{x}$ is the x component of the particle velocity as defined by Eq. (2.5), and $\triangle y \triangle z \triangle E \triangle \mu \triangle \varphi$ is the surface area. Letting $\triangle x$ go to the differential dx, we rewrite Eq. (2.33) as

$$\text{(Streaming)}_x = \triangle P \frac{\partial}{\partial x} \big[\dot{x} n(r, E, \Omega, t) \big]. \qquad (2.34)$$

Using the same procedure for the flow from the cube in the other five directions, we obtain

Streaming =

$$= \left[\frac{\partial}{\partial x}(\dot{x}n) + \frac{\partial}{\partial y}(\dot{y}n) + \frac{\partial}{\partial z}(\dot{z}n) + \frac{\partial}{\partial E}(\dot{E}n) + \frac{\partial}{\partial \mu}(\dot{\mu}n) + \frac{\partial}{\partial \varphi}(\dot{\varphi}n) \right] \triangle P, \qquad (2.35)$$

where $n = n(r, E, \Omega, t)$.

The rate of absorption within the cube is the product of the number of particles in the cube and the probability of absorption per particle per unit of time. This probability is given by the product of the absorption cross section and the particle speed v. That is,

$$\text{Absorption} = v\Sigma_a(r, E, t) n(r, E, \Omega, t) \triangle P. \qquad (2.36)$$

Using similar arguments and the fact that we need to sum the scattering from (to) E, Ω to (from) all other energies and directions E', Ω', we find

$$\text{Outscattering} = \triangle P \int_0^\infty \int_{4\pi} v\Sigma_s(r, E \to E', \Omega \cdot \Omega', t) n(r, E, \Omega, t) d\Omega' dE', \quad (2.37)$$

$$\text{Inscattering} = \triangle P \int_0^\infty \int_{4\pi} v'\Sigma_s(r, E' \to E, \Omega' \cdot \Omega, t) n(r, E', \Omega', t) d\Omega' dE', \quad (2.38)$$

where $\Sigma_s(r, E' \to E, \Omega' \cdot \Omega, t)$ is the scattering kernel as defined earlier. Since the distribution function in the integrand of Eq. (2.37) is independent of the integration variables, we can rewrite this equation (using Eq. (2.19)) as

$$\text{Outscattering} = \triangle P v \Sigma_s(r, E, t) n(r, E, \Omega, t). \qquad (2.39)$$

Finally, we need to consider the internal source of particles. We quantify this source by introducing the function $Q(r, E, \Omega, t)$ such that the rate of introduction

of particles into the cube is given by

$$\text{Source} = Q(r, E, \Omega, t) \triangle P. \tag{2.40}$$

In order to build the transport equation, we sum Eqs. (2.35-2.38, 2.40), with appropriate signs for loss and gain, to the overall rate given by Eq. (2.32). Letting $\triangle P$ approach a differential element and canceling it, we obtain

$$\frac{\partial n}{\partial t} + \frac{\partial(\dot{x}n)}{\partial x} + \frac{\partial(\dot{y}n)}{\partial y} + \frac{\partial(\dot{z}n)}{\partial z} + \frac{\partial(\dot{E}n)}{\partial E} + \frac{\partial(\dot{\mu}n)}{\partial \mu} + \frac{\partial(\dot{\varphi}n)}{\partial \varphi} = -v\Sigma_a(r, E, t)n +$$
$$+ \int_0^\infty \int_{4\pi} v'\Sigma_s(r, E' \to E, \Omega' \cdot \Omega, t)n(r, E', \Omega', t)d\Omega'dE' -$$
$$- \int_0^\infty \int_{4\pi} v\Sigma_s(r, E \to E', \Omega \cdot \Omega', t)n(r, E, \Omega, t)d\Omega'dE' + Q(r, E, \Omega, t),$$
$$\tag{2.41}$$

where $n = n(r, E, \Omega, t)$. Now, since a particle is assumed to travel in a straight line between collisions, $\dot{\mu} = \dot{\varphi} = 0$. Further, $\dot{E} = 0$ because particles stream with no change in energy. Finally, using Eqs. (2.5-2.7) and Eq. (2.10), and performing the outscattering integral as shown in Eq. (2.39), Eq. (2.41) becomes

$$\frac{1}{v}\frac{\partial \psi}{\partial t}(r, E, \Omega, t) + \Omega \cdot \nabla \psi(r, E, \Omega, t) + \Sigma_t(r, E, t)\psi(r, E, \Omega, t) =$$
$$= \int_0^\infty \int_{4\pi} \Sigma_s(r, E' \to E, \Omega' \cdot \Omega, t)\psi(r, E', \Omega', t)d\Omega'dE' + Q(r, E, \Omega, t). \tag{2.42}$$

Equation (2.42) requires both spatial and temporal boundary conditions. Assuming that the physical system of interest is nonreentrant (convex) and characterized by a volume V, it is sufficient to specify the flux of particles at all points of the bounding surface of the system in the incoming directions. This implies

$$\psi(r_s, E, \Omega, t) = \Gamma(r_s, E, \Omega, t) \quad \text{n} \cdot \Omega < 0, \tag{2.43}$$

where Γ is a specified function, r_s is a point on the surface, and n is a unit outward normal vector at this point. In the time variable, we assume the range of interest $0 \le t < \infty$ and specify the initial condition at $t = 0$, such that

$$\psi(r, E, \Omega, 0) = \alpha(r, E, \Omega), \tag{2.44}$$

where α is a specified function. In particular, Eq. (2.42) (together with the boundary and initial conditions) completely specify the linear particle transport problem.

2.3 Mixing Statistics

Consider two points x and y, with $x \le y$, on the infinite real line populated statistically with alternating segments of different materials labeled 1 and 2. Further, consider the closed interval $[x, y]$, and define $A_i(x, y)$ as the probability that this interval is made up entirely of material i. Now, define $p_i(y)$ as the probability that y is in material i, $B_i(x, y)$ as the probability that $[x, y]$ is in i *given that* y is in i, and $C_i(x, y)$ as the probability that $[x, y]$ is in i *given that* y is a material interface, with material i to the left. Following Pomraning [48], we have

$$p_i(y) = A_i(y, y), \tag{2.45}$$

$$B_i(x, y) = \frac{A_i(x, y)}{A_i(y, y)}, \tag{2.46}$$

$$C_i(x, y) = \frac{A_i(x, y) - A_i(x, y + dy)}{A_i(y, y) - A_i(y, y + dy)} = \frac{\partial A_i(x, y)/\partial y}{[\partial A_i(w, y)/\partial y]_{w=y}}. \tag{2.47}$$

As a special case of these considerations, we consider homogeneous statistics. Physically, this means that all points on the line have identical statistical properties. This implies that A_i, B_i and C_i depend only upon the single displacement argument $y - x$, and that p_i are constant, independent of y. If we simplify the notation by writing $A_i(x, y) = A_i(y - x) = A_i(z)$, we can rewrite Eqs. (2.45-2.47) by

$$p_i = A_i(0), \tag{2.48}$$

$$B_i(x, y) = \frac{A_i(z)}{A_i(0)}, \tag{2.49}$$

$$C_i(x, y) = \frac{A_i'(z)}{A_i'(0)}. \tag{2.50}$$

Now we consider a restricted class of homogeneous statistics. Let $\eta_i(\xi)$ be the probability density function for the length ξ of a segment of material i, defined such that $\eta_i(\xi)d\xi$ is the probability of a segment of material i having a length lying between ξ and $\xi + d\xi$. We then have [48]

$$C_i(z) = \int_z^\infty \eta_i(\xi)d\xi. \tag{2.51}$$

The mean chord length Λ_i in material i is given by

$$\Lambda_i = \int_0^\infty \xi \eta_i(\xi) d\xi = \int_0^\infty C_i(\xi) d\xi, \tag{2.52}$$

and the probabilities p_i are clearly related to Λ_i according to

$$p_i = \frac{\Lambda_i}{\Lambda_1 + \Lambda_2}, \tag{2.53}$$

since they are independent of position on the line. If we notice that $A_i(\infty)$ must be zero, we can deduce from Eqs. (2.48,2.50,2.52) that

$$A_i(z) = \frac{p_i}{\Lambda_i} \int_z^\infty C_i(\xi) d\xi, \tag{2.54}$$

and then Eq. (2.49) provides

$$B_i(z) = \frac{1}{\Lambda_i} \int_z^\infty C_i(\xi) d\xi. \tag{2.55}$$

If the chord lengths are exponentially distributed according to

$$\eta_i(\xi) = \frac{1}{\Lambda_i} e^{-\xi/\Lambda_i}, \tag{2.56}$$

then we have a special case of this class of homogeneous statistics, known as Markov statistics. In this case, the mean is Λ_i (as expected), and we have

$$A_i(z) = p_i e^{-z/\Lambda_i} \tag{2.57}$$

and

$$B_i(z) = C_i(z) = e^{-z/\Lambda_i}. \tag{2.58}$$

We next consider a more general Markov process without the homogeneous statistics restriction. Specifically, if the line consists of material i at position y, then the probability of $y + dy$ not being in material i is given by

$$\text{Prob}(i \to j) = \frac{dy}{\lambda_i(y)}, \tag{2.59}$$

where $\lambda_i(y)$ is a nonnegative function of y. It is the y-dependence that makes this statistics process inhomogeneous. According to Eq. (2.59), this Markov process has no memory and is completely characterized by the two Markov transition lengths

$\lambda_1(y)$ and $\lambda_2(y)$. Also, this process is shown [48] to be equivalently characterized by the unconditional probability of finding point y in material i, given by

$$p_i(y) = 1 - \int_{-\infty}^{y} \frac{1}{\lambda_i(y')} \exp\left[-\int_{y'}^{y} \left(\frac{1}{\lambda_1(\xi)} + \frac{1}{\lambda_2(\xi)} \right) d\xi \right] dy', \qquad (2.60)$$

and by the correlation length $\lambda_c(y)$, given by

$$\frac{2}{\lambda_c(y)} = \frac{1}{p_2(y)\lambda_1(y)} + \frac{1}{p_1(y)\lambda_2(y)}. \qquad (2.61)$$

Further, in the case of homogeneous Markov statistics, one can establish [43]

$$\lambda_i = \frac{\lambda_c}{1 - p_i} = \Lambda_i, \qquad (2.62)$$

and

$$\frac{1}{\lambda_c} = \frac{1}{\lambda_1} + \frac{1}{\lambda_2}. \qquad (2.63)$$

3 ATOMIC MIX MODEL

3.1 The Atomic Mix Equation

Let us consider the integro-differential transport equation given by Eq. (2.42). In a deterministic medium, the total cross section Σ_t, the scattering kernel Σ_s, and the source Q are known prescribed functions of their arguments. Thus, in order to find an expression for the angular flux ψ, one must solve this equation subject to the boundary and initial conditions given by Eqs. (2.43-2.44).

Now we consider neutron transport in a heterogeneous volume V such that the boundary ∂V of V is specified, but the interior structure of V is not. Specifically, we restrict our attention to the case in which V consists of two random immiscible materials denoted by an index i, with $i = 1, 2$. We can imagine V as a heterogeneous volume consisting of randomly distributed chunks of random sizes and shapes of material 1 imbedded in material 2. If we consider a particle traversing the mixture along a random path, it will pass through alternating segments of these two materials, as we can see in Figure 3.1.

The quantities Σ_t, Σ_s and Q are considered as discrete random variables. That is, in the ith material these elements are denoted by $\Sigma_{ti}(r, E, t)$, $\Sigma_{si}(r, E' \rightarrow E, \Omega' \cdot \Omega, t)$, and $Q_i(r, E, \Omega, t)$. The stochasticity of the problem is that we have only a probabilistic idea about which material occupies the space point r at a time t. Therefore, since we are considering Σ_t, Σ_s and Q as random variables, we must also consider the angular flux ψ as a random variable. We want to find an expression for $\langle \psi \rangle$, the ensemble-averaged angular flux (expected value) of ψ.

For convenience, let us consider the case of transport in a nonscattering medium. Thinking about $\Omega \cdot \nabla$ in Eq. (2.42) as a directional derivative, we can rewrite this equation as

$$\frac{1}{v}\frac{\partial \psi(s, t)}{\partial t} + \frac{\partial \psi(s, t)}{\partial s} + \Sigma_t(s, t)\psi(s, t) = Q(s, t), \qquad (3.1)$$
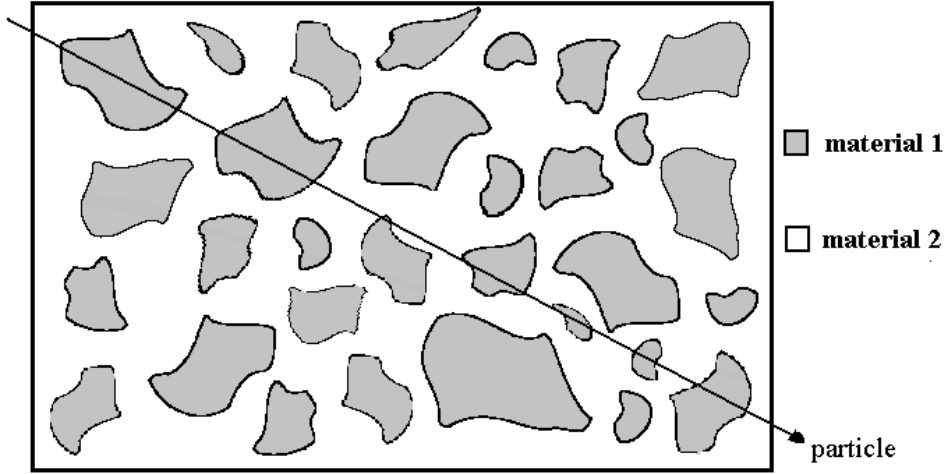
Figure 3.1: Particle traversing the mixture along a random path

where s denotes the spatial variable in the direction Ω. One must notice that Eq. (3.1) describes particle transport at each energy E and direction Ω, which are omitted since they are only parameters. We let $\langle W \rangle$ denote the ensemble average of any random variable W, and define $\tilde{W}$ as the deviation of W from $\langle W \rangle$. Then $\langle \tilde{W} \rangle = 0$, and $W = \langle W \rangle + \tilde{W}$. Using this notation we ensemble-average Eq. (3.1) to obtain

$$\frac{1}{v}\frac{\partial \langle \psi \rangle}{\partial t} + \frac{\partial \langle \psi \rangle}{\partial s} + \langle \Sigma_t \rangle \langle \psi \rangle + \langle \tilde{\Sigma}_t \tilde{\psi} \rangle = \langle Q \rangle. \tag{3.2}$$

The values of $\langle \Sigma_t \rangle$ and $\langle Q \rangle$ in this equation are defined in terms of the properties of materials 1 and 2. Defining $p_i(s,t)$ as the probability of presence of the material i at position s at time t, then

$$p_1(s,t) + p_2(s,t) = 1, \tag{3.3}$$

and we can write

$$\langle \Sigma_t(s,t) \rangle = p_1(s,t)\Sigma_{t1}(s,t) + p_2(s,t)\Sigma_{t2}(s,t), \tag{3.4}$$

$$\langle Q(s,t) \rangle = p_1(s,t)Q_1(s,t) + p_2(s,t)Q_2(s,t). \tag{3.5}$$

Now, let us define the characteristic chord length for the chunks of material i as Λ_i. Assuming that

$$\Sigma_{ti}\Lambda_i \ll 1, \quad i = 1, 2, \tag{3.6}$$

a particle between collisions is likely to travel a distance that spans many chunks of materials 1 and 2. Recalling the relationship given by Eq. (2.27), Eq. (3.6) means that Λ_i is very small when compared with the mean free path ℓ_i. On physical grounds, this assumption appropriately describes vanishingly small chunks in the mixture, which can be understood as if the two components of the system were mixed at the atomic level. When Eq. (3.6) is satisfied, it is physically intuitive that the transport process will be well-approximated by the process that holds when the chunk sizes are zero (the atomic mix limit). Moreover, when the chunk sizes shrink, the deviations in the angular flux should also shrink, and $\tilde{\psi}$ will go to zero. Hence, the cross correlation term $\langle \tilde{\Sigma}_t \tilde{\psi} \rangle$ in Eq. (3.2) is neglected, and Eq. (3.2) becomes

$$\frac{1}{v}\frac{\partial \langle \psi \rangle}{\partial t} + \frac{\partial \langle \psi \rangle}{\partial s} + \langle \Sigma_t \rangle \langle \psi \rangle = \langle Q \rangle, \tag{3.7}$$

which is closed for the ensemble-averaged angular flux $\langle \psi \rangle$. This equation represents the atomic mix description of Eq. (3.1).

Applying the same arguments above on Eqs. (2.42-2.44), the atomic mix description of stochastic transport, including scattering, is given by

$$\frac{1}{v}\frac{\partial \langle \psi(r,E,\Omega,t) \rangle}{\partial t} + \Omega \cdot \nabla \langle \psi(r,E,\Omega,t) \rangle + \langle \Sigma_t(r,E,t) \rangle \langle \psi(r,E,\Omega,t) \rangle =$$
$$= \int_0^\infty \int_{4\pi} \langle \Sigma_s(r,E' \to E, \Omega' \cdot \Omega, t) \rangle \langle \psi(r,E',\Omega',t) \rangle d\Omega' dE' + \langle Q(r,E,\Omega,t) \rangle, \tag{3.8}$$

with

$$\langle \psi(r_s,E,\Omega,t) \rangle = \langle \Gamma(r_s,E,\Omega,t) \rangle, \quad \mathrm{n} \cdot \Omega < 0, \tag{3.9}$$

$$\langle \psi(r,E,\Omega,0) \rangle = \langle \alpha(r,E,\Omega) \rangle \tag{3.10}$$

Here

$$\langle W \rangle = p_1(r,t)W_1 + p_2(r,t)W_2, \tag{3.11}$$

where W stands for Σ_t, Σ_s and Q. The neglected cross correlation terms are $\langle \tilde{\Sigma}_t \tilde{\psi} \rangle$ and $\langle \tilde{\Sigma}_s \tilde{\psi} \rangle$.
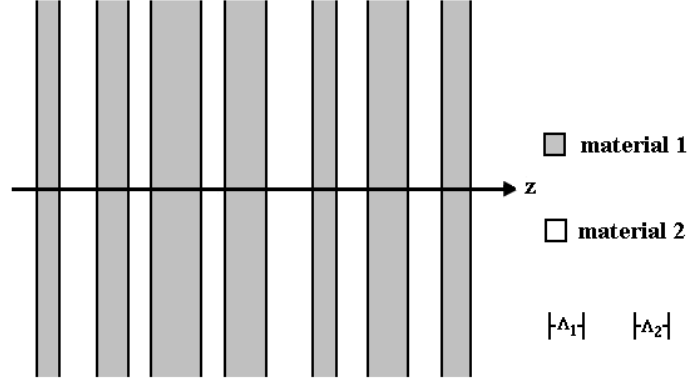
Figure 3.2: Multilayered slab - transverse volume intersection

3.2 The Multiscale Expansion Technique

In the last section we discussed only an empirical way to obtain the atomic mix equation. In Chapter 4 we will show in a rigorous way that the atomic mix equation can be deduced mathematically from the Levermore-Pomraning model, through asymptotic limits. For now, in order to illustrate the method, we will derive the atomic mix equation using the formal procedure of multiscale expansions, following the idea presented by Dumas and Golse [14].

Let us consider a three-dimensional volume in which heterogeneities occur along one spatial dimension (z) only. Moreover, let this volume consist of binary walls placed perpendicularly to the z-axis. A transverse intersection of this volume is represented by the multilayered slab in Figure 3.2, where Λ_i is the mean width of the regions of the homogeneous material i ($i = 1, 2$).

Denoting the mean free path of material i by ℓ_i, we define

$$\Lambda = \frac{\Lambda_1 + \Lambda_2}{2} \quad \text{and} \quad \ell = \frac{\ell_1 + \ell_2}{2}, \tag{3.12}$$

and assuming that Eq. (3.6) holds, which characterizes a mixture at atomic level, we define the small parameter ε by

$$\frac{\Lambda}{\ell} = \varepsilon \ll 1. \tag{3.13}$$

Now we consider the case of time independent transport in this system. For simplicity, we will assume that the scattering process is both coherent and isotropic. We will also assume the source Q to be isotropic. It is therefore clear that Σ_t, Σ_s, and Q will depend only upon the spatial variable z, since our assumptions allow us to consider energy E as a simple parameter. In this case, Eq. (2.42) becomes

$$\Omega \cdot \nabla \psi(r, \Omega) + \Sigma_t(z)\psi(r, \Omega) = \frac{\Sigma_s(z)\phi(r)}{4\pi} + \frac{Q(z)}{4\pi}, \tag{3.14}$$

where ϕ is the scalar flux as given by Eq. (2.11). The boundary condition is given by

$$\psi(r_s, \Omega) = 0, \quad \mathrm{n} \cdot \Omega < 0, \tag{3.15}$$

where r_s is a point on the surface and n is a unit outward normal vector at this point.

One must notice that the smaller is ε, the faster will be the oscillations of the functions Σ_t, Σ_s, and Q. This corresponds to the different values of these functions in each component of the mixture. For this reason, a scaling variable $w = z/\varepsilon$ is introduced [14, 21, 22, 23], and we define

$$\Sigma_t(z) = \sigma_t(w), \tag{3.16}$$

$$\Sigma_s(z) = \sigma_s(w), \tag{3.17}$$

$$Q(z) = q(w), \tag{3.18}$$

$$\psi(r, \Omega) = \hat{\psi}(r, w, \Omega). \tag{3.19}$$

Clearly, this "fast" spatial variable w describes variations in the cross sections, source and angular flux that occur over distances (along the z-axis) that are small compared to a mean free path. Rewriting Eq. (3.14) in terms of this scaling variable, we find

$$\Omega \cdot \nabla_w \hat{\psi}(r, w, \Omega) + \Omega \cdot \nabla \hat{\psi}(r, w, \Omega) + \sigma_t(w)\hat{\psi}(r, w, \Omega) = \frac{\sigma_s(w)\hat{\phi}(r, w)}{4\pi} + \frac{q(w)}{4\pi}, \tag{3.20}$$

that is,

$$\frac{\mu}{\varepsilon} \frac{\partial \hat{\psi}}{\partial w}(r, w, \Omega) + \Omega \cdot \nabla \hat{\psi}(r, w, \Omega) + \sigma_t(w)\hat{\psi}(r, w, \Omega) = \frac{\sigma_s(w)\hat{\phi}(r, w)}{4\pi} + \frac{q(w)}{4\pi}, \tag{3.21}$$

where $\hat{\phi}$ follows the scalar flux definition regarding $\hat{\psi}$.

Then, we seek $\hat{\psi}$ as a multiscale expansion of the form

$$\hat{\psi}(r, w, \Omega) = \sum_{k=0} \varepsilon^k \psi_k(r, w, \Omega). \tag{3.22}$$

Here, we remark that this expansion is performed only as a formal procedure (we will show in the next section that this analysis breaks down when we try to find an expression for the terms ψ_k with $k \geq 1$). Proceeding as in [14], we apply this expansion in Eq. (3.21), and equating the coefficients of powers ε^{-1} and ε^0, we respectively obtain

$$\mu \frac{\partial \psi_0}{\partial w}(r, w, \Omega) = 0, \tag{3.23}$$

and

$$\mu \frac{\partial \psi_1}{\partial w}(r, w, \Omega) = -\Omega \cdot \nabla \psi_0(r, w, \Omega) - \sigma_t(w) \psi_0(r, w, \Omega) + \frac{\sigma_s(w) \phi_0(r, w)}{4\pi} + \frac{q(w)}{4\pi}, \tag{3.24}$$

where ϕ_0 follows the scalar flux definition regarding ψ_0. From Eq. (3.23) we deduce that ψ_0 does not depend on w. If we define a fast spatial averaging operator [21, 22, 23] by

$$\overline{f}(r) = \lim_{\hat{w} \to \infty} \left[\frac{1}{2\hat{w}} \int_{-\hat{w}}^{\hat{w}} f(r, w) dw \right], \tag{3.25}$$

it is easy to see that

$$\overline{\frac{\partial \psi_1}{\partial w}} \to 0. \tag{3.26}$$

Hence, applying this operator in Eq. (3.24), we obtain

$$\Omega \cdot \nabla \psi_0(r, \Omega) + \overline{\sigma_t} \, \psi_0(r, \Omega) = \frac{\overline{\sigma_s} \, \phi_0(r)}{4\pi} + \frac{\overline{q}}{4\pi}, \tag{3.27}$$

which is the atomic mix representation of Eq. (3.14).

In fact, we can relate the present derivation with the discussion made in the last section. It was said that the cross correlation terms can be neglected when Eq. (3.6) is satisfied. Here, these terms can be thought of as being embodied in the evaluation of the subsequent terms of the expansion in Eq. (3.22). This is not strictly correct, since this expansion is only a formal procedure, but one can envision that the cross correlation terms must be embodied in $\psi' = \hat{\psi} - \psi_0$.

Furthermore, this derivation presents a simple approach to deal with the system heterogeneities, but we will show in the next section that we are not able to find a more accurate expression for ψ using only the mathematical tools presented here.

3.3 Limitations of the Atomic Mix Model

Atomic mix is very appealing because of its simplicity. Since the cross correlation terms are neglected, this model leads to a description that essentially does not deal with stochastic effects. Assuming that the statistics of mixing is known, the problem of solving Eq. (3.8) is not different than the one we face to solve Eq. (2.42). However, when Eq. (3.6) is not satisfied, the atomic mix description is generally inaccurate. Although there exist specified classes of problems in which atomic mix is accurate even when the chunk sizes are not optically small [21, 22], in general it fails quite badly in these situations. As an example, consider time independent transport in a nonscattering medium without internal sources, given by

$$\frac{\partial \psi(s)}{\partial s} + \Sigma_t(s)\psi(s) = 0, \tag{3.28}$$

with the boundary condition

$$\psi(0) = \Gamma_0, \tag{3.29}$$

where $(0 \leq s < \infty)$. Following Pomraning [43], let material 1 be composed of optically thin packets such that $\Sigma_{t1}\Lambda_1 \ll 1$. Then, define material 2 as very sparse optically thick chunks imbedded on material 1, in such way that $\Sigma_{t2}\Lambda_2 \gg 1$ and $p_2(s) \ll 1$. Here, Λ_i is the characteristic chord length of material i and p_2 is the probability of finding material 2 at position s. The physical description is that of a near vacuum where sparse absorbing packets of (essentialy) infinite thickness can be found. Particles travelling through this mixture tend to pass through it without undergoing an interaction, at least on the average, as can be seen from Figure 3.3. On the other hand, if we write the atomic mix description of Eqs. (3.28-3.29)
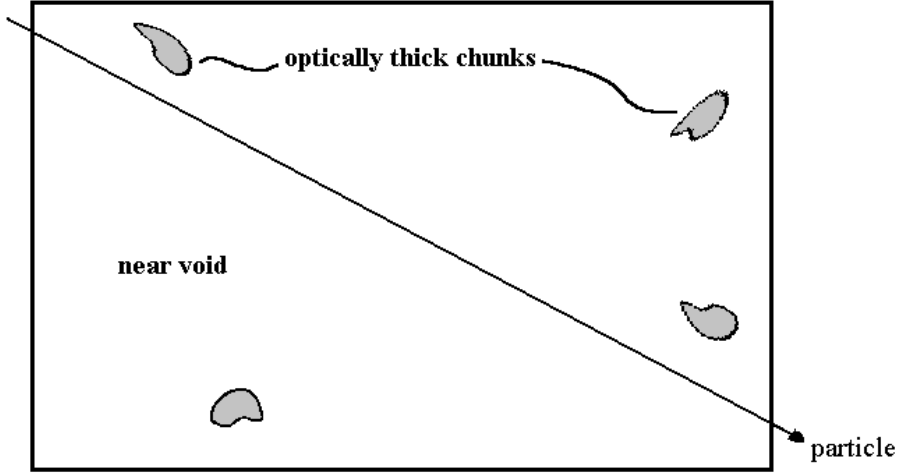
Figure 3.3: Particle travelling through a near void with sparse chunks

neglecting the cross correlation term $\langle \tilde{\Sigma}_t \tilde{\psi} \rangle$:

$$\frac{\partial \langle \psi \rangle}{\partial s} + \langle \Sigma_t \rangle \langle \psi \rangle = 0, \tag{3.30}$$

$$\langle \psi(0) \rangle = \langle \Gamma_0 \rangle, \tag{3.31}$$

we will conclude that $\langle \psi \rangle$ will be exponentially attenuated, with a scale length $1/\langle \Sigma_t \rangle$, and it is clear that $\langle \Sigma_t \rangle$ is very large, since Σ_{t2} is very large. Hence, this modelling will lead to essentialy no transmission through the system. In general, neglecting the cross correlation term will underestimate particle transmission.

Let us turn our attention to the problem with one-dimensional heterogeneities presented in last section. Since we have found an expression to ψ_0 without difficulties, we are tempted to seek an expression to ψ_1 in order to define Eq. (3.22) more accurately. Subtracting Eq. (3.27) from Eq. (3.24), we find

$$\mu \frac{\partial \psi_1}{\partial w}(r, w, \Omega) = \left[\overline{\sigma_t} - \sigma_t(w) \right] \psi_0(r, \Omega) - \frac{\left[\overline{\sigma_s} - \sigma_s(w) \right] \phi_0(r)}{4\pi} - \frac{\left[\overline{q} - q(w) \right]}{4\pi}. \tag{3.32}$$

We define

$$\sigma_t(w) = \overline{\sigma_t} + \frac{dg_t}{dw}(w), \tag{3.33}$$

$$\sigma_s(w) = \overline{\sigma_s} + \frac{dg_s}{dw}(w), \tag{3.34}$$

$$q(w) = \overline{q} + \frac{dg_q}{dw}(w), \tag{3.35}$$
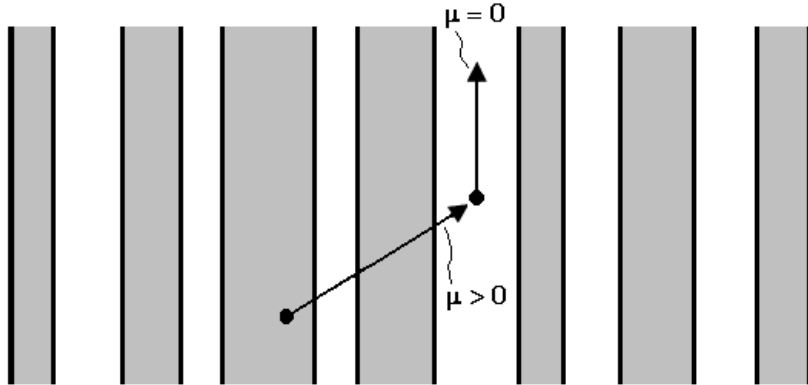
Figure 3.4: Particle travelling in direction $\mu = 0$

where the auxiliary functions g_t, g_s and g_q (and their respective derivatives) are suitable random functions with the same order of σ_t, σ_s and q regarding the scaling variable w. Thus, the randomness in functions σ_t, σ_s and q is completely due to the randomness in the g functions. Rewriting Eq. (3.32) in terms of these functions and integrating over w, we find

$$\mu\psi_1(r,w,\Omega) = -g_t(w)\psi_0(r,\Omega) + \frac{g_s(w)\phi_0(r)}{4\pi} + \frac{g_q(w)}{4\pi}. \tag{3.36}$$

However, Eq. (3.36) gives us

$$\psi_1(r,w,\Omega) = \frac{1}{\mu}\left[-g_t(w)\psi_0(r,\Omega) + \frac{g_s(w)\phi_0(r)}{4\pi} + \frac{g_q(w)}{4\pi}\right], \tag{3.37}$$

which is not bounded, given that $-1 \leq \mu \leq 1$. Hence, this analysis breaks down. In fact, it has been shown [14] that the multiscale expansion given in Eq. (3.22) cannot in general be pursued, no matter in how many directions the heterogeneities occur.

Nevertheless, in this particular case we can envision a physical explanation for this problem. While a particle travels through the medium described in Figure 3.2 with $\mu \neq 0$, it spans several walls of materials 1 and 2, as expected. But if a particle scatters to a direction in which $\mu = 0$, it will flow in a wall of one material only, as can be seen from Figure 3.4. That is, the properties of the medium in which this particle is travelling are not the same as we have in the atomic mix description. A more complex analysis would be necessary in order to derive more accurate results for this problem.

We conclude this chapter by mentioning that some important contributions have been made regarding the mathematical analysis of homogenization problems. In particular, we refer to [14] for results on the treatment of high-frequency oscillations, periodic homogenization, small divisor problems and stochastic inhomogeneities; and to [39] for strong convergence results to the solution of homogenized problems (we also refer to the literature indicated there).

4 THE LEVERMORE-POMRANING METHOD

4.1 The Levermore-Pomraning Derivation

The first derivation of the Levermore-Pomraning method [25, 44] considered time independent transport in a purely absorbing medium. However, the task of reducing this expression to an useable one when the scattering interaction is involved is exceedingly complex [43]. For this reason we will not treat this derivation in this work.

Later, Vanderhaegen [86] pointed out that in the time independent, nonscattering case, the stochastic problem is a joint Markov process, and thus the Liouville master equation applies [18, 89]. It was suggested [43, 49, 53] that the use of this master equation might produce an useful approximate model for problems with time dependence and scattering. This approach is the subject of section 4.1.1 .

In section 4.1.2 we discuss still another derivation of this model, which was introduced by Adams, Larsen and Pomraning [1]. Here, the details of this derivation follow Vasques et al. [90], in a manner that the reader may find illuminating from the physical viewpoint. We also present an argument pointing out that the Levermore-Pomraning equations, in their traditional form, are incorrect for random three dimensional geometries.

4.1.1 The Master Equation Approach

Let us consider time independent transport in a nonscattering, heterogeneous medium composed by materials 1 and 2. Then Eq. (2.42) becomes, at each energy E,

$$\frac{d\psi}{ds}(s) + \Sigma_t(s)\psi(s) = Q(s),$$

(4.1)

with the boundary condition given by

$$\psi(0) = \Gamma_0. \tag{4.2}$$

Following Vanderhaegen [86], Eq. (4.1) can be thought of as an initial value problem, with the spatial variable s playing the role of time. Hence, if we define in terms of Eq. (2.59) the probability of not finding material i at $s + ds$ *given that* the position s consists of material i, then we have a joint Markov process, and the Liouville master equation [18, 89] applies. This equation describes the joint probability density $P_i(\psi, s)$, defined such that $P_i d\psi$ is the probability of finding material i at position s, and having the stochastic solution lie between ψ and $\psi + d\psi$. Thus, for $i = 1, 2$ and $j \neq i$, we have the coupled equations

$$\frac{\partial P_i}{\partial s} - \frac{\partial}{\partial \psi}\left[(\Sigma_{ti}\psi - Q_i)P_i\right] = \frac{P_j}{\lambda_j} - \frac{P_i}{\lambda_i}. \tag{4.3}$$

The boundary conditions of Eq. (4.3) are given by

$$P_i(\psi, 0) = p_i(0)\delta(\psi - \Gamma_0), \tag{4.4}$$

where $p_i(s)$, the probability of finding material i at position s, is related to $P_i(\psi, s)$ according to

$$p_i(s) = \int_0^\infty P_i(\psi, s)d\psi. \tag{4.5}$$

If we define $\psi_i(s)$ as the ensemble average of $\psi(s)$ over all physical realizations such that s is in material i, then we have

$$p_i(s)\psi_i(s) = \int_0^\infty \psi P_i(\psi, s)d\psi, \tag{4.6}$$

and

$$\langle \psi(s) \rangle = p_1(s)\psi_1(s) + p_2(s)\psi_2(s). \tag{4.7}$$

Further, if we multiply Eqs. (4.3-4.4) by ψ and integrate over $0 \leq \psi < \infty$, we find:

$$\frac{d(p_i\psi_i)}{ds} + \Sigma_{ti}p_i\psi_i = p_iQ_i + \frac{p_j\psi_j}{\lambda_j} - \frac{p_i\psi_i}{\lambda_i}, \tag{4.8}$$

subject to the boundary conditions

$$\psi_i(0) = \Gamma_0. \tag{4.9}$$

Equations (4.8) and (4.9) give an exact description for the ensemble-averaged angular flux in binary Markovian mixtures for the problem given by Eq. (4.1). Unfortunately, when scattering is included, the transport equation cannot be thought of as an initial value problem, and therefore it does not describe a Markov process even if the mixing process is assumed to be Markovian [88]. Hence the Liouville master equation, if applied, would not produce an exact formulation.

On the other hand, it is possible to obtain a useful approximation for particle transport in Markovian mixtures with scattering using the Liouville master equation [43, 49, 53]. Let us consider the inscattering term given by Eq. (2.38). The basic approximation consists of treating this term in the same way as the internal source term Q. This approximation is performed in such way that the continuous random variable $\psi(r, E', \Omega', t)$ is replaced by a discrete random variable $\psi_i(r, E', \Omega', t)$, such that ψ_i is the ensemble average of ψ over the continuous states found when the system is in material i at given r and t. In analogy with the non-scattering case, we find the two coupled equations (with time dependence included)

$$\left(\frac{1}{v}\frac{\partial}{\partial t} + \Omega \cdot \nabla\right)P_i - \frac{\partial}{\partial \psi}\left\{\left[\Sigma_{ti}\psi + (S_i - \Sigma_{si})\psi_i - Q_i\right]P_i\right\} = \frac{P_j}{\lambda_j} - \frac{P_i}{\lambda_i}, \qquad (4.10)$$

where S_i is the scattering operator for material i, defined by

$$S_i\psi_i = \Sigma_{si}\psi_i - \int_0^\infty \int_{4\pi} \Sigma_{si}(r, E' \to E, \Omega' \cdot \Omega, t)\psi_i(r, E', \Omega', t)d\Omega'dE'. \qquad (4.11)$$

In Eq. (4.10), $P_i(\psi, r, E, \Omega, t)d\psi$ is the probability of finding material i at position r and time t, and having the stochastic solution lie between ψ and $\psi + d\psi$. We define $p_i(r, t)$, the probability of finding material i at position r and time t, in analogy to Eq. (4.5). Hence $\psi_i(r, E, \Omega, t)$ is given in terms of P_i in analogy to Eq. (4.6). Further, the Markov transition functions in Eq. (4.10) depend upon angle, space and time; that is, $\lambda_i = \lambda_i(r, \Omega, t)$.

If we assign boundary and initial conditions for the transport equation of the form

$$\psi(r_s, E, \Omega, t) = \Gamma(r_s, E, \Omega, t), \quad \mathrm{n} \cdot \Omega < 0, \qquad (4.12)$$

$$\psi(r, E, \Omega, 0) = \alpha(r, E, \Omega), \qquad (4.13)$$

where r_s is a point on the surface of the system and n is a unit outward normal vector at r_s, then the boundary and initial conditions on Eq. (4.10) are given by

$$P_i(\psi, r_s, E, \Omega, t) = p_i(r_s, t)\delta(\psi - \Gamma), \quad \text{n} \cdot \Omega < 0, \tag{4.14}$$

$$P_i(\psi, r, E, \Omega, 0) = p_i(r, 0)\delta(\psi - \alpha). \tag{4.15}$$

Again, multiplying Eqs. (4.10,4.14-4.15) by ψ and integrating over $0 \leq \psi < \infty$, we find

$$\frac{1}{v}\frac{\partial(p_i\psi_i)}{\partial t} + \Omega \cdot \nabla(p_i\psi_i) + (\Sigma_{ai} + S_i)(p_i\psi_i) = p_iQ_i + \frac{p_j\psi_j}{\lambda_j} - \frac{p_i\psi_i}{\lambda_i}, \tag{4.16}$$

subject to the boundary and initial conditions

$$\psi_i(r_s, E, \Omega, t) = \Gamma(r_s, E, \Omega, t), \quad \text{n} \cdot \Omega < 0, \tag{4.17}$$

$$\psi_i(r, E, \Omega, 0) = \alpha(r, E, \Omega). \tag{4.18}$$

Thus, the overall ensemble average of the angular flux is related to ψ_i according to

$$\langle \psi(r, E, \Omega, t)\rangle = p_1(r, t)\psi_1(r, E, \Omega, t) + p_2(r, t)\psi_2(r, E, \Omega, t). \tag{4.19}$$

Equations (4.16-4.18) are the "classic" Levermore-Pomraning equations.

4.1.2 Stochastic Balance Method

Now we will present a second derivation of this model. Following Adams, Larsen and Pomraning [1] and Vasques et al. [90], we will initially restrict our considerations to time-independent statistics (i.e., the configuration of materials 1 and 2 in any given physical realization of the mixing statistics is static).

For notation simplicity, we consider the transport equation with an isotropic internal source, and we assume that the scattering process is both coherent and isotropic. Thus we have

$$\frac{1}{v}\frac{\partial \psi}{\partial t}(r, \Omega, t) + \Omega \cdot \nabla\psi(r, \Omega, t) + \Sigma_t\psi(r, \Omega, t) = \frac{\Sigma_s}{4\pi}\int_{4\pi}\psi(r, \Omega', t)d\Omega' + \frac{Q(r, t)}{4\pi}, \tag{4.20}$$

and we define boundary and initial conditions

$$\psi(r_s, \Omega, t) = \Gamma(r_s, \Omega, t), \quad \mathrm{n} \cdot \Omega < 0, \tag{4.21}$$

$$\psi(r, \Omega, 0) = \alpha(r, \Omega), \tag{4.22}$$

where r_s is a point on the surface of the system and n is a unit outward normal vector at r_s.

Now, we introduce the characteristic functions

$$\chi_i(r) = \begin{cases} 1, & \text{if } r \text{ is in material } i \\ 0, & \text{if } r \text{ is in material } j \neq i \end{cases}. \tag{4.23}$$

The basic issue is that we do not know the functions $\chi_1(r)$ and $\chi_2(r)$, but we know that they satisfy

$$\chi_1(r) + \chi_2(r) = 1. \tag{4.24}$$

Multiplying Eq. (4.20) by $\chi_i(r)$, and using:

$$\chi_i(\Omega \cdot \nabla \psi) = \Omega \cdot \nabla(\chi_i \psi) - \psi(\Omega \cdot \nabla \chi_i), \tag{4.25}$$

$$\chi_i(r)\Sigma_t(r) = \Sigma_{ti}\chi_i(r), \tag{4.26}$$

$$\chi_i(r)\Sigma_s(r) = \Sigma_{si}\chi_i(r), \tag{4.27}$$

$$\chi_i(r)Q(r, t) = Q_i\chi_i(r), \tag{4.28}$$

we find, for $i = 1, 2$,

$$\frac{1}{v}\frac{\partial(\chi_i\psi)}{\partial t} + \Omega \cdot \nabla(\chi_i\psi) + \Sigma_{ti}(\chi_i\psi) = \frac{\Sigma_{si}}{4\pi}\int_{4\pi}\chi_i\psi(r, \Omega', t)d\Omega' + \frac{Q_i\chi_i}{4\pi} + \psi(\Omega \cdot \nabla\chi_i). \tag{4.29}$$

The next step is to ensemble-average this result over all statistical realizations. The probability of finding material i at point r is given by

$$p_i(r) = \langle \chi_i(r) \rangle, \tag{4.30}$$

and therefore we define

$$\psi_i(r, \Omega, t) = \frac{\langle \chi_i(r)\psi(r, \Omega, t) \rangle}{\langle \chi_i(r) \rangle}, \tag{4.31}$$

where, again, ψ_i is the ensemble average of $\psi(r, \Omega, t)$ over all physical realizations such that r is in material i. Hence Eq. (4.29) becomes

$$\frac{1}{v}\frac{\partial(p_i\psi_i)}{\partial t} + \Omega\cdot\nabla(p_i\psi_i) + \Sigma_{ti}(p_i\psi_i) =$$
$$= \frac{\Sigma_{si}}{4\pi}\int_{4\pi} p_i\psi_i(r, \Omega', t)d\Omega' + \frac{p_iQ_i}{4\pi} + \left\langle\psi(\Omega\cdot\nabla\chi_i)\right\rangle. \tag{4.32}$$

Further, from Eqs. (4.24,4.30-4.31) we deduce that

$$\left\langle\psi(r, \Omega, t)\right\rangle = p_1(r)\psi_1(r, \Omega, t) + p_2(r)\psi_2(r, \Omega, t), \tag{4.33}$$

which is the overall ensemble average of the angular flux as defined earlier. Boundary and initial conditions for $\psi_i(r, \Omega, t)$ are obtained by multiplying Eqs. (4.21-4.22) by $\chi_i(r)$ and ensemble-averaging them:

$$\psi_i(r_s, \Omega, t) = \Gamma(r_s, \Omega, t), \quad \mathrm{n}\cdot\Omega < 0, \tag{4.34}$$

$$\psi_i(r, \Omega, 0) = \alpha(r, \Omega). \tag{4.35}$$

Now, in order to obtain a closed system of equations and boundary conditions for ψ_1 and ψ_2, it is necessary to evaluate the term

$$\left\langle f_i(r, \Omega, t)\right\rangle = \left\langle\psi(r, \Omega, t)[\Omega\cdot\nabla\chi_i]\right\rangle \tag{4.36}$$

on the right hand side of Eq. (4.32). To do this, we consider the average value of $f_i(r, \Omega, t)$ over a volume V and take the limit as V approaches zero:

$$\left\langle f_i(r, \Omega, t)\right\rangle = \lim_{V\to 0}\left\langle\psi(r, \Omega, t)\left(\frac{1}{V}\int_V \Omega\cdot\nabla\chi_i(r)dr\right)\right\rangle. \tag{4.37}$$

The ensemble-average in Eq. (4.37) is over all realizations. However, for a given realization, we have $\int_V \Omega\cdot\nabla\chi_i(r)dr \neq 0$ only if there is an interface between materials 1 and 2 intersecting V. Therefore, we write

$$\left\langle\psi(r, \Omega, t)\left(\frac{1}{V}\int_V \Omega\cdot\nabla\chi_i(r)dr\right)\right\rangle = P^*\left\langle\psi(r, \Omega, t)\left(\frac{1}{V}\int_V \Omega\cdot\nabla\chi_i(r)dr\right)\right\rangle^*, \tag{4.38}$$

where P^* is the probability that a realization has an interface that intersects V, and $\left\langle\,\cdot\,\right\rangle^*$ is a restricted average defined to be an ensemble-average over all realizations having an interface that intersects V.
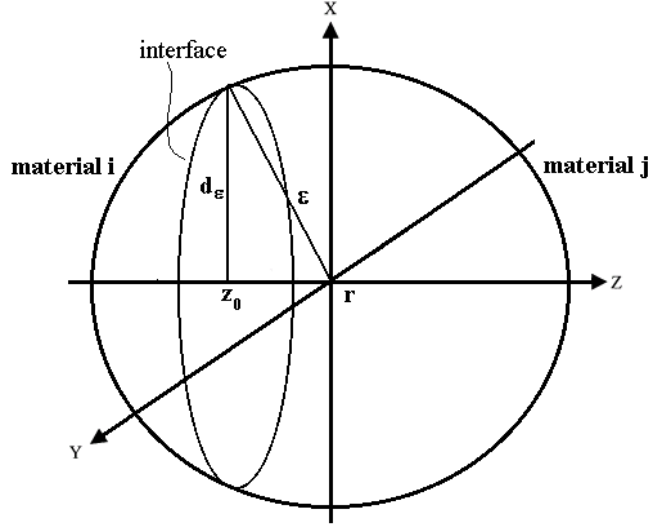
Figure 4.1: Intersection of the interface with the sphere V

Now we consider V to be a sphere of radius ε centered at r. Assuming that there exists an interface intersecting this sphere, for ε small enough we can regard this interface as a plane with normal vector n_i pointing out of region i. If we chose the z-axis perpendicular to this planar interface as shown in Figure 4.1, then the intersection of the interface with the sphere is a disc of radius $d_\varepsilon = \sqrt{\varepsilon^2 - z_0^2}$ given by the intersection of the plane $z = z_0$ with the sphere, and $\mathrm{n}_i = \hat{e}_z$. In this coordinate system we have $\nabla \chi(r) = -\mathrm{n}_i \delta(z - z_0)$; thus

$$
\frac{1}{V} \int_V \Omega \cdot \nabla \chi_i(r) dr = \frac{3}{4\pi\varepsilon^3} \int_V (-\Omega \cdot \mathrm{n}_i) \delta(z - z_0) dx\, dy\, dz =
$$
$$
= \frac{3}{4\pi\varepsilon^3}(-\Omega \cdot \mathrm{n}_i)\pi d_\varepsilon^2 = \frac{3}{4\varepsilon^3}(-\Omega \cdot \mathrm{n}_i)d_\varepsilon^2,
$$
(4.39)

and Eq. (4.37) becomes

$$
\langle f_i(r, \Omega, t)\rangle = \lim_{\varepsilon \to 0}\left[-\frac{3}{4\varepsilon^3}P^*\left\langle (\Omega \cdot \mathrm{n}_i)\psi(r, \Omega, t)d_\varepsilon^2 \right\rangle^* \right].
$$
(4.40)

Let us define $\langle \cdot \rangle^*_{\Omega \cdot \mathrm{n}_i > 0}$ to be the ensemble-average over all realizations such that an interface intersects V and Ω points out of material i. Then, since $\mathrm{n}_i = -\mathrm{n}_j$,

$$
\left\langle (\Omega \cdot \mathrm{n}_i)\psi(r, \Omega, t)d_\varepsilon^2 \right\rangle^* =
$$
$$
= \left\langle (\Omega \cdot \mathrm{n}_i)\psi(r, \Omega, t)d_\varepsilon^2 \right\rangle^*_{\Omega \cdot \mathrm{n}_i > 0} + \left\langle (\Omega \cdot \mathrm{n}_i)\psi(r, \Omega, t)d_\varepsilon^2 \right\rangle^*_{\Omega \cdot \mathrm{n}_i < 0}
$$
(4.41)
$$
= \left\langle (\Omega \cdot \mathrm{n}_i)\psi(r, \Omega, t)d_\varepsilon^2 \right\rangle^*_{\Omega \cdot \mathrm{n}_i > 0} - \left\langle (\Omega \cdot \mathrm{n}_j)\psi(r, \Omega, t)d_\varepsilon^2 \right\rangle^*_{\Omega \cdot \mathrm{n}_j > 0},
$$
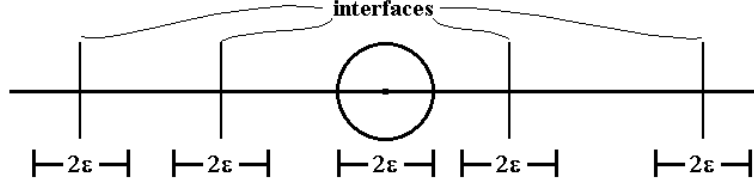
Figure 4.2: Arbitrary infinite line intersecting interfaces perpendicularly

and defining

$$\Psi_i^\varepsilon = \frac{\left\langle (\Omega \cdot n_i)\psi(r,\Omega,t)d_\varepsilon^2 \right\rangle_{\Omega \cdot n_i > 0}^*}{\left\langle (\Omega \cdot n_i)d_\varepsilon^2 \right\rangle_{\Omega \cdot n_i > 0}^*}, \tag{4.42}$$

we can rewrite Eq. (4.40) as

$$\left\langle f_i(r,\Omega,t) \right\rangle =$$
$$= \lim_{\epsilon \to 0} \left[\frac{3}{4\varepsilon^3} P^* \left(\Psi_j^\varepsilon \left\langle (\Omega \cdot n_j)d_\varepsilon^2 \right\rangle_{\Omega \cdot n_j > 0}^* - \Psi_i^\varepsilon \left\langle (\Omega \cdot n_i)d_\varepsilon^2 \right\rangle_{\Omega \cdot n_i > 0}^* \right) \right]. \tag{4.43}$$

The geometrical quantities $\left\langle (\Omega \cdot n_i)d_\varepsilon^2 \right\rangle_{\Omega \cdot n_i > 0}^*$ in Eq. (4.43) are equal for $i = 1, 2$ and can be explicitly evaluated if we assume that:

1) the points z_0 in Figure 4.1 are uniformly distributed on $-\varepsilon < z_0 < \varepsilon$;

2) the normal vectors of interfaces passing through V are uniformly distributed on the unit sphere.

Then, using $\Omega \cdot n_i = \mu$ and $d_\varepsilon^2 = \varepsilon^2 - z_0^2$, we obtain for $i = 1$ and 2

$$\left\langle (\Omega \cdot n_i)d_\varepsilon^2 \right\rangle_{\Omega \cdot n_i > 0}^* = \left\langle \mu(\varepsilon^2 - z_0^2) \right\rangle_{\mu > 0}^*$$
$$= \int_0^1 \left(\frac{1}{2\varepsilon} \int_{-\varepsilon}^\varepsilon \mu(\varepsilon^2 - z_0^2)dz_0 \right) d\mu \tag{4.44}$$
$$= \frac{\varepsilon^2}{3}.$$

Introducing this result into Eq. (4.43), we get

$$\left\langle f_i(r,\Omega,t) \right\rangle = \lim_{\epsilon \to 0} \left[\frac{3}{4\varepsilon^3} \frac{\varepsilon^2}{3} P^* \left(\Psi_j^\varepsilon - \Psi_i^\varepsilon \right) \right] = \lim_{\epsilon \to 0} \left[\frac{1}{4\varepsilon} P^* \left(\Psi_j^\varepsilon - \Psi_i^\varepsilon \right) \right]. \tag{4.45}$$

Further, it is possible to calculate P^*. To do this, let us consider an arbitrary infinite line through the point r, and let us assume (for the moment) that the interfaces all intersect the line perpendicularly. Then, it can be seen from Figure 4.2 that an

interface intersects V only if the point r lies within a distance ε of an interface. This creates a line segment of width 2ε about each interface, such that if r is in one of these segments, then an interface intersects V. Over a very large length of this line, spanning m chunks of material i and m chunks of material j, we have

$$(2m)(2\varepsilon) = 4m\varepsilon$$

$$= \begin{pmatrix} \text{the length of the line segments such that if } r \text{ lies on} \\ \text{one of these segments, then an interface intersects } V \end{pmatrix}, \tag{4.46}$$

and

$$m(\Lambda_1 + \Lambda_2) \approx (\text{total length of the line}). \tag{4.47}$$

The ratio of Eqs. (4.46) and (4.47) is P^*. That is,

$$P^* = \frac{4\varepsilon}{\Lambda_1 + \Lambda_2}. \tag{4.48}$$

One can easily see that this expression has the right qualitative behavior. It correctly limits to zero as $\varepsilon \to 0$, and as $\Lambda_1, \Lambda_2 \to \infty$.

Introducing Eq. (4.48) into Eq. (4.45), we obtain

$$\langle f_i(r, \Omega, t) \rangle = \lim_{\epsilon \to 0} \left[\frac{1}{4\varepsilon} \left(\frac{4\varepsilon}{\Lambda_1 + \Lambda_2} \right) \left(\Psi_j^\varepsilon - \Psi_i^\varepsilon \right) \right] = \lim_{\epsilon \to 0} \left[\frac{1}{\Lambda_1 + \Lambda_2} \left(\Psi_j^\varepsilon - \Psi_i^\varepsilon \right) \right]. \tag{4.49}$$

Finally, defining $\Psi_i = \lim\limits_{\varepsilon \to 0} \Psi_i^\varepsilon$ and using Eq. (2.53), we have

$$\begin{aligned} \langle f_i(r, \Omega, t) \rangle &= \frac{1}{\Lambda_1 + \Lambda_2} \left(\Psi_j - \Psi_i \right) \\ &= \left(\frac{\Lambda_j}{\Lambda_1 + \Lambda_2} \right) \left(\frac{\Psi_j}{\Lambda_j} \right) - \left(\frac{\Lambda_i}{\Lambda_1 + \Lambda_2} \right) \left(\frac{\Psi_i}{\Lambda_i} \right) \\ &= \frac{p_j \Psi_j}{\Lambda_j} - \frac{p_i \Psi_i}{\Lambda_i}, \end{aligned} \tag{4.50}$$

and this result is the Levermore-Pomraning expression for $\langle f_i \rangle$. Combining Eq. (4.32) with Eq. (4.50), we obtain

$$\begin{aligned} \frac{1}{v} \frac{\partial (p_i \psi_i)}{\partial t} &+ \Omega \cdot \nabla (p_i \psi_i) + \Sigma_{ti}(p_i \psi_i) = \\ &= \frac{\Sigma_{si}}{4\pi} \int_{4\pi} p_i \psi_i(r, \Omega', t) d\Omega' + \frac{p_i Q_i}{4\pi} + \frac{p_j \Psi_j}{\Lambda_j} - \frac{p_i \Psi_i}{\Lambda_i}. \end{aligned} \tag{4.51}$$

Unfortunately, this result consists of two equations with four unknown functions, namely ψ_1, ψ_2, Ψ_1 and Ψ_2; thus, a closure is needed to make this formalism useful. No simple exact relationship seems to exist relating ψ_i (the ensemble average of ψ over all physical realizations such that r is in material i) and Ψ_i (the ensemble average of ψ at interface points for which $\Omega \cdot n_i > 0$). Nevertheless, in analogy with upwind differencing encountered in the numerical analysis of hyperbolic equations, we approximate Ψ_i by simply equating it to ψ_i. Rewriting Eq. (4.51) with this closure, we find

$$\frac{1}{v}\frac{\partial(p_i\psi_i)}{\partial t} + \Omega\cdot\nabla(p_i\psi_i) + \Sigma_{ti}(p_i\psi_i) =$$
$$= \frac{\Sigma_{si}}{4\pi}\int_{4\pi}p_i\psi_i(r,\Omega',t)d\Omega' + \frac{p_iQ_i}{4\pi} + \frac{p_j\psi_j}{\Lambda_j} - \frac{p_i\psi_i}{\Lambda_i}, \tag{4.52}$$

and the general case (general scattering, arbitrary source) is straightforwardly given by

$$\frac{1}{v}\frac{\partial(p_i\psi_i)}{\partial t} + \Omega\cdot\nabla(p_i\psi_i) + (\Sigma_{ai} + S_i)(p_i\psi_i) = p_iQ_i + \frac{p_j\psi_j}{\Lambda_j} - \frac{p_i\psi_i}{\Lambda_i}, \tag{4.53}$$

where S_i is the scattering operator as defined by Eq. (4.11). Again, the coupled equations ($i = 1, 2$) given by Eq. (4.53) are known as the "classic" Levermore-Pomraning equations.

It is important to notice that this derivation applies to arbitrary homogeneous statistics (the homogeneity condition is implicit in assumptions 1 and 2 in page 41). Particularly, in the case of Markov statistics we know from Eq. (2.62) that $\Lambda_i = \lambda_i$, i.e., the characteristic chord lengths are simply the Markov transition functions λ_i. Thus, when the mixture is taken as Markovian, Eq. (4.53) is identical to the Liouville master equation result given by Eq. (4.16). Therefore, the exactness for time independent, purely absorbing mixtures is clearly explained within the present context, since the approximation $\Psi_i = \psi_i$ is in this case exact. According to Pomraning [43], this follows from the fact that for purely absorbing, time independent transport, the solution at any point depends only upon the optical depths from this point to the system boundary and the source points. For Markov statistics, the ensemble-averaged optical depth between two spatial points is the same if one of the points is an interface, or if this point is chosen at random in one of the materials.

In order to extend these considerations to nonstatic physical realizations of the mixing, we define

$$\chi_i(r,t) = \begin{cases} 1, & \text{if } r \text{ is in material } i \text{ at time } t \\ 0, & \text{if } r \text{ is in material } j \neq i \text{ at time } t \end{cases}. \tag{4.54}$$

Multiplying Eq. (4.20) by $\chi_i(r,t)$, a new term will appear, given by (h_i) in

$$\frac{1}{v}\left(\chi_i \frac{\partial \psi}{\partial t}\right) = \frac{1}{v}\frac{\partial(\chi_i \psi)}{\partial t} - \underbrace{\frac{1}{v}\left(\psi \frac{\partial \chi_i}{\partial t}\right)}_{(h_i)}. \tag{4.55}$$

We define $p_i(r,t)$, the probability of finding material i at point r and time t, by

$$p_i(r,t) = \langle \chi_i(r,t) \rangle, \tag{4.56}$$

and the ensemble-averaged angular flux over all physical realizations such that r is in material i at time t by

$$\psi_i(r,E,\Omega,t) = \frac{\langle \chi_i(r,t)\psi(r,E,\Omega,t)\rangle}{\langle \chi_i(r,t)\rangle}. \tag{4.57}$$

Treating $\langle h_i \rangle$ in analogy with the way we treated $\langle f_i \rangle$, we find [43]

$$\frac{1}{v}\frac{\partial(p_i \psi_i)}{\partial t} + \Omega \cdot \nabla(p_i \psi_i) + (\Sigma_{ai} + S_i)(p_i \psi_i) = p_i Q_i +$$
$$+ \left(\frac{p_j \Psi_j}{\Lambda_j} - \frac{p_i \Psi_i}{\Lambda_i}\right) + \left(\frac{p_j \hat{\Psi}_j}{\hat{\lambda}_j} - \frac{p_i \hat{\Psi}_i}{\hat{\lambda}_i}\right), \tag{4.58}$$

where

$$\frac{p_i(r,t)}{\hat{\lambda}_i(r,t)} = \frac{1}{v}\lim_{T\to 0}\left[\frac{1}{T}\langle N_i \rangle\right] \tag{4.59}$$

and

$$\hat{\Psi}_i = \langle \psi \rangle_{i \to j}^{\ddagger}. \tag{4.60}$$

In Eq. (4.59), T is a time interval and N_i is the number of transitions from material i to material $j \neq i$ in T at space point r. In Eq. (4.60), the operator $\langle \cdot \rangle_{i \to j}^{\ddagger}$ is a restricted average, defined to be an ensemble average over realizations that undergo a transition from material i to material j at a given space point r at a time t.
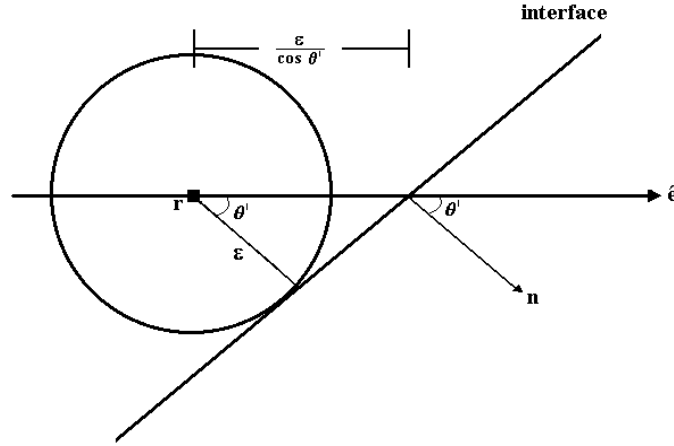
Figure 4.3: Interface intersecting an arbitrary line at an arbitrary angle

Again, a simple closure is obtained by setting $\Psi_i = \hat{\Psi}_i = \psi_i$. Also, we can define a composite coupling coefficient $\tilde{\lambda}_i$ according to

$$\frac{1}{\tilde{\lambda}_i} = \frac{1}{\Lambda_i} + \frac{1}{\hat{\lambda}_i},$$
(4.61)

and applying these arguments in Eq. (4.58), it becomes identical to Eq. (4.53) (with the terms Λ_i replaced by $\tilde{\lambda}_i$).

We remark that the model we have just presented can be also derived through other techniques. In the case of Markovian mixing statistics, one can obtain the same result by using techniques of nuclear reactor noise analysis [67], or by assuming that each particle track is independent of prior tracks [68].

At this point we must turn our attention to the assumption made in Figure 4.2 that the interfaces all intersect an arbitrary line perpendicularly. This assumption does lead to the "classic" Levermore-Pomraning equations, but we get a different result when we relax this unphysical constraint.

Let us examine the case in which interfaces can intersect an arbitrary line at arbitrary angles. In this case, Eq. (4.48) is incorrect. Let us consider an arbitrary line through r pointing in a direction $\hat{e}$, and let the normal n to an arbitrary interface have an angle θ' measured with respect to this line. It can be seen from Figure 4.3 that, if the point r lies within a distance $\dfrac{\varepsilon}{|\hat{e} \cdot \text{n}|}$ of the interface, then the
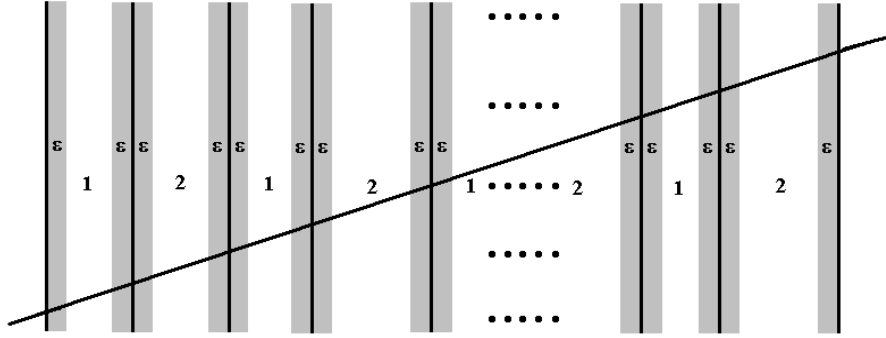
Figure 4.4: Arbitrary line through a slab in a planar geometry system

interface will intersect V. Hence, the intervals previously of width 2ε become wider, and Eq. (4.48) must be written

$$P^* = \left\langle \frac{1}{|\underline{e} \cdot \mathrm{n}|} \right\rangle \left(\frac{4\varepsilon}{\Lambda_1 + \Lambda_2} \right) = \beta \left(\frac{4\varepsilon}{\Lambda_1 + \Lambda_2} \right). \qquad (4.62)$$

It is easy to check that β is equal to unity in the case of one dimensional planar geometries. To do this, let us consider an arbitrary line with direction μ through a slab composed of m chunks of material 1 and m chunks of material 2. We can see from Figure 4.4 that, if we place a sphere of radius ε in this slab, then this sphere will intersect an interface only if its center lies inside the shaded areas. That is, if the center of this sphere is located outside the shaded areas, the sphere will not intersect an interface. The length of the line segments within the shaded areas is $4m\varepsilon/|\mu|$, and the total length of the line is $m(\Lambda_1 + \Lambda_2)/|\mu|$. The ratio of these two quantities is P^*:

$$P^* = \frac{4m\varepsilon/|\mu|}{m(\Lambda_1 + \Lambda_2)/|\mu|} = \frac{4\varepsilon}{(\Lambda_1 + \Lambda_2)}, \qquad (4.63)$$

and therefore we conclude that, in planar geometry systems, $\beta = 1$. However, this is not true for random three dimensional geometries, as we shall see from the next discussion.

Let us consider a large binary system consisting of materials 1 and 2. We assume the chunks of material 1 as being uniform, non-overlapping spheres of radius ρ, suspended in material 2 (the "host" medium). As a technical example, this system is consistent with the geometry of a pebble bed reactor core. We seek
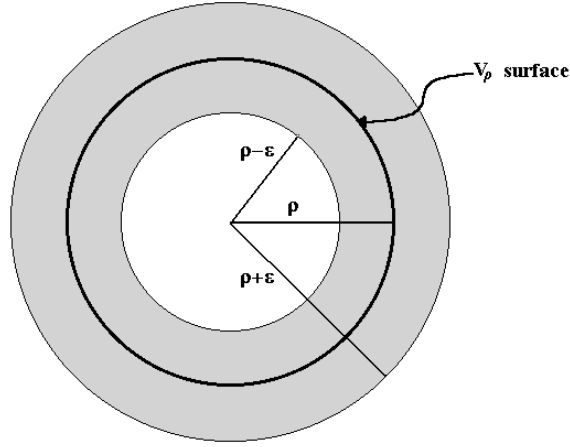
Figure 4.5: Shell associated with a V_ρ sphere

an expression to describe P_ε, the probability that a sphere V_ε of radius ε randomly placed in this system will intersect the surface of a sphere of material 1.

We will denote any sphere of material 1 by V_ρ. The mean chord length across a chunk of material 1 is given by

$$\Lambda_1 = \frac{\text{Volume of the sphere}}{\text{Cross-sectional area of the sphere}} = \frac{\frac{4}{3}\pi\rho^3}{\pi\rho^2} = \frac{4}{3}\rho. \tag{4.64}$$

Bearing in mind that the statistics is assumed to be homogeneous, equation (2.53) holds, and therefore we can calculate Λ_2 by using

$$\frac{\Lambda_1}{\Lambda_2} = \frac{p_1}{p_2} = \frac{p_1}{1 - p_1}, \tag{4.65}$$

which gives us

$$\Lambda_2 = \Lambda_1\left(\frac{1 - p_1}{p_1}\right) = \frac{4}{3}\rho\left(\frac{1 - p_1}{p_1}\right). \tag{4.66}$$

To calculate P_ε, we first assume that the spheres V_ρ are greater than a distance 2ε apart from each other. In this case V_ε cannot intersect the surfaces of two spheres of material 1. In a large volume V of the binary system the number M of spheres V_ρ in V satisfies

$$p_1 = \frac{M}{V}\frac{4}{3}\pi\rho^3 \implies M = V\frac{3p_1}{4\pi\rho^3}. \tag{4.67}$$

The sphere V_ε intersects the surface of a V_ρ only if the center of V_ε lies within a distance ε of the surface of V_ρ. This defines a shell of volume

$$V_{shell} = \frac{4}{3}\pi\left((\rho + \varepsilon)^3 - (\rho - \varepsilon)^3\right) = \frac{4}{3}\pi(6\rho^2\varepsilon + 2\varepsilon^2) = 8\pi\rho^2\varepsilon\left(1 + \frac{\varepsilon^2}{3\rho^2}\right) \tag{4.68}$$
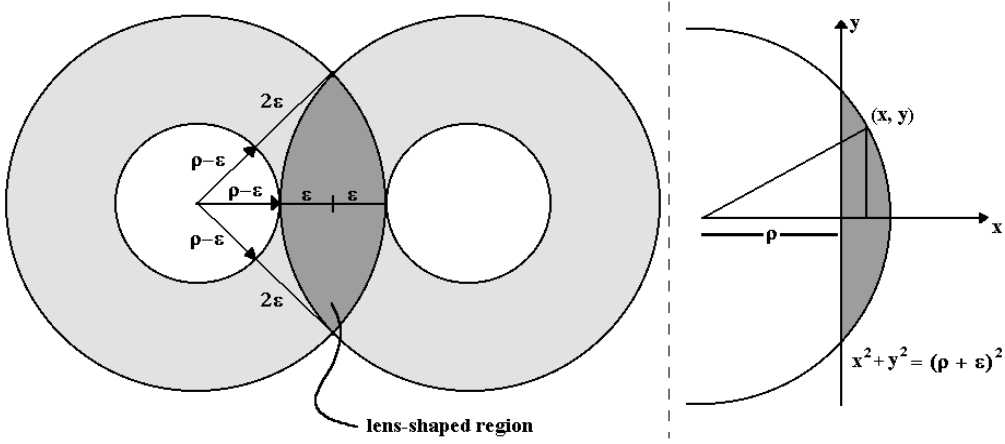
Figure 4.6: Lens-shaped region formed by two overlapping shells

associated with each V_ρ, as can be seen in Figure 4.5. If the center of V_ε lies within any of these disjoint shells, then V_ε intersects the surface of one chunk of material 1. We can now calculate

$$P_\varepsilon = \frac{MV_{shell}}{V} = \frac{1}{V}\left(V\frac{3p_1}{4\pi\rho^3}\right)(8\pi\rho^2\varepsilon)\left(1+\frac{\varepsilon^2}{3\rho^2}\right) = 6\varepsilon\frac{p_1}{\rho}\left(1+\frac{\varepsilon^2}{3\rho^2}\right). \qquad (4.69)$$

However, we have from Eqs. (4.64) and (4.66)

$$\Lambda_1 + \Lambda_2 = \frac{4}{3}\frac{\rho}{p_1} \implies \frac{p_1}{\rho} = \frac{4}{3}\frac{1}{\Lambda_1 + \Lambda_2}, \qquad (4.70)$$

and therefore

$$P_\varepsilon = 6\varepsilon\left(\frac{4}{3}\frac{1}{\Lambda_1 + \Lambda_2}\right)\left(1+\frac{\varepsilon^2}{3\rho^2}\right) = \frac{8\varepsilon}{\Lambda_1 + \Lambda_2}\left(1+\frac{\varepsilon^2}{3\rho^2}\right). \qquad (4.71)$$

This result holds if the chunks of material 1 are greater than 2ε apart from each other. Next, let us assume that the spheres V_ρ can touch each other, and that the average number of spheres V_ρ in direct contact with a specific random V_ρ' is m. When two spheres of material 1 are in contact, a lens-shaped region of overlap between the two shells occurs. The volume of this lens-shaped region (Figure 4.6) is given by

$$V_{lens} = 2\int_\rho^{\rho+\varepsilon} \pi y^2 dx = 2\pi\int_\rho^{\rho+\varepsilon}\left((\rho+\varepsilon)^2 - x^2\right)dx = 2\pi\left(\rho\varepsilon^2 + \frac{2\varepsilon^3}{3}\right)$$
$$= 2\pi\varepsilon^2\left(\rho+\frac{2\varepsilon}{3}\right). \qquad (4.72)$$

Now, we can rewrite Eq. (4.69):

$$P_\varepsilon = \frac{M(V_{shell} - mV_{lens})}{V} = \frac{3p_1}{4\pi\rho^3}\left((8\pi\rho^2\varepsilon)\left(1+\frac{\varepsilon^2}{3\rho^2}\right) - m(2\pi\rho^2)\left(\rho+\frac{2\varepsilon}{3}\right)\right), \qquad (4.73)$$

and using Eq. (4.70) we obtain

$$P_\varepsilon = \frac{8\varepsilon}{\Lambda_1 + \Lambda_2}\big(1 + O(\varepsilon)\big). \tag{4.74}$$

This result holds under all possible circumstances of non-overlapping spheres of radius ρ (material 1) suspended in a host medium (material 2). Equation (4.74) differs from the "classic" Levermore-Pomraning estimate by a factor of 2; that is, the factor β in Eq. (4.62) should be replaced by 2 in this particular system. The main point of this discussion is that Eq. (4.48) is not correct for random three dimensional geometries.

4.2   Physical Interpretation of the Levermore-Pomraning Model

In order to illustrate the physical relevance of the present model, we will present a phenomenological interpretation developed by Sahni [68] and discuss a possible deficiency of the model for isotropic scattering. We will also introduce an idea for a corrected model for isotropic scattering, with a Sahni-like interpretation [20, 24].

Let us assume static (time independent) homogeneous mixing statistics. In this case, the (closed) Levermore-Pomraning equations are given by Eq. (4.53). Now let us define Σ_{li} by

$$\Sigma_{li} = \frac{1}{\Lambda_i}. \tag{4.75}$$

One should be attentive to the fact that Σ_{li}^{-1}, in analogy to Eqs. (2.28-2.29), can be thought of as the mean distance a particle must travel to "leak" out of material i. Hence Eq. (4.53) can be written

$$\frac{1}{v}\frac{\partial(p_i\psi_i)}{\partial t} + \Omega\cdot\nabla(p_i\psi_i) + (\Sigma_{ti}+\Sigma_{li})(p_i\psi_i) = (\Sigma_{si}-S_i)(p_i\psi_i) + p_iQ_i + \Sigma_{lj}(p_j\psi_j). \tag{4.76}$$

Now, suppose that a particle is "born" at a point in material i. We already know that Σ_{si} and Σ_{ai} are the respective probabilities per unit path length that the particle
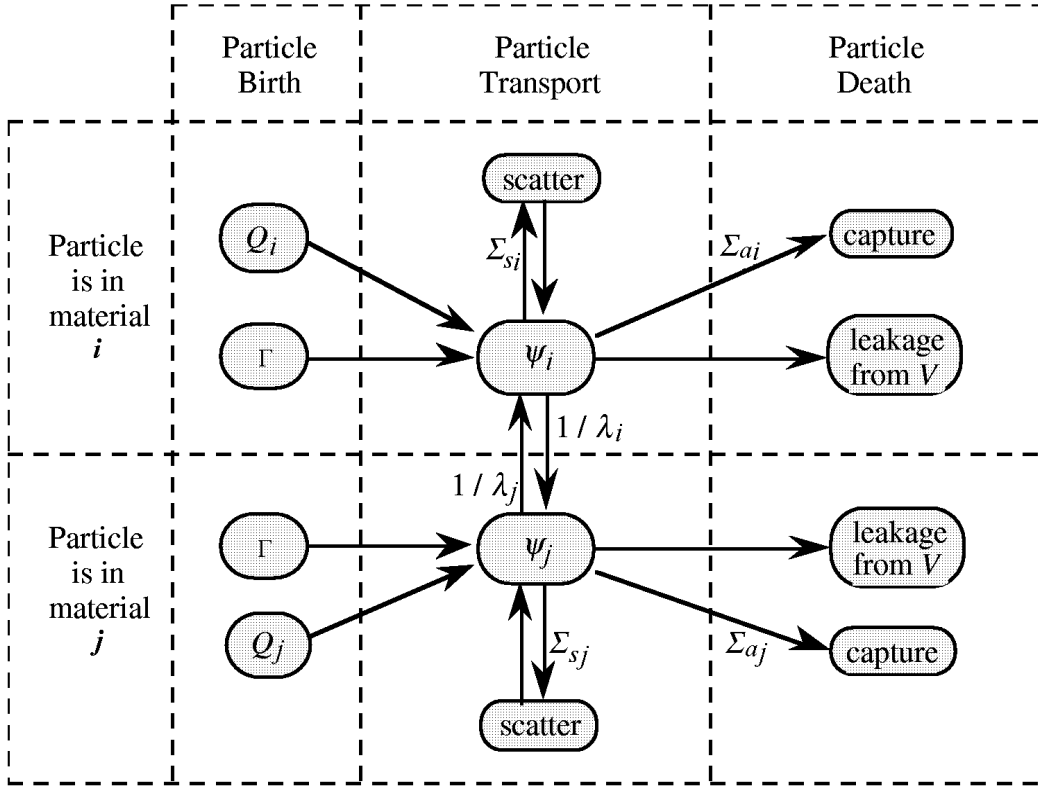
Figure 4.7: Flow diagram for the Levermore-Pomraning equations

will scatter or be absorbed. We then notice that Σ_{li} is the probability per unit path length that the particle will "leak" out of material i into a chunk of material $j \neq i$. Thus, within this chunk of material i, three different "events" may occur regarding this particle. We define the probabilities

$$
\begin{aligned}
p_{si} &= \frac{\Sigma_{si}}{\Sigma_{si} + \Sigma_{ai} + \Sigma_{li}}, \\
p_{ai} &= \frac{\Sigma_{ai}}{\Sigma_{si} + \Sigma_{ai} + \Sigma_{li}}, \\
p_{li} &= \frac{\Sigma_{li}}{\Sigma_{si} + \Sigma_{ai} + \Sigma_{li}},
\end{aligned}
\tag{4.77}
$$

which determine wheter the particle scatters, is absorbed, or leaks into material j. If the particle scatters, then a new direction of flight is selected and the particle continues on its history (in material i). If the particle is absorbed, the particle's history ends. If the particle leaks out of material i, then it is assumed to enter material j with no change of direction.
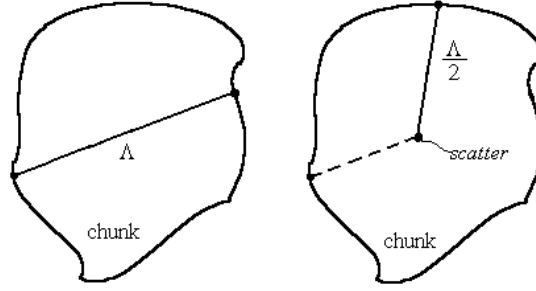
Figure 4.8: Mean distance to exit a chunk

Therefore, in Eq. (4.76) the term $\Sigma_{li}(p_i\psi_i)$ on the left side describes particles that leak out of material i and enter material j, and the term $\Sigma_{lj}(p_j\psi_j)$ on the right side describes particles that leak out of material j and enter material i. Further, one must notice that particles are neither created nor destroyed by "leaking" from one material into another. In this interpretation particles travel a mean distance of Λ_i in material i before passing into material j, and they travel a mean distance of Λ_j in material j before passing into material i.

We present in Figure 4.7 a flow diagram for the Levermore-Pomraning equations, where the processes that particles can experience are shown together with their respective probability of occurrence per unit path length. Sahni's interpretation of this model is quite reasonable from the physical viewpoint. It assures that ψ_i and ψ_j are positive, and that the model cannot produce an unphysical negative mean angular flux. However, a possible flaw in the model can be seen.

The present interpretation assumes that, for all particles, the mean distance to exit a chunk of material i is given by Λ_i. Actually, this is true only for particles that have not yet experienced a collision within the chunk. If a particle scatters isotropically in a chunk with mean chord length given by Λ, then the mean distance to this scattered particle exit this chunk will be given by $\Lambda/2$ (Figure 4.8). That is, scattered particles are twice as likely to leak out of a chunk than unscattered particles.

Following Larsen [20, 24], we define ψ_i^u to be the flux of particles that have leaked into a chunk of material i but have not yet experienced a collision within this chunk, and ψ_i^s to be the flux of particles within a chunk of material i that: (i) have experienced at least one scattering within this chunk; or (ii) have been born from a source inside this chunk. Then we can build an improved system of Levermore-Pomraning equations:

$$\frac{1}{v}\frac{\partial(p_i\psi_i^u)}{\partial t} + \Omega\cdot\nabla(p_i\psi_i^u) + (\Sigma_{ti} + \Sigma_{li})(p_i\psi_i^u) = \Sigma_{lj}(p_j\psi_j^u) + 2\Sigma_{lj}(p_j\psi_j^s), \quad (4.78)$$

$$\frac{1}{v}\frac{\partial(p_i\psi_i^s)}{\partial t} + \Omega\cdot\nabla(p_i\psi_i^s) + (\Sigma_{ti} + 2\Sigma_{li})(p_i\psi_i^s) = p_iQ_i + (\Sigma_{si} - S_i)(p_i\psi_i^s + p_i\psi_i^u). \quad (4.79)$$

This is to say that ψ_i^u describes particles that "see" a mean distance to exit a chunk of material i of Λ_i, and that ψ_i^s describes particles that "see" a mean distance to exit a chunk of material i of $\Lambda_i/2$.

In the absence of scattering and internal sources, one has $\psi_i^s = 0$, and the above equations reduce to the original model. In this case, Eqs. (4.78-4.79) are identical to the Levermore-Pomraning equations and, therefore, are exact. In Figure 4.9 a flow diagram for these equations can be seen.

A quantitative argument to justify this idea is as follows. Suppose that the scalar flux within a chunk of average width Λ ($-\Lambda/2 < x < \Lambda/2$) is well-represented by the two-term power series expansion

$$\phi(x) = \phi + x\phi', \tag{4.80}$$

where ϕ and ϕ' are $O(1)$ constants (the error of this equation is $O(\Lambda^2)$). Then for $\mu > 0$ the mean distance a scattered particle (travelling in direction μ) must travel to exit the chunk is exactly

$$Dist(\mu) = \frac{1}{\mu}\left[\int_{-\Lambda/2}^{\Lambda/2}\left(\frac{\Lambda}{2} - x\right)\left(\frac{\Sigma_s}{2}\phi(x)\right)dx\right]\left[\int_{-\Lambda/2}^{\Lambda/2}\left(\frac{\Sigma_s}{2}\phi(x)\right)dx\right]^{-1}, \quad 0 < \mu \leq 1. \tag{4.81}$$

Introducing Eq. (4.80) into Eq. (4.81) and evaluating the integrals, we obtain

$$Dist(\mu) = \frac{1}{\mu}\left(\frac{\Lambda}{2} - \frac{\phi'}{\phi}\frac{\Lambda^2}{12}\right) + O(\Lambda^3), \quad 0 < \mu \leq 1. \tag{4.82}$$
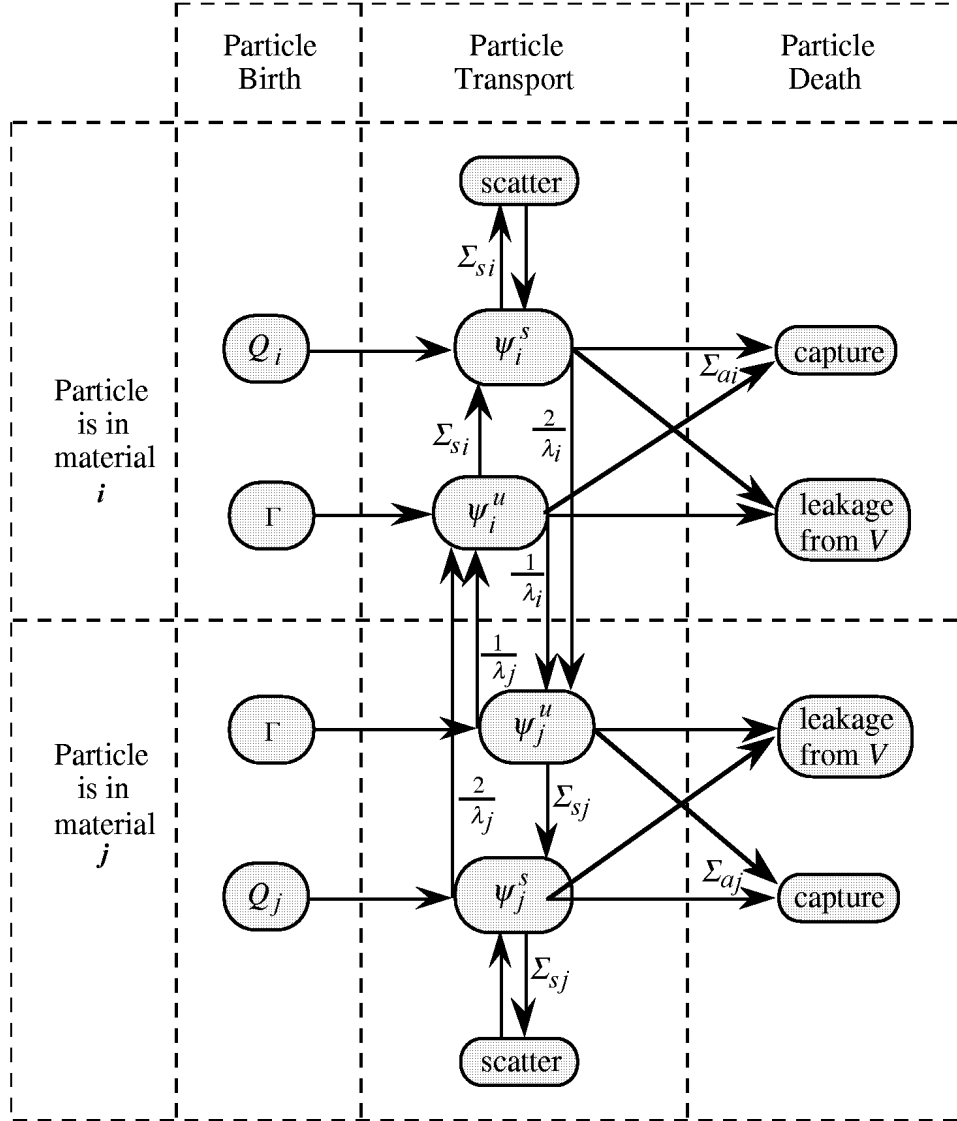
Figure 4.9: Flow diagram for the revised equations

The Levermore-Pomraning method predicts, for $0 < \mu \leq 1$,

$$Dist_{LP}(\mu) \approx \frac{\Lambda}{\mu}, \tag{4.83}$$

and comparing Eq. (4.83) with Eq. (4.82) we see that the error in Eq. (4.83) is $O(\Lambda)$. The revised method predicts

$$Dist_*(\mu) \approx \frac{\Lambda}{2\mu}, \tag{4.84}$$

and the error in this is $O(\Lambda^2 \phi'/\phi)$. This error is $O(\Lambda^2)$ provided that $\phi'/\phi = O(1)$, which is smaller than the Levermore-Pomraning error when Λ is small. Also, if $\phi'/\phi = \varepsilon$ is small, then this error can be small even if $\Lambda = O(1)$.

In the future we intend to work carefully in the development of this idea, in order to obtain a theoretical procedure that would confirm the hypothesized accuracy of the revised model over the Levermore-Pomraning method. At the present moment we are working on numerical experiments to determine how much effect these corrections will have.

4.3   Complementary Results

Thus far, we have discussed the derivation and physical interpretation of the Lever-more-Pomraning method. We have also mentioned that Eq. (4.53) is exact in the time independent, purely absorbing case. There is, in fact, an exact formalism for treating a restricted class of stochastic problems with the scattering interaction included [27, 45, 46, 47, 88]. The key to this analysis is the introduction of an optical depth variable, defined in terms of the total cross section. This formalism treats a class of planar geometry problems for which the total cross section Σ_t, the scattering kernel Σ_s and the source Q all obey the same statistics, in the sense that the functions Σ_s/Σ_t and Q/Σ_t are nonstochastic.

In this section we briefly discuss some developments that have arised during the last two decades. In particular, we show that the Atomic Mix model can be deduced from the Levermore-Pomraning equations through the use of asymptotic limits. For the rest of this section we will assume the mixing to be given by homogeneous Markov statistics.

4.3.1   Asymptotic Limits of the Levermore-Pomraning Model

Let us consider Eq. (4.53). It is easy to see that if both Λ_i increase without bound, then the interface terms vanish, and the equations for ψ_1 and ψ_2 decouple. Also, if one of the Λ_i vanishes, this equation is shown to be exact [28]. This follows from the fact that if Λ_1 is vanishingly small and Λ_2 is nonvanishing,

then $p_1 = 0$ and $p_2 = 1$. In this case, $\langle\psi\rangle = \psi_2$, and the addition of Eq. (4.53) for $i = 1$ and $i = 2$ gives the nonstochastic transport equation for material 2.

Now, we change dependent variables in Eq. (4.53) from ψ_1 and ψ_2 to $\langle\psi\rangle$ and ϑ [25, 43, 44, 62, 64] according to

$$\langle\psi\rangle = p_1\psi_1 + p_2\psi_2, \tag{4.85}$$

$$\vartheta = \sqrt{p_1 p_2}\,(\psi_1 - \psi_2). \tag{4.86}$$

The inverse of this transformation is given by

$$\psi_1 = \langle\psi\rangle + \left(\frac{p_2}{p_1}\right)^{1/2}\vartheta, \tag{4.87}$$

$$\psi_2 = \langle\psi\rangle - \left(\frac{p_1}{p_2}\right)^{1/2}\vartheta, \tag{4.88}$$

and Eq. (4.53) can be written in an algebraically different, but equivalent, form [43, 62]:

$$\left(\frac{1}{v}\frac{\partial}{\partial t}+\Omega\cdot\nabla\right)\langle\psi\rangle + \langle\Sigma_t\rangle\langle\psi\rangle + \nu\vartheta = \langle Q\rangle +$$
$$+ \int_0^\infty \int_{4\pi} \langle\Sigma_s(r, E' \to E, \Omega' \to \Omega, t)\rangle\langle\psi(r, E', \Omega', t)\rangle d\Omega' dE' + \tag{4.89}$$
$$+ \int_0^\infty \int_{4\pi} \langle\nu_s(r, E' \to E, \Omega' \to \Omega, t)\vartheta(r, E', \Omega', t)d\Omega' dE',$$

$$\left(\frac{1}{v}\frac{\partial}{\partial t}+\Omega\cdot\nabla\right)\vartheta + \nu\langle\psi\rangle + \hat\Sigma_t\vartheta = U +$$
$$+ \int_0^\infty \int_{4\pi} \nu_s(r, E' \to E, \Omega' \to \Omega, t)\langle\psi(r, E', \Omega', t)\rangle d\Omega' dE' + \tag{4.90}$$
$$+ \int_0^\infty \int_{4\pi} \langle\hat\Sigma_s(r, E' \to E, \Omega' \to \Omega, t)\vartheta(r, E', \Omega', t)d\Omega' dE'.$$

Here, $\langle\Sigma_t\rangle$, $\langle\Sigma_s\rangle$ and $\langle Q\rangle$ are defined in analogy with the general random variable W in Eq. (3.11); and

$$U = \sqrt{p_1 p_2}\,(Q_1 - Q_2), \tag{4.91}$$

$$\nu = \sqrt{p_1 p_2}\,(\Sigma_{t1} - \Sigma_{t2}), \tag{4.92}$$

$$\nu_s = \sqrt{p_1 p_2}\,(\Sigma_{s1} - \Sigma_{s2}), \tag{4.93}$$

$$\hat\Sigma_s = p_2\Sigma_{s1} + p_1\Sigma_{s2}, \tag{4.94}$$

$$\hat{\Sigma}_t = p_2 \Sigma_{t1} + p_1 \Sigma_{t2} + \lambda_c^{-1}, \tag{4.95}$$

where λ_c is the correlation length defined by Eq. (2.61). For simplicity, we rewrite Eqs. (4.89-4.90) assuming that the scattering process is both coherent and isotropic:

$$\left(\frac{1}{v}\frac{\partial}{\partial t} + \Omega \cdot \nabla\right) \begin{bmatrix} \langle \psi \rangle \\ \vartheta \end{bmatrix} + \begin{bmatrix} \langle \Sigma_t \rangle & \nu \\ \nu & \hat{\Sigma}_t \end{bmatrix} \begin{bmatrix} \langle \psi \rangle \\ \vartheta \end{bmatrix} = \frac{1}{4\pi} \begin{bmatrix} \langle \Sigma_s \rangle & \nu_s \\ \nu_s & \hat{\Sigma}_s \end{bmatrix} \begin{bmatrix} \langle \phi \rangle \\ \zeta \end{bmatrix} + \begin{bmatrix} \langle Q \rangle \\ U \end{bmatrix}, \tag{4.96}$$

where

$$\langle \phi \rangle = \int_{4\pi} \langle \psi \rangle d\Omega \quad \text{and} \quad \zeta = \int_{4\pi} \vartheta d\Omega. \tag{4.97}$$

Now we consider the case when the average chord length through the chunks of material i is small when compared to the particle mean free path in that material. It can be seen from Eq. (2.61) that small chord lengths imply a small correlation length. In this case, we have

$$\lambda_c \Sigma_{ti} \ll 1, \tag{4.98}$$

and looking to Eqs. (4.92-4.95), we notice that $\hat{\Sigma}_t \gg \langle \Sigma_t \rangle$, $\langle \Sigma_s \rangle$, $\hat{\Sigma}_s$, ν, ν_s. Thus, we introduce a smallness parameter ε into Eq. (4.96) by replacing $\hat{\Sigma}_t$ with $\hat{\Sigma}_t/\varepsilon$. We seek a solution for this equation as a power series in ε:

$$\langle \psi \rangle = \sum_{k=0} \varepsilon^k \langle \psi^{(k)} \rangle, \tag{4.99}$$

$$\vartheta = \sum_{k=0} \varepsilon^k \vartheta^{(k)}, \tag{4.100}$$

where the power (k) in $\langle \psi^{(k)} \rangle$ and $\vartheta^{(k)}$ is just an index denoting the kth term in the asymptotic expansion. Inserting Eqs. (4.99-4.100) into Eq. (4.96), with $\hat{\Sigma}_t$ replaced by $\hat{\Sigma}_t/\varepsilon$, and equating coefficients of powers of ε, we find for $O(\varepsilon^{-1})$ that $\vartheta^{(0)} = 0$, and for $O(1)$ that

$$\left(\frac{1}{v}\frac{\partial}{\partial t} + \Omega \cdot \nabla\right) \langle \psi^{(0)} \rangle + \langle \Sigma_t \rangle \langle \psi^{(0)} \rangle + \nu \vartheta^{(0)} = \frac{1}{4\pi} \left(\langle \Sigma_s \rangle \langle \phi^{(0)} \rangle + \nu_s \zeta^{(0)} \right) + \langle Q \rangle, \tag{4.101}$$

where

$$\langle \phi^{(0)} \rangle = \int_{4\pi} \langle \psi^{(0)} \rangle d\Omega \quad \text{and} \quad \zeta^{(0)} = \int_{4\pi} \vartheta^{(0)} d\Omega. \tag{4.102}$$

Since $\vartheta^{(0)} = 0$, we have $\zeta^{(0)} = 0$, and recalling that $\langle\psi\rangle = \langle\psi^{(0)}\rangle + O(\varepsilon)$, Eq. (4.101) becomes

$$\left(\frac{1}{v}\frac{\partial}{\partial t} + \Omega \cdot \nabla\right)\langle\psi\rangle + \langle\Sigma_t\rangle\langle\psi\rangle = \frac{\langle\Sigma_s\rangle\langle\phi\rangle}{4\pi} + \langle Q\rangle + O(\varepsilon). \qquad (4.103)$$

One must notice that Eq. (4.103) is just the atomic mix description of Eq. (4.53) in the case of coherent and isotropic scattering, where ε is a measure of the smallness of the correlation length compared with the smallest particle mean free path in the two materials 1 and 2. We conclude that this is a valid model when the assumptions that lead to Eq. (4.98) are verified.

Another important asymptotic limit is that corresponding to a mixing of a small amount of the large cross section material i with a large amount of the small cross section material j [28]. In this case we find (for coherent and isotropic scattering)

$$\frac{1}{v}\frac{\partial\langle\psi\rangle}{\partial t} + \Omega \cdot \nabla\langle\psi\rangle + \Sigma_{t,eff}\langle\psi\rangle = \frac{\Sigma_{s,eff}\langle\phi\rangle}{4\pi} + Q_{eff}, \qquad (4.104)$$

where $\Sigma_{t,eff}$, $\Sigma_{s,eff}$ and Q_{eff} are nonstochastic "effective" quantities, given by

$$\Sigma_{t,eff} = \langle\Sigma_t\rangle - \frac{\nu^2}{\hat{\Sigma}_t}, \qquad (4.105)$$

$$\Sigma_{s,eff} = \langle\Sigma_s\rangle - \frac{\nu^2}{\hat{\Sigma}_t} - \frac{(\nu - \nu_s)^2}{\hat{\Sigma}_t - \hat{\Sigma}_s}, \qquad (4.106)$$

$$Q_{eff} = \langle Q\rangle - \left(\frac{\hat{\Sigma}_t(\nu - \nu_s) + 2\nu\hat{\Sigma}_s}{\hat{\Sigma}_t(\hat{\Sigma}_t - \hat{\Sigma}_s)}\right)U. \qquad (4.107)$$

Again, $\langle\Sigma_t\rangle$, $\langle\Sigma_s\rangle$ and $\langle Q\rangle$ are defined in analogy with the general random variable W in Eq. (3.11), and U, ν, ν_s, $\hat{\Sigma}_s$ and $\hat{\Sigma}_t$ are given by Eqs. (4.91-4.95). By using these definitions in Eqs. (4.105-4.107), an algebraic calculation establishes that $\Sigma_{t,eff}$, $\Sigma_{s,eff}$ and Q_{eff} can never be negative for any nonnegative parameters p_i, Σ_{ti}, Σ_{si}, Q_i and λ_c.

One should notice that Eq. (4.104) contains atomic mix as a limiting case. This follows from the fact that when $\lambda_c \to 0$, $\hat{\Sigma}_t \to \infty$, and therefore the quantities $\Sigma_{t,eff}$, $\Sigma_{s,eff}$ and Q_{eff} respectively converge to $\langle\Sigma_t\rangle$, $\langle\Sigma_s\rangle$ and $\langle Q\rangle$. Work involving effective parameters as numerical calculations [30], and generalizations for

arbitrary number of components in the mixture [29] and anisotropic scattering [59] are available in the literature. Further, the development of a first order correction in λ_c has also been reported [58, 60, 83].

Besides these cases, asymptotic limits leading to a diffusive description of stochastic particle transport were obtained away from the atomic mix optics, and were generalized to a mixture consisting of an arbitrary number of components [31, 70]. Asymptotic diffusive descriptions have also been obtained in the presence of anisotropic statistics [54]. Finally, there are still other results regarding diffusive descriptions that did not arise from asymptotic analysis, as flux-limited diffusion theories [56, 69] and spherical harmonic approximations [82].

We finish this section with an important remark. Although there is a considerable literature applying a great deal of analysis to the Levermore-Pomraning equations, there seems to be very few papers where the same analysis is applied to the underlying physically correct Boltzmann equation. The analysis leading to Eqs. (4.104-4.107) is an example of this; to our knowledge, it is still an open question whether this result is physically correct. Indeed, there is a large number of such problems in which a rigorous mathematical analysis is required in order to prove (or disprove) the physical correctness of the results obtained. We hope to contemplate this subject in the future.

4.3.2   Alternate Closures and Higher-Order Models

In section 4.1.2 we presented an upwind strategy to close Eq. (4.51) consisting of the simple replacement of Ψ_i by ψ_i. Here, we briefly discuss alternate closures for this equation, as well as the existence of higher-order models for problems with scattering.

Within the context of monoenergetic particle transport with isotropic scattering, we can mention two alternate closures [80] for the Levermore-Pomraning

model, which have been suggested to improve the simpler closure presented early:

$$\Psi_i = \frac{\sqrt{\langle\Sigma_a\rangle\langle\Sigma_t\rangle}\left[\langle\Sigma_a\rangle(\Sigma_{t1}-\Sigma_{t2})^2 + \langle\Sigma_t\rangle(\Sigma_{a1}-\Sigma_{a2})^2\right]}{\left[\langle\Sigma_a\rangle(\Sigma_{t1}-\Sigma_{t2})\right]^2 + \left[\langle\Sigma_t\rangle(\Sigma_{a1}-\Sigma_{a2})\right]^2}\psi_i, \tag{4.108}$$

where $\langle\Sigma_a\rangle = \langle\Sigma_t\rangle - \langle\Sigma_s\rangle$; and

$$\Psi_i = \left(\psi_i - \frac{\langle\Sigma_s\rangle}{\langle\Sigma_t\rangle}\frac{\phi_i}{4\pi}\right)\left(\frac{\langle\Sigma_t\rangle}{\langle\Sigma_t\rangle - \langle\Sigma_s\rangle}\right)^{1/2}. \tag{4.109}$$

It is easy to see that both closures reduce to $\Psi_i = \psi_i$ in the absence of scattering, as one should expect. The qualitative difference between these two closures is that Eq. (4.109) mixes the different directions through ϕ_i, the scalar flux term. Based upon representative numerical calculations [80], both closures are shown to be, in general, not inferior to the classic upwind closure, and in some cases they are even better.

Beyond the task of finding a closure for Eq. (4.51), one may expect to achieve better accuracy by going to higher order. By higher-order models we mean that a stochastic balance equation for Ψ_i is derived, containing still more restricted statistical ensemble averages. Then a closure is introduced for these terms, and Eq. (4.51) is maintained in its exact form. Here we restrict ourselves to simply present an example of this kind of model, without details, in order to illustrate the idea of the method.

Consider source-free monoenergetic particle transport with isotropic scattering in planar geometry. In this case Eq. (4.51) is written

$$\frac{1}{v}\frac{\partial(p_i\psi_i)}{\partial t} + \mu\frac{\partial(p_i\psi_i)}{\partial z} + \Sigma_{ti}(p_i\psi_i) = \frac{\Sigma_{si}(p_i\phi_i)}{4\pi} + \frac{p_j\Psi_j}{\Lambda_j} - \frac{p_i\Psi_i}{\Lambda_i}. \tag{4.110}$$

An equation for Ψ_i is then derived, by introducing a closure for the higher statistical averages that occur in the exact balance equation [51, 55]:

$$\frac{1}{v}\frac{\partial(p_i\Psi_i)}{\partial t} + \mu\frac{\partial(p_i\Psi_i)}{\partial z} + \Sigma_{ti}(p_i\Psi_i) = \frac{\Sigma_{si}(p_iU_i)}{4\pi} + \frac{p_j\Psi_j}{\Lambda_j} - \frac{p_i\Psi_i}{\Lambda_i}, \tag{4.111}$$

where U_i is a collision term given by

$$\frac{U_i}{2\pi} = \begin{cases} \int_{-1}^0 \Psi_j(\mu')d\mu' + \int_0^1 \Psi_i(\mu')d\mu' & \mu > 0 \\ \int_{-1}^0 \Psi_i(\mu')d\mu' + \int_0^1 \Psi_j(\mu')d\mu' & \mu < 0 \end{cases}. \tag{4.112}$$

This model is known as the interface model. One should notice that, since a closure is required to obtain Eq. (4.111), this equation is only an approximate description for Ψ_i, and therefore this model describes $\langle\psi\rangle = p_1\psi_1 + p_2\psi_2$ also as an approximation. However, in the case of purely absorbing systems, the interface model clearly imply the exact expression $\Psi_i = \psi_i$, as we should expect.

This model, which is reasonably accurate for purely scattering problems, was later modified by including an interpolation between its closure and the classic closure, which is exact for purely absorbing problems. Equation (4.110) is then written as [81]

$$\frac{1}{v}\frac{\partial(p_i\psi_i)}{\partial t} + \mu\frac{\partial(p_i\psi_i)}{\partial z} + \Sigma_{ti}(p_i\psi_i) = \frac{\Sigma_{si}(p_i\phi_i)}{4\pi} + \frac{p_j(a\psi_j + b\Psi_j)}{\Lambda_j} - \frac{p_i(a\psi_i + b\Psi_i)}{\Lambda_i},$$
(4.113)

where Ψ_i satisfies Eq. (4.111) and

$$a = \left(\frac{\langle\Sigma_a\rangle}{\langle\Sigma_t\rangle}\right)^{1/2},$$

$$b = \frac{\langle\Sigma_a\rangle\langle\Sigma_s\rangle(\Sigma_{t1} - \Sigma_{t2})^2}{\langle\Sigma_t\rangle\left[\langle\Sigma_a\rangle(\Sigma_{t1} - \Sigma_{t2})^2 + \langle\Sigma_t\rangle(\Sigma_{a1} - \Sigma_{a2})^2\right]}.$$
(4.114)

The classic closure is clearly recovered for purely absorbing problems, since Eq. (4.114) in this case yield $a = 1$ and $b = 0$. Similarly, with $\Sigma_{ai} = 0$, Eq. (4.114) imply $a = 0$ and $b = 1$, and the interface model is characterized. Also, if $\Sigma_{t1} = \Sigma_{t2}$, then $b = 0$ and the present model reduces to the model given by Eq. (4.108).

5   NUMERICAL RESULTS

In this chapter we present numerical results for time independent transport problems in planar geometry. The medium is assumed to be composed of two randomly mixed materials, and the statistics of the mixing is taken as a homogeneous Markov process. In this case, assuming isotropic and coherent scattering as well as isotropic internal sources, Eq. (2.42) is written

$$\mu\frac{\partial\psi}{\partial z}(z,\mu) + \Sigma_t(z)\psi(z,\mu) = \frac{\Sigma_s(z)}{2}\int_{-1}^{1}\psi(z,\mu')d\mu' + \frac{Q(z)}{2}, \qquad (5.1)$$

where μ is the cosine of the angle between the z-axis and the particle's direction of travel. We take Eq. (5.1) to hold on the interval $0 \leq z \leq Z$, and we define the isotropic boundary conditions

$$\begin{cases} \psi(0,\mu) = \Gamma_0, \ \ \mu > 0 \\ \psi(Z,\mu) = \Gamma_Z, \ \ \mu < 0 \end{cases}, \qquad (5.2)$$

where Γ_0 and Γ_Z are constants.

In order to well-represent this problem, the atomic mix equation (3.8) is written

$$\mu\frac{\partial\langle\psi\rangle}{\partial z} + \langle\Sigma_t\rangle\langle\psi\rangle = \frac{\langle\Sigma_s\rangle}{2}\int_{-1}^{1}\langle\psi(z,\mu')\rangle d\mu' + \frac{\langle Q\rangle}{2}, \qquad (5.3)$$

and its boundary conditions are given by

$$\begin{cases} \langle\psi(0,\mu)\rangle = \Gamma_0, \ \ \mu > 0 \\ \langle\psi(Z,\mu)\rangle = \Gamma_Z, \ \ \mu < 0 \end{cases}. \qquad (5.4)$$

Also, the Levermore-Pomraning equations (4.53) are written

$$\mu\frac{\partial(p_i\psi_i)}{\partial z} + \Sigma_{ti}(p_i\psi_i) = \frac{\Sigma_{si}}{2}\int_{-1}^{1}p_i\psi_i(z,\mu')d\mu' + |\mu|\left(\frac{p_j\psi_j}{\Lambda_j} - \frac{p_i\psi_i}{\Lambda_i}\right) + \frac{p_iQ_i}{2}, \quad (5.5)$$

with the boundary conditions:

$$\begin{cases} \psi_i(0,\mu) = \Gamma_0, \ \ \mu > 0 \\ \psi_i(Z,\mu) = \Gamma_Z, \ \ \mu < 0 \end{cases}. \qquad (5.6)$$
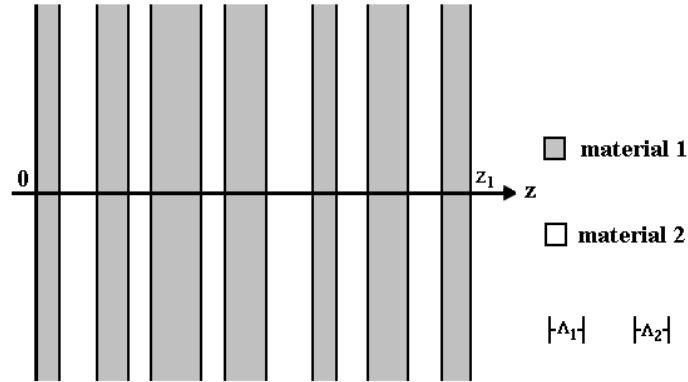
Figure 5.1: Binary planar system

At this point we must explain the term $|\mu|$ multiplying the gain-loss term between the parenthesis at the right hand side of Eq. (5.5). If the mean slab thickness of material i is Λ_i, then the mean chord length seen by a particle traveling at an angle characterized by its cosine μ is $\Lambda_i/|\mu|$. That is, the mean chord length through material i is angularly dependent in planar geometry systems.

Next we will discuss the procedure used to obtain the benchmark results, as well as the atomic mix and Levermore-Pomraning predictions.

5.1   Numerical Procedure

Let us consider time independent stochastic transport (including scattering) in a layered planar geometry under the assumption of homogeneous Markov mixing statistics for the two components of the random medium. The system is taken to be statistically composed of alternating slabs of two materials (Figure 5.1), such that each material has spatially independent cross sections Σ_t and Σ_s, and independent internal sources Q. We already know from the previous discussion (section 2.3) that, if the statistics of this situation is assumed to be a homogeneous Markov process, then the thickness of each slab of material i is chosen at random from an

exponential distribution given by Eq. (2.56), reproduced here for convenience:

$$\eta_i(\xi) = \Lambda_i^{-1} e^{-\xi/\Lambda_i}. \tag{5.7}$$

We remind the reader that in this equation $\eta_i(\xi)d\xi$ is the probability of a segment of material i having a length lying between ξ and $\xi + d\xi$, and Λ_i is the mean slab thickness of material i.

At any point in this system, the probability p_i of finding material i is given by Eq. (2.53). Aiming at the attainment of ensemble-averaged results for the scalar flux $\phi(z)$, we have first generated a physical realization of the statistics using a Monte Carlo procedure, and for this realization we have solved the corresponding transport problem using the LTS$_N$ formulation for a multi-region slab [75].

To obtain a physical realization we first choose the material present at $z = 0$ statistically according to the probabilities p_i. Then we sample from Eq. (5.7) for the value of i so determined to establish the width ξ of the first segment of this material, with its left-hand boundary at $z = 0$. We next sample from Eq. (5.7) with the other material index to determine the width ξ of the next segment. We then sample from Eq. (5.7) with the original index i to determine the width ξ of the third segment. We continue this process until the entire interval $0 \leq z \leq Z$ is populated with alternating segments of the two materials.

Repeating this process for a large number of physical realizations, ensemble-averaged results for the scalar flux $\phi(z)$ follow from simple numerical averages:

$$\langle \phi(z) \rangle = \frac{1}{K} \sum_{k=1}^{K} \phi_k(z), \tag{5.8}$$

where the index k denotes a particular realization of the statistics, and K represents the number of realizations computed. We have also calculated the standard deviation $\sigma\big(\phi(z)\big)$ of these results according to

$$\sigma\big(\phi(z)\big) = \left| \langle \phi(z) \rangle^2 - \frac{1}{K} \sum_{k=1}^{K} \phi_k^2(z) \right|^{1/2}, \tag{5.9}$$

which gives an indication of the spread of the solutions about the means, and allows us to use the results of the Central Limit Theorem [35].

The Central Limit Theorem is a fundamental result within the Stochastic Processes Theory. Basically, it states that if a random variable can be represented by the sum of any K independent random variables, provided that the contribution of each one of these variables to the sum is small, then for K large enough the distribution of this sum will be approximately the normal distribution. We present a simple version of this theorem [35]:

Theorem 5.1.1. *Let $X_1, X_2, ..., X_K$ be K independent random variables with the same distribution. Let $E(X_i)$ and $V(X_i)$ be respectively the expected value and the variance of these variables, and $X = \sum_{i=1}^{K} X_i$. Then $E(X) = KE(X_i)$ and $V(X) = KV(X_i)$, and for K large enough the distribution of*

$$T_K = \frac{X - KE(X_i)}{V(X_i)\sqrt{K}} \tag{5.10}$$

will be approximately the N(0,1) distribution. That is to say that

$$\lim_{K \to \infty} P(T_K \leq t) = \frac{1}{\sqrt{2\pi}} \int_{-\infty}^{t} e^{-x^2/2} dx, \tag{5.11}$$

the N(0,1) distribution function.

In particular, Theorem (5.1.1) states that, for K large enough, the arithmetic mean $\frac{1}{K}\sum_{i=1}^{K} X_i$ of K realizations of the same random variable has (approximately) a normal distribution.

Now, if we call $\langle \phi(z) \rangle$ the "real" ensemble-averaged scalar flux, $\langle \phi_K(z) \rangle$ the "sample" (after K realizations) ensemble-averaged scalar flux, and $\sigma_K = \sigma_K(\phi(z))$ the "sample" standard deviation, then we know from the theorem above and from the properties of the normal distribution that

$$\left| \langle \phi_K(z) \rangle - \langle \phi(z) \rangle \right| < \frac{\sigma_K}{\sqrt{K}}, \quad \text{with probability } (\approx) \ 0.68, \tag{5.12}$$

$$\left| \langle \phi_K(z) \rangle - \langle \phi(z) \rangle \right| < \frac{2\sigma_K}{\sqrt{K}}, \quad \text{with probability } (\approx) \ 0.95, \tag{5.13}$$

$$\left|\langle\phi_K(z)\rangle - \langle\phi(z)\rangle\right| < \frac{3\sigma_K}{\sqrt{K}}, \text{ with probability } (\approx) \ 0.99. \qquad (5.14)$$

Let us choose Eq. (5.13). Dividing this equation by $\langle\phi_K(z)\rangle$ we get

$$\left|1 - \frac{\langle\phi(z)\rangle}{\langle\phi_K(z)\rangle}\right| < \frac{2\sigma_K}{\langle\phi_K(z)\rangle\sqrt{K}}. \qquad (5.15)$$

The left side of this inequality is the relative error. The benchmark results for the scalar flux were obtained for 50 points of z within the interval $[0, 10]$, in order to plot its behaviour. The number of realizations K was chosen for each problem in such way that, for each one of these 50 points,

$$\frac{2\sigma_K}{\langle\phi_K(z)\rangle\sqrt{K}} < 0.01. \qquad (5.16)$$

That is, the statistical relative error in the benchmark results is less than 1% with 95% confidence, for all simulations performed. This procedure consumed a large computation time for those problems where the variation was not small, due to the fact that we need $K > 40,000 \dfrac{\sigma_K^2}{\langle\phi_K(z)\rangle^2}$ to achieve this relative error of 1%. We underline the power of the LTS$_N$ method in performing these benchmark calculations, since there were cases where the number of physical realizations was much larger than 1,000,000.

The atomic mix and Levermore-Pomraning predictions were also obtained through the use of the LTS$_N$ method. Each realization of the benchmark simulations, as well as the atomic mix and Levermore-Pomraning predictions, was performed using an 8-point Gauss-Legendre quadrature set in the discrete ordinates angular approximation ($N = 8$). The benchmark code run time varied between one minute for the less expensive problems (Λ_i large, K small) to more than two days for the most expensive problems (Λ_i small, K large). For comparison, both the atomic mix and Levermore-Pomraning codes finished in approximately one second for all problems. All numerical calculations were done on a Pentium III 1.0 GHz. Further, the codes reproduced very accurately the results for the mean presented in [1] and [12], as well as the standard deviations in the benchmark case.
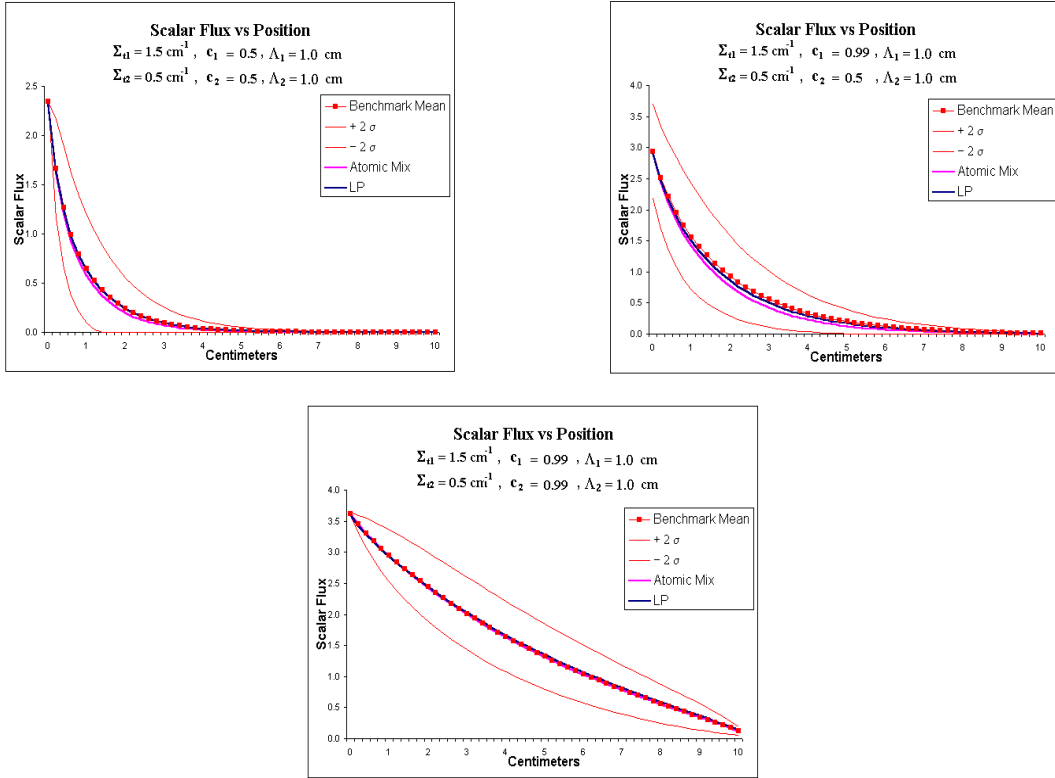
Figure 5.2: Models approximations to a benchmark ensemble-averaged scalar flux - Set 1

In section 5.2 we present numerical results for the Reflection/Transmission problem without internal sources. Simulations for problems with internal sources will be presented in section 5.3.

5.2 The Reflection/Transmission Problem

Let us consider Eq. (5.1) without internal sources,

$$\mu\frac{\partial\psi(z,\mu)}{\partial z} + \Sigma_t(z)\psi(z,\mu) = \frac{\Sigma_s(z)}{2}\int_{-1}^{1}\psi(z,\mu')d\mu'. \qquad (5.17)$$

Also, we consider an isotropic intensity normalized to a unit incoming flux incident upon the planar system at $z = 0$; and no intensity incident upon the system at $z = Z$. This corresponds to the boundary conditions

$$\left\{ \begin{array}{ll} \psi(0,\mu) = 2, & \mu > 0 \\ \psi(Z,\mu) = 0, & \mu < 0 \end{array} \right. . \qquad (5.18)$$

Table 5.1: Set 1 - Parameters Simulated for the Reflection/Transmission Problems

$\Sigma_{t1} = 1.5$ cm^{-1}, $\quad \Sigma_{s1} = c_1\Sigma_{t1}$, $\quad \Lambda_1 = 0.125, 0.5, 1, 2, 8$ cm $\Sigma_{t2} = 0.5$ cm^{-1}, $\quad \Sigma_{s2} = c_2\Sigma_{t2}$, $\quad \Lambda_2 = \Lambda_1/2, \Lambda_1, 2\Lambda_1$ cm						
$Z = 10$ cm	Set 1.1	Set 1.2	Set 1.3	Set 1.4	Set 1.5	Set 1.6
c_1	0.99	0.99	0.99	0.5	0.5	0.0
c_2	0.99	0.5	0.0	0.5	0.99	0.99
Number of Cases	15	15	15	15	15	15

According to the previous discussion, we computed the ensemble-averaged scalar flux for the system as well as the probabilities of reflection R and transmission T as given by

$$R = \int_0^1 \mu\psi(0, -\mu)d\mu, \quad T = \int_0^1 \mu\psi(Z, \mu)d\mu. \tag{5.19}$$

The probability of absorption A follows from particle conservation, such that $A = 1 - R - T$.

There are seven variable parameters that can be varied when considering this particular problem, namely: the system length (Z), the mean chord length in each material (Λ_i), the total cross section in each material (Σ_{ti}) and the single scatter albedo in each material ($c_i = \Sigma_{si}/\Sigma_{ti}$). Since the main goal of these simulations is to compare and contrast the accuracy of the atomic mix and Levermore-Pomraning models, the set of parameters was chosen in order to facilitate the achievement of this objective.

The Reflection/Transmission problem is the subject of several papers dealing with benchmark results and approximations; however, to our knowledge, a comparison of atomic mix, Levermore-Pomraning, and benchmark calculations is treated in only two of these papers [12, 90]. In particular, Davis, Palmer and Larsen [12] provide an interesting and elucidating examination of this problem for "Solid-Void" mixtures. By "Solid-Void" we mean that one of the materials within the system is a void ($\Sigma_t = \Sigma_s = 0$). In order to provide a new contribution to the literature, we chose not to work with mixtures containing a void material.
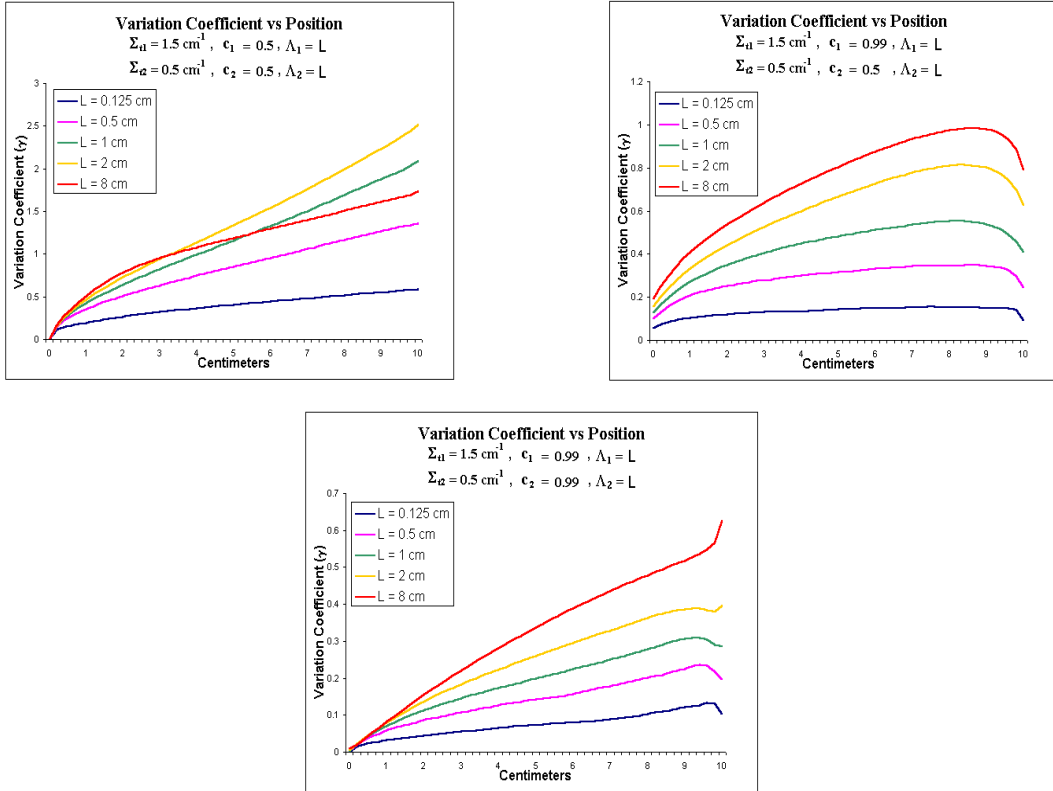
Figure 5.3: Variation coefficient comparison for different values of Λ_i - Set 1

Further, it was shown [94] that in systems of small length the probability of reflection and transmission does not vary with mixing statistics in planar geometry. Therefore, we have fixed the system length at 10 cm for all problems, in order to guarantee the influence of the mixing statistics to the problems. The set of problems considered contains 90 cases in which the total cross sections of material 1 and 2 were respectively set to 1.5 cm^{-1} and 0.5 cm^{-1}. The mean chord lengths and the single scatter albedo of each material vary according to the values given at Table 5.1.

It was found that, in the totality of the simulated problems, both the atomic mix and Levermore-Pomraning predictions lie well within ± 2 standard deviations σ of the mean, as can be seen from the examples shown in Figure 5.2. Next, we will examine in detail how the standard deviation of the benchmark solution and the relative errors of the atomic mix and Levermore-Pomraning predictions vary with changes in the mean chord lengths Λ_i and in the scatter albedo c_i.
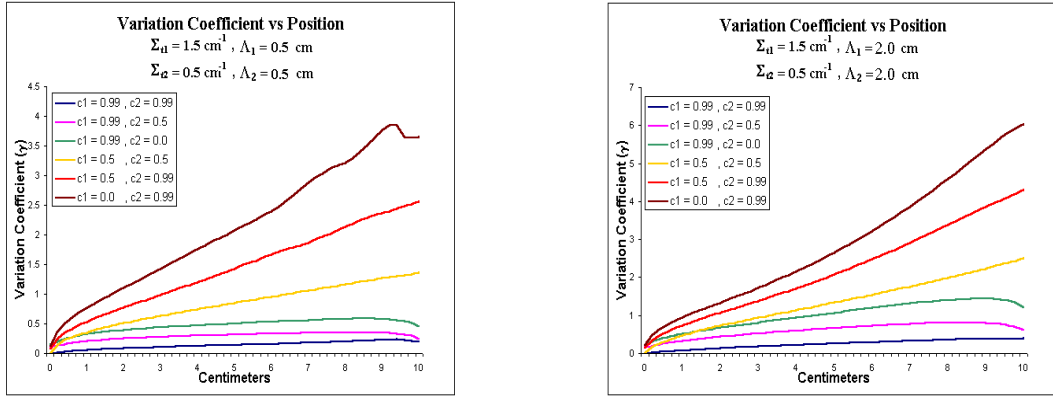
Figure 5.4: Variation coefficient comparison for different values of c_i - Set 1

When examining the standard deviation of these problems, we must pay special attention to the variation coefficient γ given by

$$\gamma(z) = \frac{\sigma\big(\phi(z)\big)}{\langle\phi(z)\rangle},\tag{5.20}$$

since this quantity (also known as the relative standard deviation) provides a good idea of the solution's variation. As expected, there is more variation at the right edge of the system than at the left edge. This is due to the material interfaces in the interior of the system. It was observed that the variation coefficient generally grows when the mean chord lengths increase. Also, there seems to be a relationship connecting the variation coefficient to the system's diffusivity. Both of these behaviours were observed in the computation process: in general, in order to obtain the relative error of 1% with 95% confidence, problems with larger Λ_i required many more realizations than those with smaller Λ_i; and systems with low diffusivity required more realizations than highly diffusive systems. However, there is another interesting detail: the variation coefficient increases when the single scatter albedo of material 2 (which is optically thinner than material 1 in all cases - $\Sigma_{t2}\Lambda_2 < \Sigma_{t1}\Lambda_1$) becomes greater than the single scatter albedo of material 1. This happens *even when the system becomes more diffusive*. These trends can be seen in Figures 5.3 and 5.4, where we present some plots comparing γ for different combinations of Λ_i and c_i.

Figure 5.5: Comparison of the atomic mix relative error ($\pm 1\%$ with 95% confidence) for different values of Λ_i - Set 1

The errors of the atomic mix and Levermore-Pomraning models relative to the benchmark results were calculated by

$$
\text{Atomic Mix Relative Error}\,(\%) = 100\frac{\left|\langle\phi\rangle_{AM} - \langle\phi\rangle_{Benchmark}\right|}{\langle\phi\rangle_{Benchmark}},
$$
$$
\text{Levermore-Pomraning Relative Error}\,(\%) = 100\frac{\left|\langle\phi\rangle_{LP} - \langle\phi\rangle_{Benchmark}\right|}{\langle\phi\rangle_{Benchmark}}.
$$
$$(5.21)$$

One must notice that since each benchmark result has itself a relative error of 1% with 95% confidence, the true relative errors obtained by the formulas in Eq. (5.21) will vary in 1% with 95% confidence. That is, if the relative error calculated by Eq. (5.21) is (for example) 5%, then with 95% confidence the true relative error will lie between 4% and 6%.

Bearing this information in mind we can examine the predictions errors. As expected, the atomic mix accuracy deteriorates when Eq. (3.6) is not satisfied; i.e, when the Λ_i become greater. The relative error increases as we get closer to
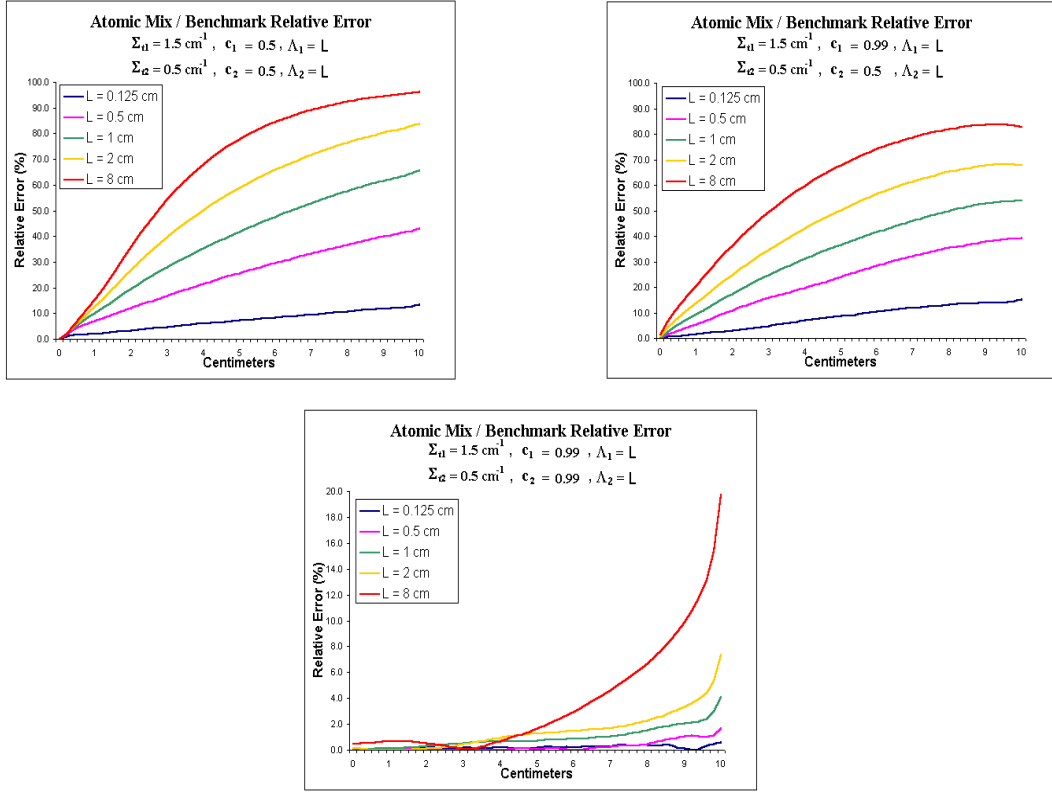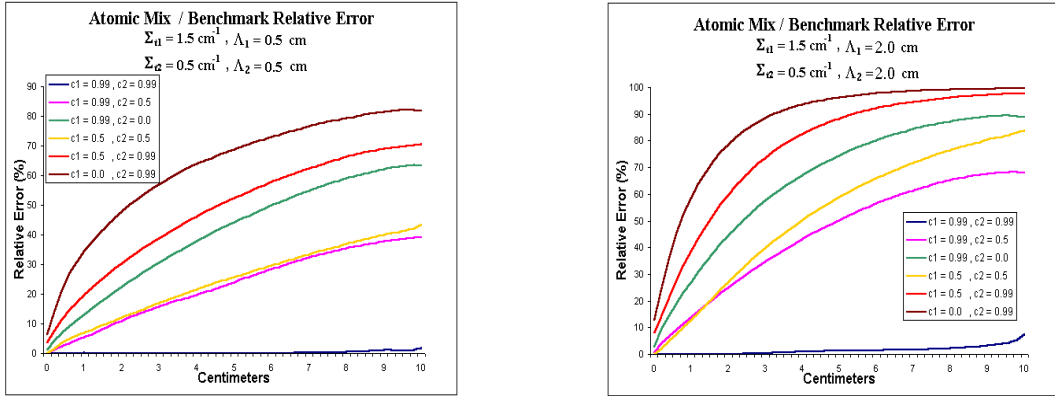
Figure 5.6: Comparison of the atomic mix relative error ($\pm 1\%$ with 95% confidence) for different values of c_i - Set 1

the right edge of the system, due to the solution's variation. This can be checked by examining the plots in Figure 5.5. Also, the changes in the system's diffusivity seem to affect the atomic mix result in the same way that affects the benchmark solution's variation. Comparing the plots in Figure 5.6 with those in Figure 5.4 we see that the accuracy of the atomic mix model gets better (in general) when the values of γ diminish.

In analogy to what happens with the atomic mix model, the accuracy of the Levermore-Pomraning method also worsens when the mean chord lengths increase. This is not unexpected, since we have proved that the Levermore-Pomraning equations reduce to the atomic mix equation when the mean chord lengths tend to zero. However, this bad effect in the prediction accuracy is weaker in the Levermore-Pomraning model. Figure 5.7 contains representative plots of this behaviour. Again, one must notice that the relative error is in general greater away from the left edge of the system, due to the solution's variation. Further, we know that the Levermore-Pomraning equations are exact when considering nonscattering problems, and that approximations are done to include the scattering process into the model. Therefore we expect the accuracy of this method to be better in systems with low diffusivity.

In fact, the system's diffusivity plays a fundamental role in the Levermore-Pomraning prediction. As an example, we can see from Figure 5.8 that the Levermore-Pomraning prediction achieves excelent results when $c_1 = c_2 = 0.5$, despite the high
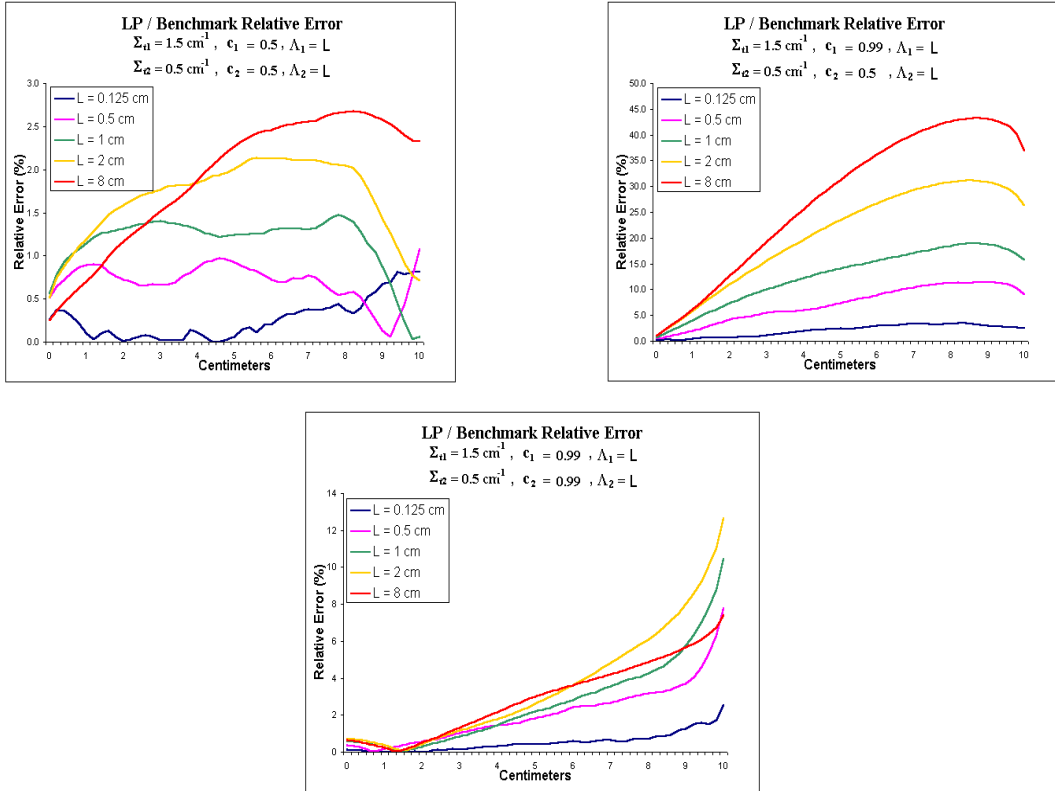
Figure 5.7: Comparison of the Levermore-Pomraning relative error ($\pm 1\%$ with 95% confidence) for different values of Λ_i - Set 1

values of γ for this case. As the system becomes more diffusive, the solution's variation has a stronger effect in the error of this method.

In the next pages, we present tables with the probabilities of Reflection and Transmission obtained by the benchmark, atomic mix and Levermore-Pomraning methods for the 90 problems simulated (Tables 5.2-5.7). The number of realizations simulated for each problem is displayed in the last column of these tables. After each table, we present the respective plots of the models relative errors (Figures 5.9-5.14).

For the systems with high diffusivity shown in Set 1.1, the atomic mix model is more accurate than the Levermore-Pomraning for almost all choices of Λ_i. However, as the mean chord lengths increase, the difference between the relative errors of both methods diminish. In fact the Levermore-Pomraning predictions are superior when compared with the predictions calculated using the atomic mix
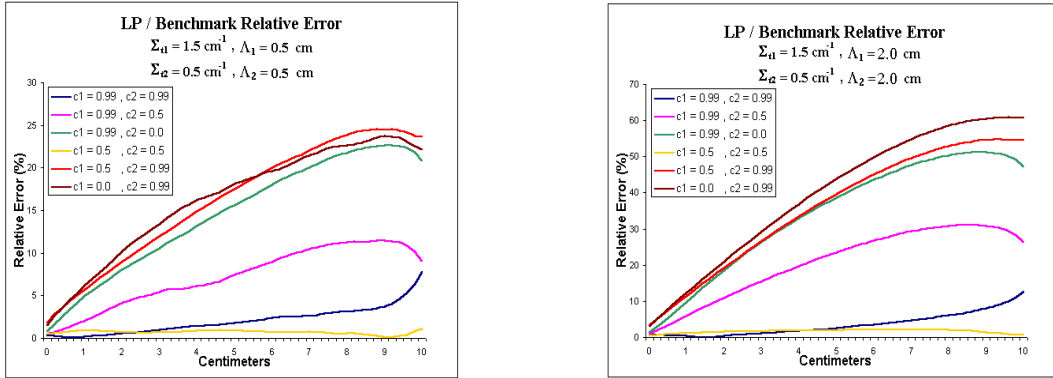
Figure 5.8: Comparison of the Levermore-Pomraning relative error ($\pm 1\%$ with 95% confidence) for different values of c_i - Set 1

model for all other sets of problems. In particular, we underline the excellence of its predictions in the lowest diffusive systems contained in Set 1.4. Further, all trends mentioned in the above discussion, such as accuracy degradation with Λ_i increasing and the variation's solution influence in the relative error, can be seen by examining this data. We ask the reader to pay special attention to the Tables in which the Reflection/Transmission probabilities are displayed. Although the relative error of the methods is quite large in some cases, this does not mean that the absolute difference between the predictions and the benchmark results is also large. Indeed, the absolute difference between the Levermore-Pomraning predictions and the benchmark solutions never exceeds the second decimal digit. Another interesting point to be remarked is the number of realizations calculated for the benchmark solution of the 10th problem of Set 1.6: 12,960,000. Again we remark the suitability of the LTS_N method in solving this kind of problem.

Table 5.2: Reflection and Transmission Results - Set 1.1

$Z = 10$ cm		**	Benchmark	Atomic	Levermore	Number of
Λ_1	Λ_2	**	Result	Mix	Pomraning	Realizations
-	-	-	-	-	-	-
	0.0625	$\langle R \rangle$	0.800747	0.800784	0.799590	1024
		$\langle T \rangle$	0.049501	0.049468	0.050286	
0.125	0.125	$\langle R \rangle$	0.796492	0.796689	0.794280	1024
		$\langle T \rangle$	0.066907	0.066516	0.068405	
	0.25	$\langle R \rangle$	0.788964	0.789233	0.785658	1024
		$\langle T \rangle$	0.090316	0.090058	0.093171	
	0.25	$\langle R \rangle$	0.800513	0.800784	0.796737	1024
		$\langle T \rangle$	0.050200	0.049468	0.052307	
0.5	0.5	$\langle R \rangle$	0.796046	0.796689	0.789168	1600
		$\langle T \rangle$	0.067646	0.066516	0.072569	
	1.0	$\langle R \rangle$	0.787562	0.789233	0.779003	2500
		$\langle T \rangle$	0.092786	0.090058	0.099163	
	0.5	$\langle R \rangle$	0.800278	0.800784	0.793997	2500
		$\langle T \rangle$	0.050720	0.049468	0.054349	
1.0	1.0	$\langle R \rangle$	0.795184	0.796689	0.784920	3600
		$\langle T \rangle$	0.069324	0.066516	0.076225	
	2.0	$\langle R \rangle$	0.786147	0.789233	0.774233	4900
		$\langle T \rangle$	0.094832	0.090058	0.103680	
	1.0	$\langle R \rangle$	0.799723	0.800784	0.790457	4900
		$\langle T \rangle$	0.051953	0.049468	0.057188	
2.0	2.0	$\langle R \rangle$	0.793750	0.796689	0.780218	6400
		$\langle T \rangle$	0.071787	0.066516	0.080611	
	4.0	$\langle R \rangle$	0.783534	0.789233	0.769649	6400
		$\langle T \rangle$	0.098940	0.090058	0.108394	
	4.0	$\langle R \rangle$	0.796411	0.800784	0.784018	16900
		$\langle T \rangle$	0.058176	0.049468	0.063926	
8.0	8.0	$\langle R \rangle$	0.787175	0.796689	0.773787	16900
		$\langle T \rangle$	0.082836	0.066516	0.088911	
	16.0	$\langle R \rangle$	0.775251	0.789233	0.764646	12100
		$\langle T \rangle$	0.112087	0.090058	0.115903	

$\Sigma_{t1} = 1.5$ cm^{-1}, $\Sigma_{s1} = c_1 \Sigma_{t1}$, $c_1 = 0.99$

$\Sigma_{t2} = 0.5$ cm^{-1}, $\Sigma_{s2} = c_2 \Sigma_{t2}$, $c_2 = 0.99$

Figure 5.9: Relative errors of the atomic mix and Levermore-Pomraning methods ($\pm 1\%$ with 95% confidence) - Set 1.1

Table 5.3: Reflection and Transmission Results - Set 1.2

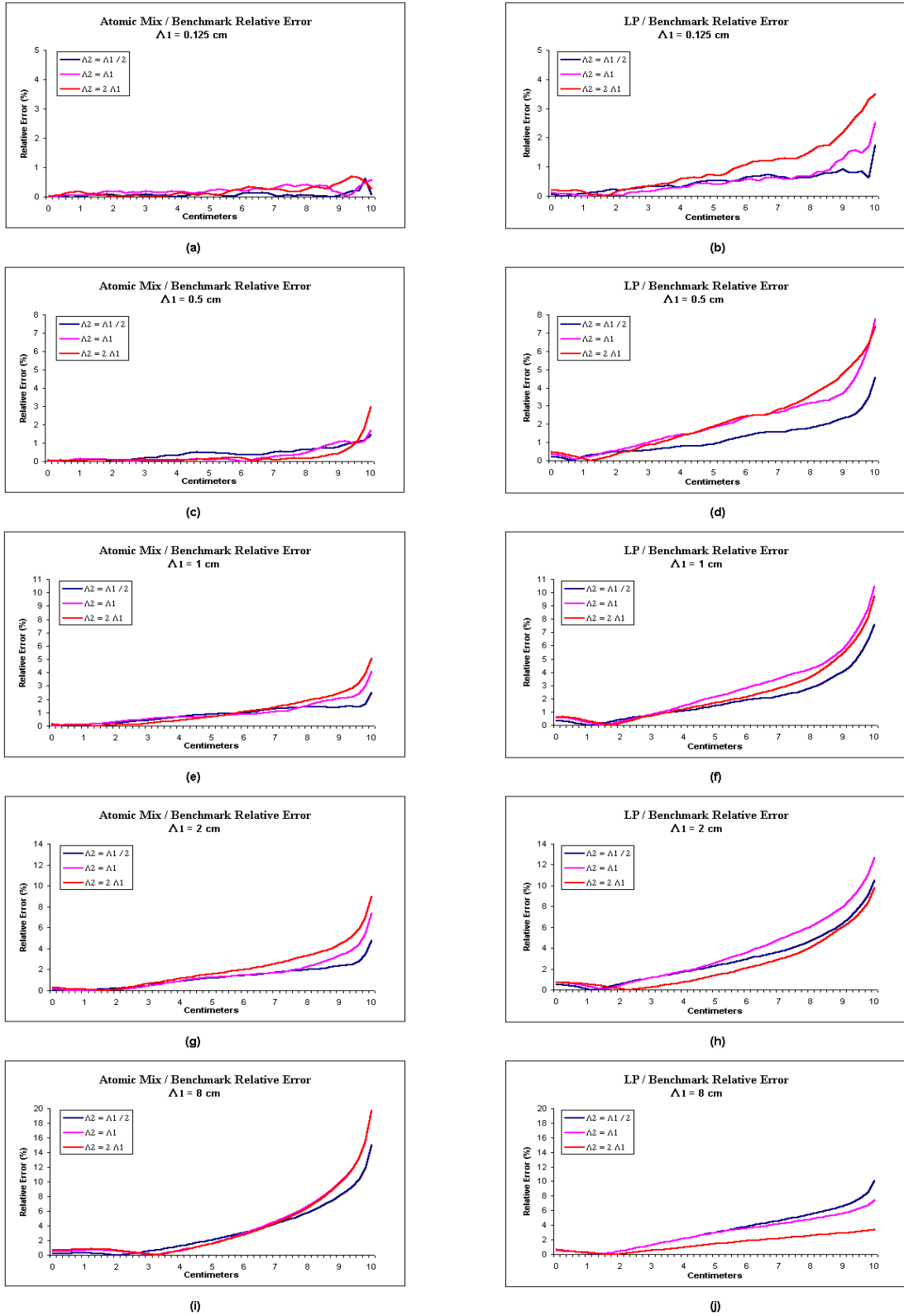| $\Sigma_{t1} = 1.5$ cm^{-1}, $\Sigma_{s1} = c_1\Sigma_{t1}$, $c_1 = 0.99$						
$\Sigma_{t2} = 0.5$ cm^{-1}, $\Sigma_{s2} = c_2\Sigma_{t2}$, $c_2 = 0.5$						
$Z = 10$ cm		**	Benchmark	Atomic	Levermore	Number of
Λ_1	Λ_2	**	Result	Mix	Pomraning	Realizations
-	-	-	-	-	-	-
	0.0625	$\langle R \rangle$	0.533021	0.528754	0.529840	1600
		$\langle T \rangle$	0.003167	0.002807	0.003050	
0.125	0.125	$\langle R \rangle$	0.437939	0.434291	0.434307	1024
		$\langle T \rangle$	0.002354	0.001992	0.002287	
	0.25	$\langle R \rangle$	0.344390	0.344518	0.342775	1024
		$\langle T \rangle$	0.002384	0.002001	0.002364	
	0.25	$\langle R \rangle$	0.544783	0.528754	0.532523	6400
		$\langle T \rangle$	0.004213	0.002807	0.003677	
0.5	0.5	$\langle R \rangle$	0.443228	0.434291	0.434964	4900
		$\langle T \rangle$	0.003300	0.001992	0.002999	
	1.0	$\langle R \rangle$	0.350940	0.344518	0.340812	4900
		$\langle T \rangle$	0.003273	0.002001	0.003139	
	0.5	$\langle R \rangle$	0.552743	0.528754	0.535411	12100
		$\langle T \rangle$	0.005439	0.002807	0.004358	
1.0	1.0	$\langle R \rangle$	0.448936	0.434291	0.436484	14400
		$\langle T \rangle$	0.004390	0.001992	0.003703	
	2.0	$\langle R \rangle$	0.351174	0.344518	0.340826	12100
		$\langle T \rangle$	0.004216	0.002001	0.003807	
	1.0	$\langle R \rangle$	0.558819	0.528754	0.540050	22500
		$\langle T \rangle$	0.007528	0.002807	0.005403	
2.0	2.0	$\langle R \rangle$	0.457872	0.434291	0.439901	28900
		$\langle T \rangle$	0.006291	0.001992	0.004683	
	4.0	$\langle R \rangle$	0.356969	0.344518	0.342756	32400
		$\langle T \rangle$	0.005639	0.002001	0.004616	
	4.0	$\langle R \rangle$	0.575749	0.528754	0.555493	25600
		$\langle T \rangle$	0.013679	0.002807	0.008754	
8.0	8.0	$\langle R \rangle$	0.470134	0.434291	0.453013	40000
		$\langle T \rangle$	0.011445	0.001992	0.007431	
	16.0	$\langle R \rangle$	0.361543	0.344518	0.352028	62500
		$\langle T \rangle$	0.009276	0.002001	0.006555	

Figure 5.10: Relative errors of the atomic mix and Levermore-Pomraning methods ($\pm 1\%$ with 95% confidence) - Set 1.2

Table 5.4: Reflection and Transmission Results - Set 1.3

$Z = 10$ cm		**	Benchmark	Atomic	Levermore	Number of
Λ_1	Λ_2	**	Result	Mix	Pomraning	Realizations
-	-	-	-	-	-	-
	0.0625	$\langle R \rangle$	0.417642	0.407756	0.413145	3600
		$\langle T \rangle$	0.000650	0.000493	0.000591	
0.125	0.125	$\langle R \rangle$	0.305174	0.297147	0.302292	2500
		$\langle T \rangle$	0.000435	0.000311	0.000407	
	0.25	$\langle R \rangle$	0.205589	0.197812	0.200832	2500
		$\langle T \rangle$	0.000484	0.000350	0.000468	
	0.25	$\langle R \rangle$	0.440016	0.407756	0.424945	16900
		$\langle T \rangle$	0.001198	0.000493	0.000877	
0.5	0.5	$\langle R \rangle$	0.325281	0.297147	0.312546	14400
		$\langle T \rangle$	0.000850	0.000311	0.000676	
	1.0	$\langle R \rangle$	0.215634	0.197812	0.206919	12100
		$\langle T \rangle$	0.000861	0.000350	0.000760	
	0.5	$\langle R \rangle$	0.458710	0.407756	0.435649	40000
		$\langle T \rangle$	0.002023	0.000493	0.001236	
1.0	1.0	$\langle R \rangle$	0.338940	0.297147	0.321485	40000
		$\langle T \rangle$	0.001467	0.000311	0.000994	
	2.0	$\langle R \rangle$	0.225537	0.197812	0.212690	40000
		$\langle T \rangle$	0.001344	0.000350	0.001054	
	1.0	$\langle R \rangle$	0.476954	0.407756	0.449818	62500
		$\langle T \rangle$	0.003743	0.000493	0.001887	
2.0	2.0	$\langle R \rangle$	0.355673	0.297147	0.333289	90000
		$\langle T \rangle$	0.002809	0.000311	0.001525	
	4.0	$\langle R \rangle$	0.237063	0.197812	0.220770	122500
		$\langle T \rangle$	0.002291	0.000350	0.001474	
	4.0	$\langle R \rangle$	0.512546	0.407756	0.484557	52900
		$\langle T \rangle$	0.010449	0.000493	0.004821	
8.0	8.0	$\langle R \rangle$	0.380788	0.297147	0.361876	78400
		$\langle T \rangle$	0.008096	0.000311	0.003739	
	16.0	$\langle R \rangle$	0.254961	0.197812	0.240707	136900
		$\langle T \rangle$	0.005890	0.000350	0.002967	

$\Sigma_{t1} = 1.5$ cm^{-1}, $\quad \Sigma_{s1} = c_1\Sigma_{t1}$, $\quad c_1 = 0.99$
$\Sigma_{t2} = 0.5$ cm^{-1}, $\quad \Sigma_{s2} = c_2\Sigma_{t2}$, $\quad c_2 = 0.0$
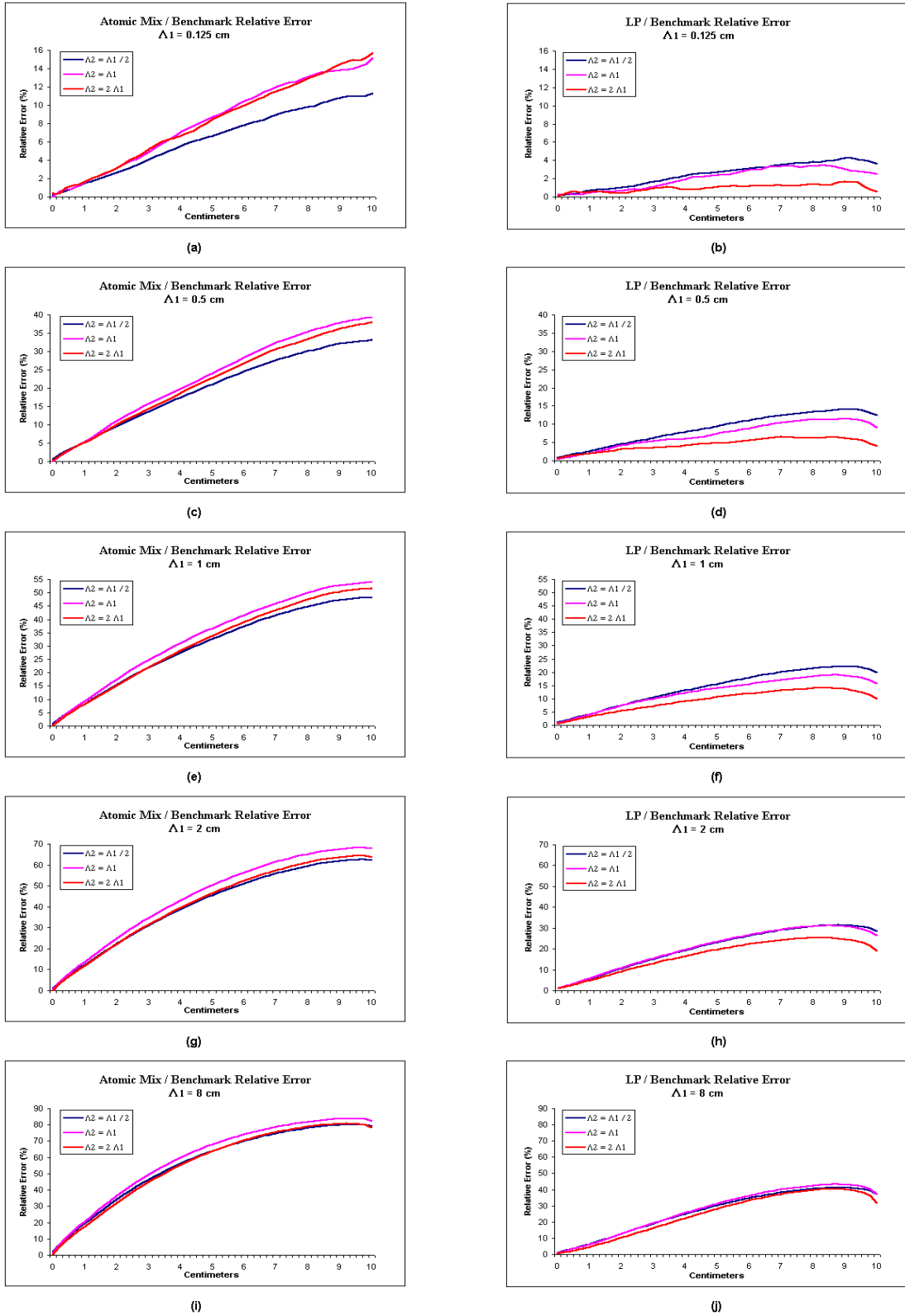
Figure 5.11: Relative errors of the atomic mix and Levermore-Pomraning methods ($\pm 1\%$ with 95% confidence) - Set 1.3

Table 5.5: Reflection and Transmission Results - Set 1.4

$Z = 10$ cm		**	Benchmark	Atomic	Levermore	Number of
Λ_1	Λ_2	**	Result	Mix	Pomraning	Realizations
-	-	-	-	-	-	-
	0.0625	$\langle R \rangle$	0.151766	0.151766	0.150430	8100
		$\langle T \rangle$	0.000009	0.000008	0.000009	
0.125	0.125	$\langle R \rangle$	0.151766	0.151766	0.149376	14400
		$\langle T \rangle$	0.000047	0.000040	0.000047	
	0.25	$\langle R \rangle$	0.151766	0.151766	0.148694	16900
		$\langle T \rangle$	0.000241	0.000204	0.000242	
	0.25	$\langle R \rangle$	0.151766	0.151766	0.148290	62500
		$\langle T \rangle$	0.000012	0.000008	0.000012	
0.5	0.5	$\langle R \rangle$	0.151766	0.151766	0.146455	40000
		$\langle T \rangle$	0.000071	0.000040	0.000072	
	1.0	$\langle R \rangle$	0.151766	0.151766	0.145885	122500
		$\langle T \rangle$	0.000374	0.000204	0.000375	
	0.5	$\langle R \rangle$	0.151766	0.151766	0.147159	160000
		$\langle T \rangle$	0.000017	0.000008	0.000017	
1.0	1.0	$\langle R \rangle$	0.151766	0.151766	0.145517	202500
		$\langle T \rangle$	0.000118	0.000040	0.000118	
	2.0	$\langle R \rangle$	0.151766	0.151766	0.145530	108900
		$\langle T \rangle$	0.000575	0.000204	0.000575	
	1.0	$\langle R \rangle$	0.151766	0.151766	0.146659	562500
		$\langle T \rangle$	0.000034	0.000008	0.000034	
2.0	2.0	$\langle R \rangle$	0.151766	0.151766	0.145723	302500
		$\langle T \rangle$	0.000250	0.000040	0.000248	
	4.0	$\langle R \rangle$	0.151766	0.151766	0.146372	108900
		$\langle T \rangle$	0.000981	0.000204	0.000974	
	4.0	$\langle R \rangle$	0.151766	0.151766	0.148260	422500
		$\langle T \rangle$	0.000325	0.000008	0.000317	
8.0	8.0	$\langle R \rangle$	0.151766	0.151766	0.148548	122500
		$\langle T \rangle$	0.001115	0.000040	0.001090	
	16.0	$\langle R \rangle$	0.151765	0.151766	0.149362	62500
		$\langle T \rangle$	0.002288	0.000204	0.002251	

$\Sigma_{t1} = 1.5$ cm^{-1}, $\Sigma_{s1} = c_1 \Sigma_{t1}$, $c_1 = 0.5$
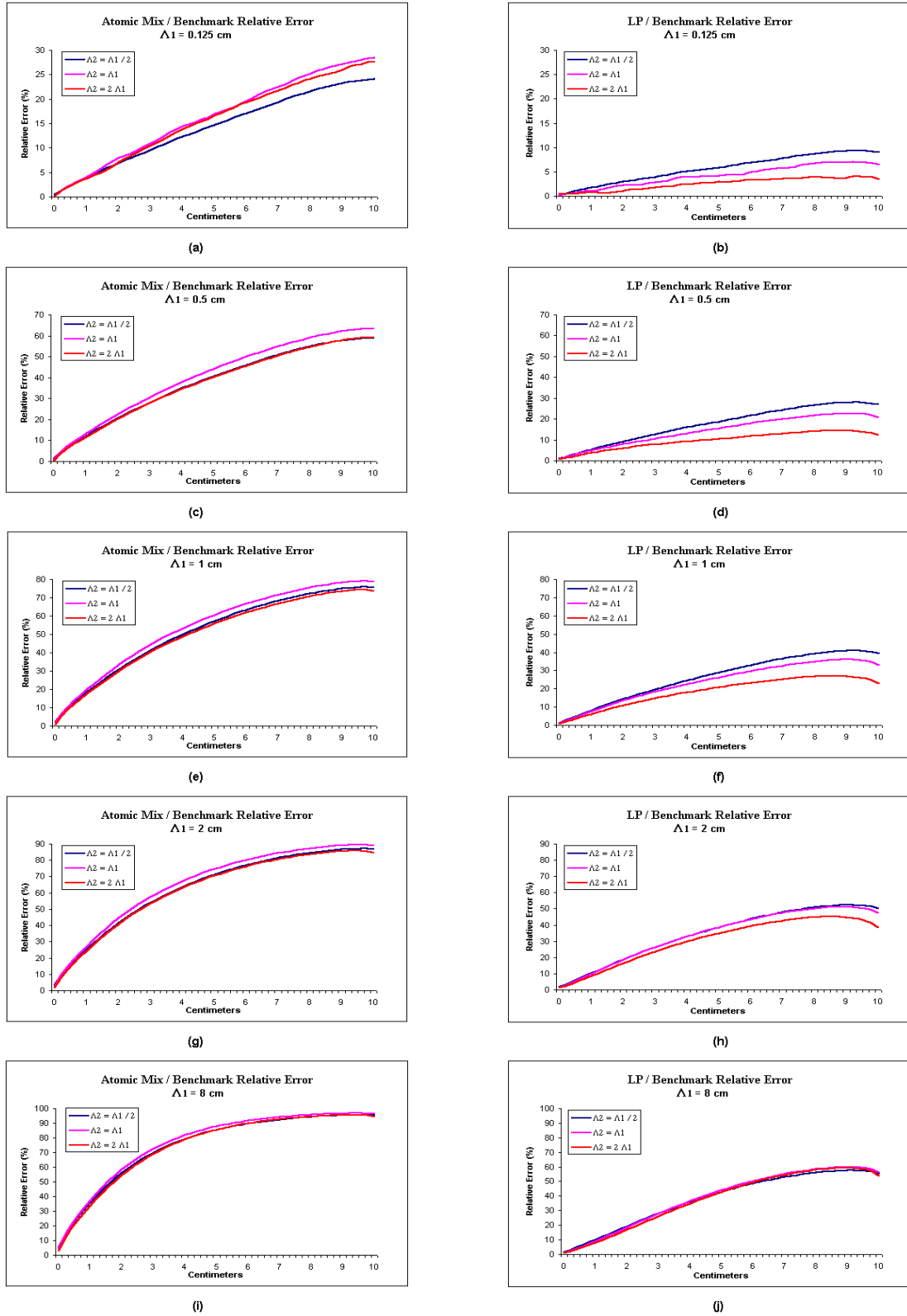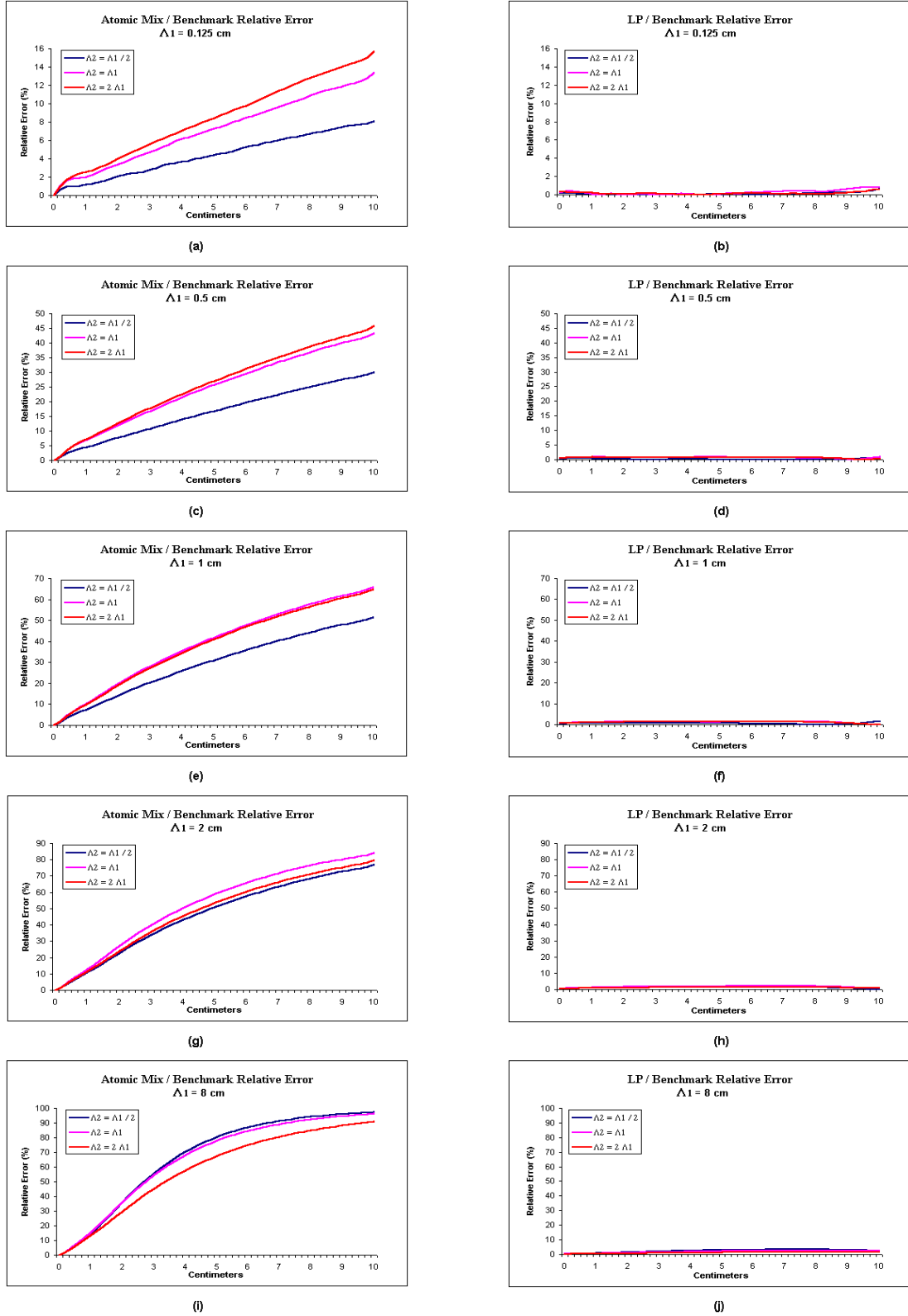$\Sigma_{t2} = 0.5$ cm^{-1}, $\Sigma_{s2} = c_2 \Sigma_{t2}$, $c_2 = 0.5$

Figure 5.12: Relative errors of the atomic mix and Levermore-Pomraning methods ($\pm$1% with 95% confidence) - Set 1.4

Table 5.6: Reflection and Transmission Results - Set 1.5

| $\Sigma_{t1} = 1.5$ cm^{-1}, $\Sigma_{s1} = c_1\Sigma_{t1}$, $c_1 = 0.5$					
$\Sigma_{t2} = 0.5$ cm^{-1}, $\Sigma_{s2} = c_2\Sigma_{t2}$, $c_2 = 0.99$					
$Z = 10$ cm		**	Benchmark	Atomic	Levermore	Number of
Λ_1	Λ_2	**	Result	Mix	Pomraning	Realizations
-	-	-	-	-	-	-
	0.0625	$\langle R \rangle$	0.190241	0.185130	0.186986	14400
		$\langle T \rangle$	0.000016	0.000014	0.000015	
0.125	0.125	$\langle R \rangle$	0.226168	0.213852	0.219074	25600
		$\langle T \rangle$	0.000126	0.000095	0.000121	
	0.25	$\langle R \rangle$	0.287015	0.261261	0.272731	40000
		$\langle T \rangle$	0.001150	0.000750	0.001027	
	0.25	$\langle R \rangle$	0.202419	0.185130	0.192409	102400
		$\langle T \rangle$	0.000025	0.000014	0.000023	
0.5	0.5	$\langle R \rangle$	0.254473	0.213852	0.232827	302500
		$\langle T \rangle$	0.000308	0.000095	0.000238	
	1.0	$\langle R \rangle$	0.337296	0.261261	0.299420	250000
		$\langle T \rangle$	0.003364	0.000750	0.002238	
	0.5	$\langle R \rangle$	0.215414	0.185130	0.198973	902500
		$\langle T \rangle$	0.000052	0.000014	0.000041	
1.0	1.0	$\langle R \rangle$	0.280586	0.213852	0.247838	902500
		$\langle T \rangle$	0.000874	0.000095	0.000533	
	2.0	$\langle R \rangle$	0.378615	0.261261	0.325588	302500
		$\langle T \rangle$	0.008593	0.000750	0.004714	
	1.0	$\langle R \rangle$	0.233952	0.185130	0.210080	4000000
		$\langle T \rangle$	0.000229	0.000014	0.000126	
2.0	2.0	$\langle R \rangle$	0.315984	0.213852	0.270836	810000
		$\langle T \rangle$	0.003786	0.000095	0.001755	
	4.0	$\langle R \rangle$	0.427258	0.261261	0.361977	202500
		$\langle T \rangle$	0.022207	0.000750	0.011519	
	4.0	$\langle R \rangle$	0.286330	0.185130	0.249066	640000
		$\langle T \rangle$	0.008102	0.000014	0.003425	
8.0	8.0	$\langle R \rangle$	0.391656	0.213852	0.338022	160000
		$\langle T \rangle$	0.032186	0.000095	0.017538	
	16.0	$\langle R \rangle$	0.504661	0.261261	0.450394	62500
		$\langle T \rangle$	0.069793	0.000750	0.048187	
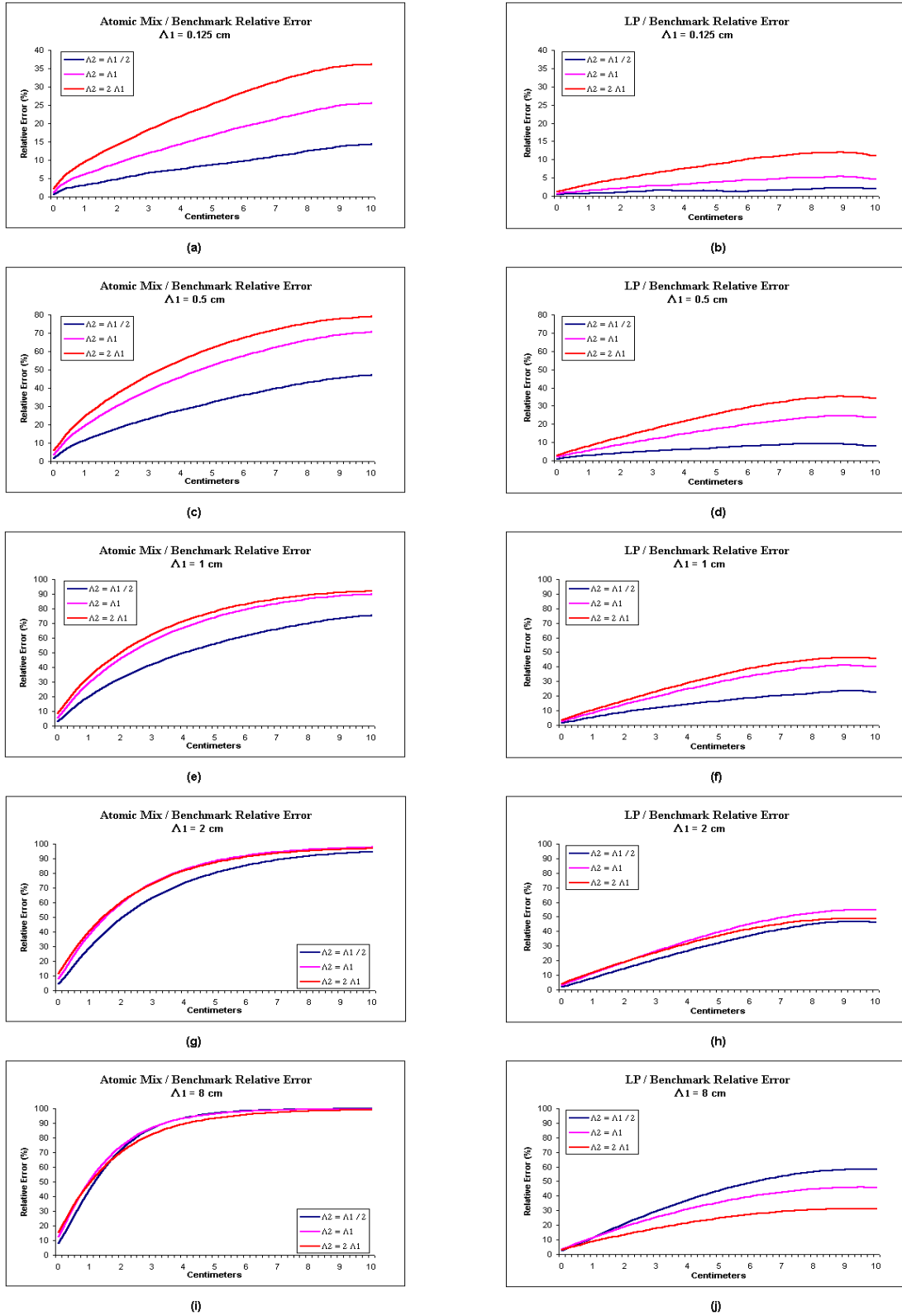
Figure 5.13: Relative errors of the atomic mix and Levermore-Pomraning methods ($\pm 1\%$ with 95% confidence) - Set 1.5

Table 5.7: Reflection and Transmission Results - Set 1.6

| $\Sigma_{t1} = 1.5$ cm^{-1}, $\Sigma_{s1} = c_1\Sigma_{t1}$, $c_1 = 0.0$					
$\Sigma_{t2} = 0.5$ cm^{-1}, $\Sigma_{s2} = c_2\Sigma_{t2}$, $c_2 = 0.99$					
$Z = 10$ cm		**	Benchmark	Atomic	Levermore	Number of
Λ_1	Λ_2	**	Result	Mix	Pomraning	Realizations
-	-	-	-	-	-	-
	0.0625	$\langle R \rangle$	0.040363	0.032882	0.039170	16900
		$\langle T \rangle$	0.000002	0.000002	0.000002	
0.125	0.125	$\langle R \rangle$	0.080941	0.061623	0.076557	40000
		$\langle T \rangle$	0.000019	0.000013	0.000019	
	0.25	$\langle R \rangle$	0.149746	0.109973	0.138605	62500
		$\langle T \rangle$	0.000235	0.000127	0.000213	
	0.25	$\langle R \rangle$	0.058279	0.032882	0.053062	202500
		$\langle T \rangle$	0.000004	0.000002	0.000003	
0.5	0.5	$\langle R \rangle$	0.121741	0.061623	0.106375	640000
		$\langle T \rangle$	0.000064	0.000013	0.000051	
	1.0	$\langle R \rangle$	0.223664	0.109973	0.190218	640000
		$\langle T \rangle$	0.001239	0.000127	0.000761	
	0.5	$\langle R \rangle$	0.076358	0.032882	0.066174	1960000
		$\langle T \rangle$	0.000009	0.000002	0.000008	
1.0	1.0	$\langle R \rangle$	0.157910	0.061623	0.132296	2890000
		$\langle T \rangle$	0.000312	0.000013	0.000172	
	2.0	$\langle R \rangle$	0.280510	0.109973	0.231575	640000
		$\langle T \rangle$	0.005064	0.000127	0.002402	
	1.0	$\langle R \rangle$	0.101806	0.032882	0.084515	12960000
		$\langle T \rangle$	0.000078	0.000002	0.000040	
2.0	2.0	$\langle R \rangle$	0.204516	0.061623	0.166214	1690000
		$\langle T \rangle$	0.002350	0.000013	0.000951	
	4.0	$\langle R \rangle$	0.344098	0.109973	0.281992	250000
		$\langle T \rangle$	0.017844	0.000127	0.008261	
	4.0	$\langle R \rangle$	0.169394	0.032882	0.136115	902500
		$\langle T \rangle$	0.006956	0.000002	0.002775	
8.0	8.0	$\langle R \rangle$	0.300405	0.061623	0.250111	202500
		$\langle T \rangle$	0.029699	0.000013	0.015765	
	16.0	$\langle R \rangle$	0.442592	0.109973	0.389464	62500
		$\langle T \rangle$	0.067397	0.000127	0.045569	
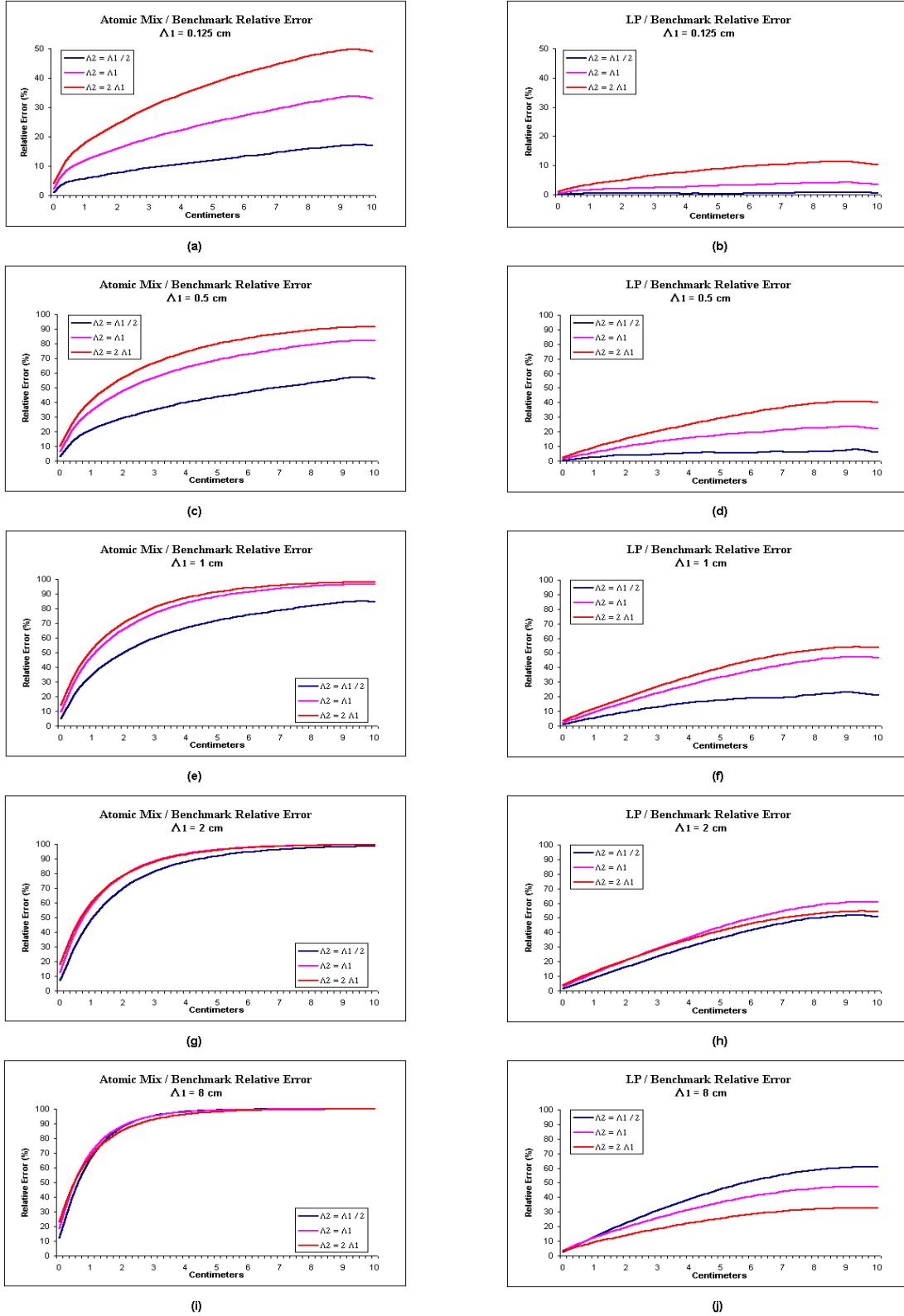
Figure 5.14: Relative errors of the atomic mix and Levermore-Pomraning methods ($\pm 1\%$ with 95% confidence) - Set 1.6
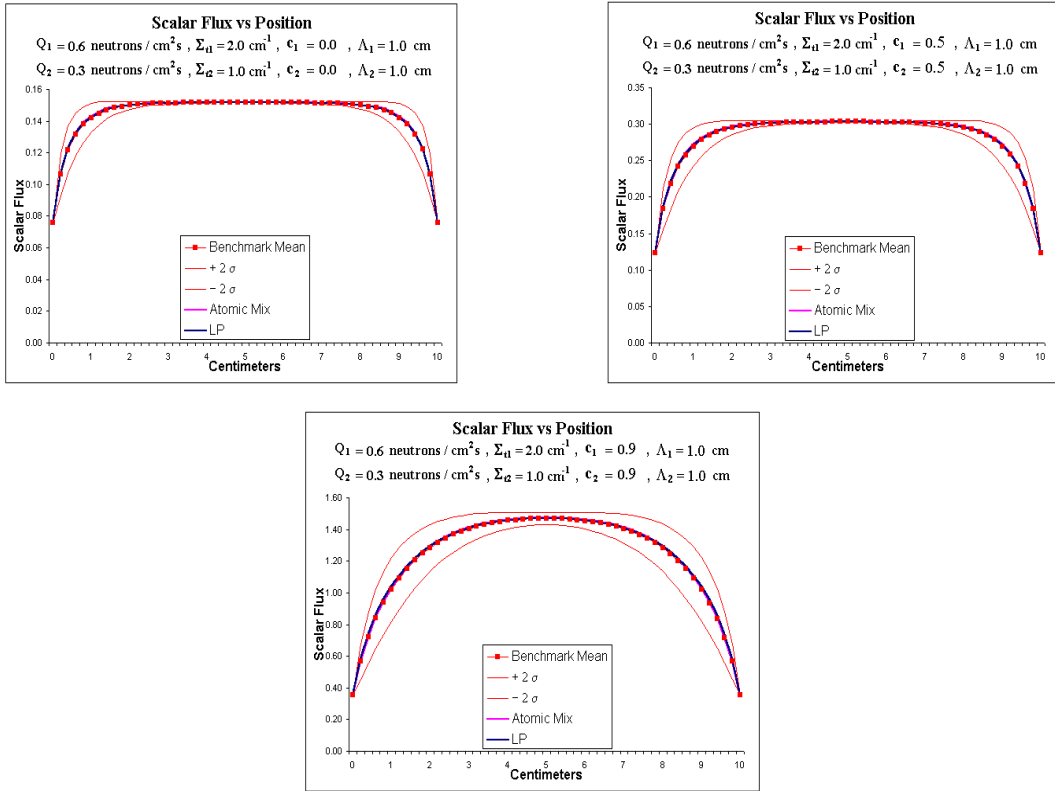
Figure 5.15: Models approximations to a benchmark ensemble-averaged scalar flux - Set 2

5.3 Problems With Constant Internal Sources

Here we consider Eq. (5.1) with vacuum boundary conditions at both sides of the slab,

$$
\begin{cases}
\psi(0, \mu) = 0, & \mu > 0 \\
\psi(Z, \mu) = 0, & \mu < 0
\end{cases}
\quad , \tag{5.22}
$$

and constant internal sources Q_i. There are nine variable parameters that we can vary when considering the analysis of this problem: the same seven parameters mentioned at the last section plus the internal source Q_i of each material. As in the last section, we have fixed the system length in 10 cm for all problems. The set of problems considered contains 27 cases, in which the total cross sections of material 1 and 2 were respectively set to 2.0 cm^{-1} and 1.0 cm^{-1}, and the internal sources were defined by

$$
Q_1 = 0.6 \frac{\text{neutrons}}{\text{cm}^2\text{s}}, \quad Q_2 = 0.3 \frac{\text{neutrons}}{\text{cm}^2\text{s}} \ . \tag{5.23}
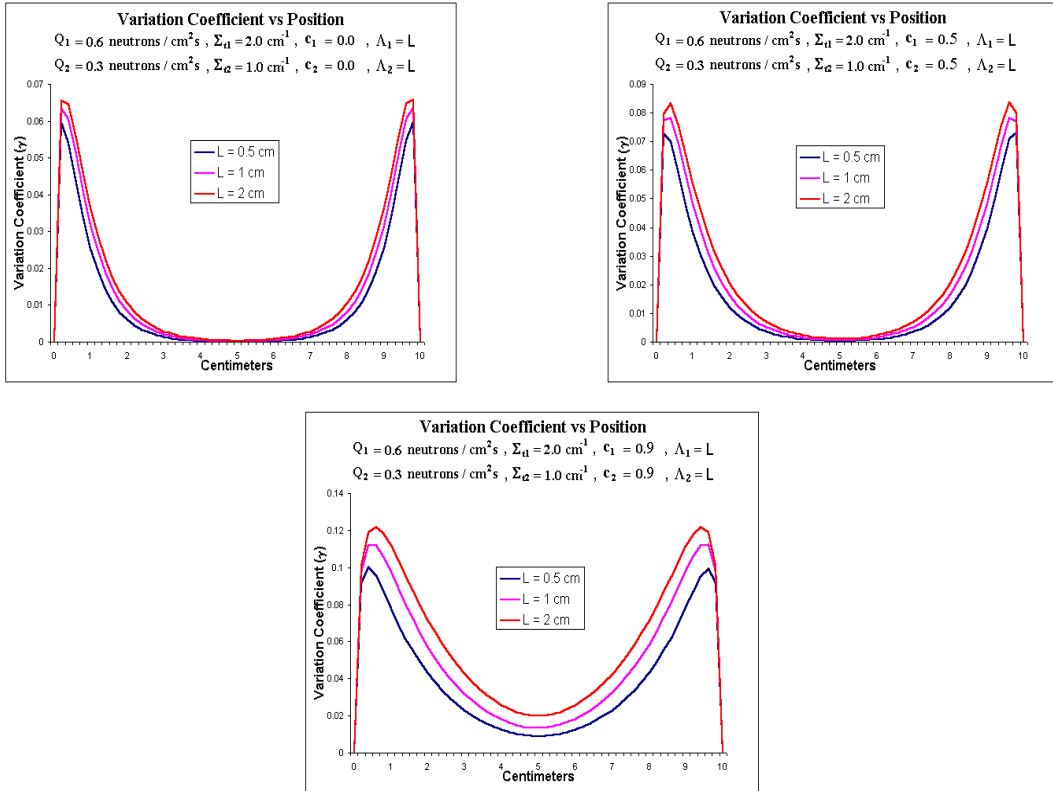$$

Figure 5.16: Variation coefficient comparison for different values of Λ_i - Set 2

The single scatter albedos of the materials were chosen such that $c_1 = c_2$ for all cases. This choice of parameters was made in order to simulate a medium containing slabs of two different densities of the same material. The three sets of parameters simulated are shown in Table 5.8.

Table 5.8: Set 2 - Parameters Simulated for the Source Problems

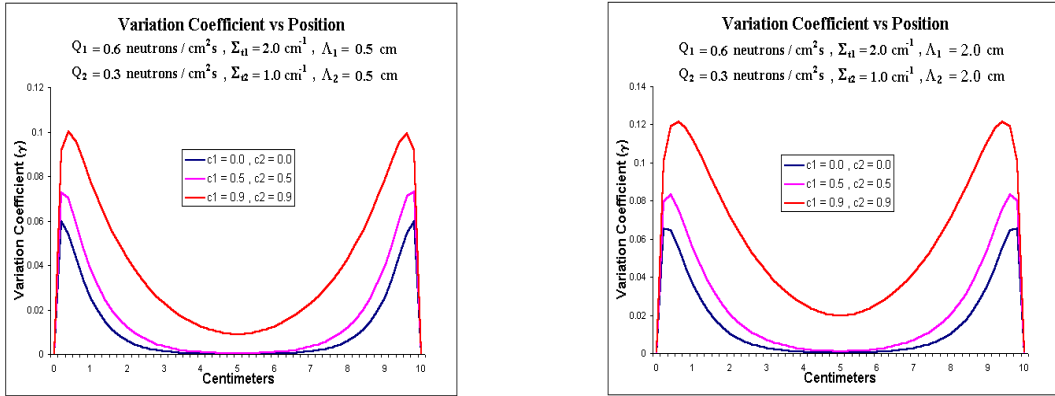| $\Sigma_{t1} = 2.0$ cm^{-1}, $\Sigma_{s1} = c_1\Sigma_{t1}$, $\Lambda_1 = 0.5, 1, 2$ cm,		$Q_1 = 0.6$ neutrons/cm^{2}s	
$\Sigma_{t2} = 1.0$ cm^{-1}, $\Sigma_{s2} = c_2\Sigma_{t2}$, $\Lambda_2 = \Lambda_1/2, \Lambda_1, 2\Lambda_1$ cm,		$Q_2 = 0.3$ neutrons/cm^{2}s	
$Z = 10$ cm	Set 2.1	Set 2.2	Set 2.3
c_1	0.0	0.5	0.9
c_2	0.0	0.5	0.9
Number of Cases	9	9	9

Figure 5.17: Variation coefficient comparison for different values of c_i - Set 2

In analogy with what was shown in the last section, the atomic mix and Levermore-Pomraning predictions in all problems lie well within ± 2 standard deviations σ of the mean. In Figure 5.15 the reader can see examples of this fact. We outline the rest of this section following the same structure presented in the last one: we first examine the variation of the benchmark solution and the behaviour of the predictions when the parameters vary; then we present the data regarding the relative errors of the complete set of problems.

Calculating the variation coefficient as given by Eq. (5.20), we see that it assumes symmetric values within the system, as expected. Its maximum values are localized near the edges, and the minimum values at the boundaries (due to the vacuum condition prescribed) and at the center of the system. This trend is due mainly to the fact that, in these systems, we allow only $N(z)$ to vary, i.e., we allow only the *density* of the material to vary randomly. In this situation, a particular simple "infinite-medium" solution of the transport problem always exists:

$$\psi(z,\mu) = \frac{1}{2} \frac{\langle Q \rangle}{\langle \Sigma_a \rangle}, \tag{5.24}$$

which is independent of z, independent of μ, and in particular independent of $N(z)$, hence has *zero variance*. If these physical systems were all very thick, the solution of all these problems would limit, a few mean free paths away from the outer boundaries, to this infinite-medium solution, where the variance is zero. Near the outer boundaries ($z = 0$ and $z = 10$), boundary layers exist, and there the variance is not
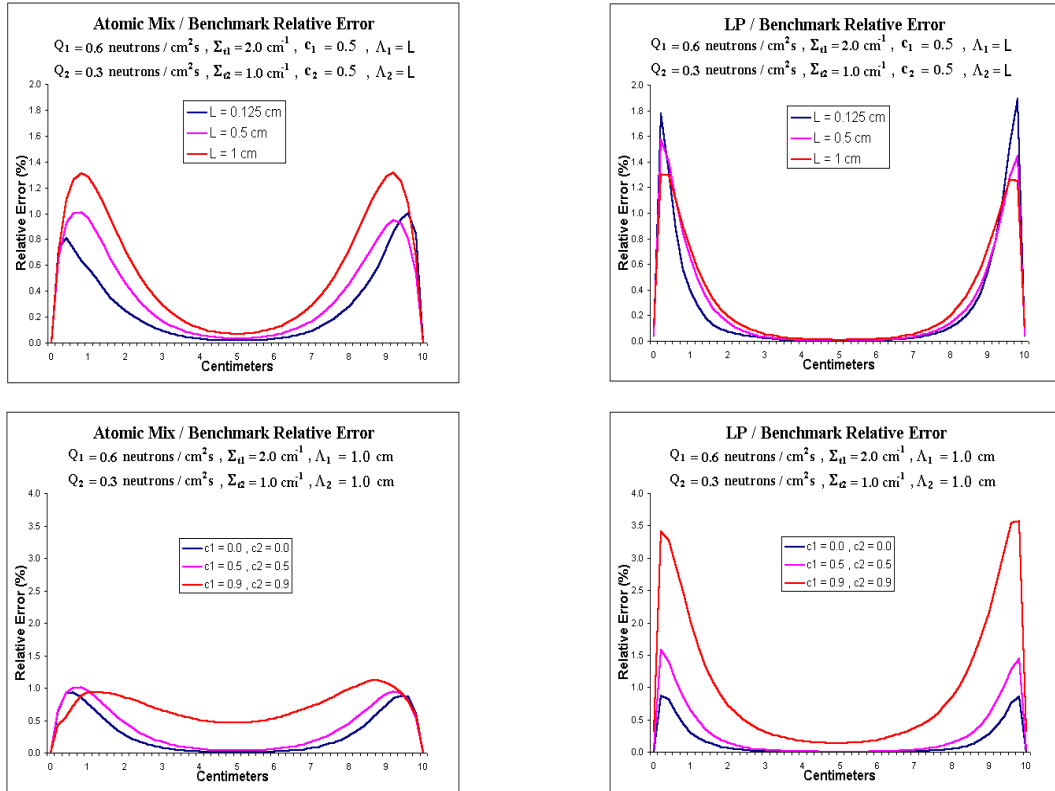
Figure 5.18: Comparison of the atomic mix and Levermore-Pomraning relative errors ($\pm 1\%$ with 95% confidence) for different values of Λ_i and c_i - Set 2

zero. Again, the values of γ increase when the mean chord lengths grow (Figure 5.16). On the other hand, in contrast with the results of the last section, we observe that the lower the diffusivity of the system, the smaller the solution's variation. This is not unexpected, since for problems with low diffusivity, the boundary layers are narrow, and the solution moves to the infinite-medium solution already mentioned. However, in the problems with higher diffusivity, the boundary layers are wider and extend deeper into the slab; hence the variance does not go to zero at the center - although it does have a local minimum. One can make these observations by examining the examples ploted in Figure 5.17.

Analysing the atomic mix and Levermore-Pomraning predictions for this class of problems we see that, due to the small variation of the benchmark mean, the relative errors obtained are also small. Their accuracy generally deteriorates when the mean chord lengths increase and when the system becomes more diffusive, except

for the points where the relative error is close to its maximum (Figure 5.18). In these points we have observed some alternance in these trends. We have also observed that these relative error curves present certain assymetric shapes (we will get back to this subject soon). Further, we can observe that the behaviour of the relative errors is strongly connected with the solution's variation, as in the Reflection/Transmission problems.

In the next pages we present the plots of the relative errors obtained through the comparison of the benchmark, atomic mix, and Levermore-Pomraning methods for this set of 27 problems (Figures 5.19-5.21). The reader will see that the maximum error peaks of the Levermore-Pomraning method are generally greater than those obtained by the atomic mix method, particularly in the mildly and highly diffusive systems contained in Sets 2.2 and 2.3. Nevertheless, the Levermore-Pomraning prediction is always more accurate than the atomic mix prediction at the center of all systems, away from these peaks. We remark that, in comparison with the relative errors obtained for the Reflection/Transmission problem, the errors obtained for these particular source problems are considerably small. This leads us to believe that both the numerical and the statistical errors have a significatively greater effect in these results, which explains the assymmetric shapes encountered in some curves. Finally, we mention that all trends discussed above, such as accuracy degradation with increasing values of Λ_i and the variation's solution influence in the relative error, can be seen by examining this data. All benchmark simulations were calculated for 10,000 physical realizations of the problem, although 1,000 realizations would be enough for almost all cases.
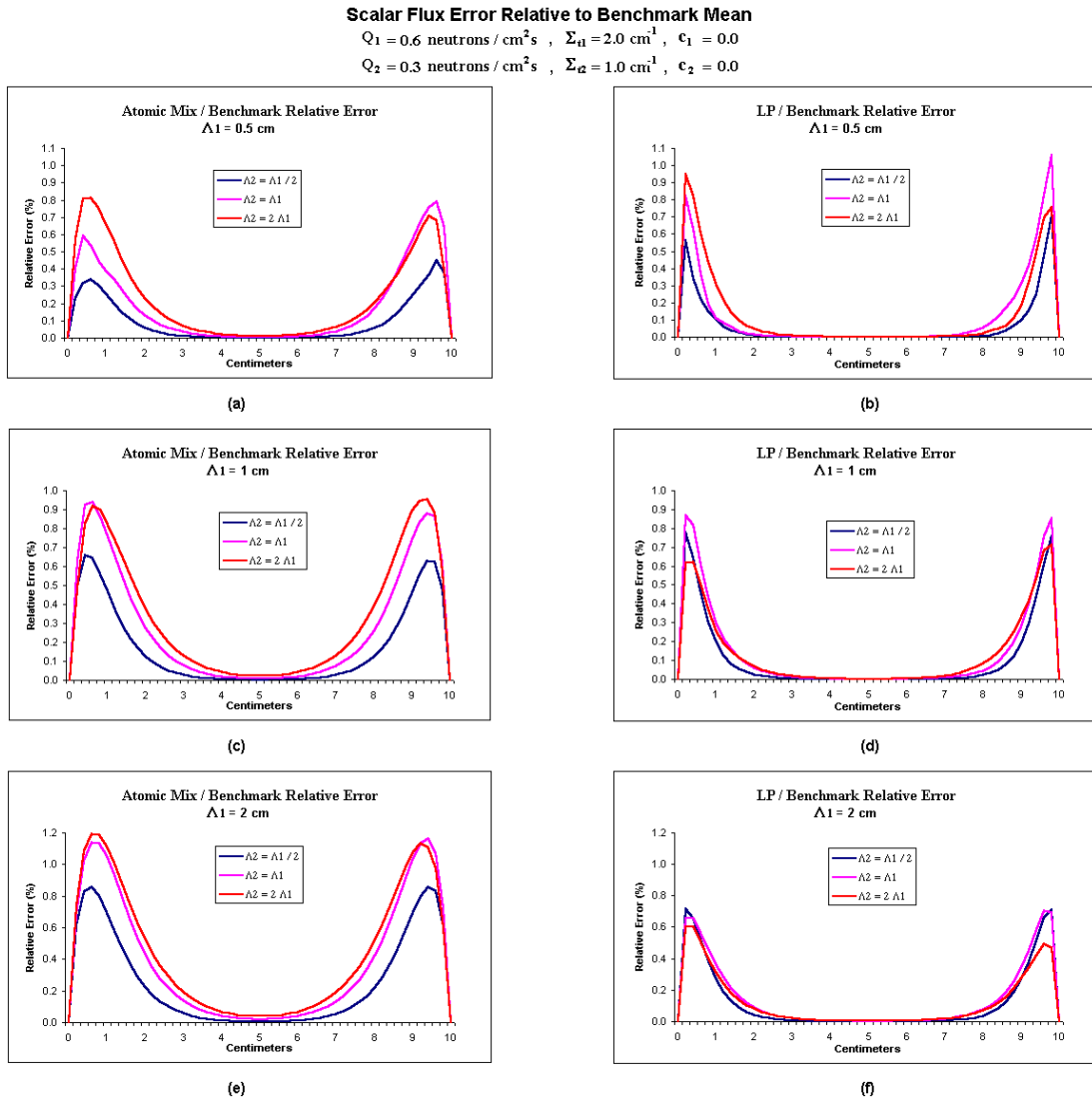
Figure 5.19: Relative errors of the atomic mix and Levermore-Pomraning methods ($\pm 1\%$ with 95% confidence) - Set 2.1
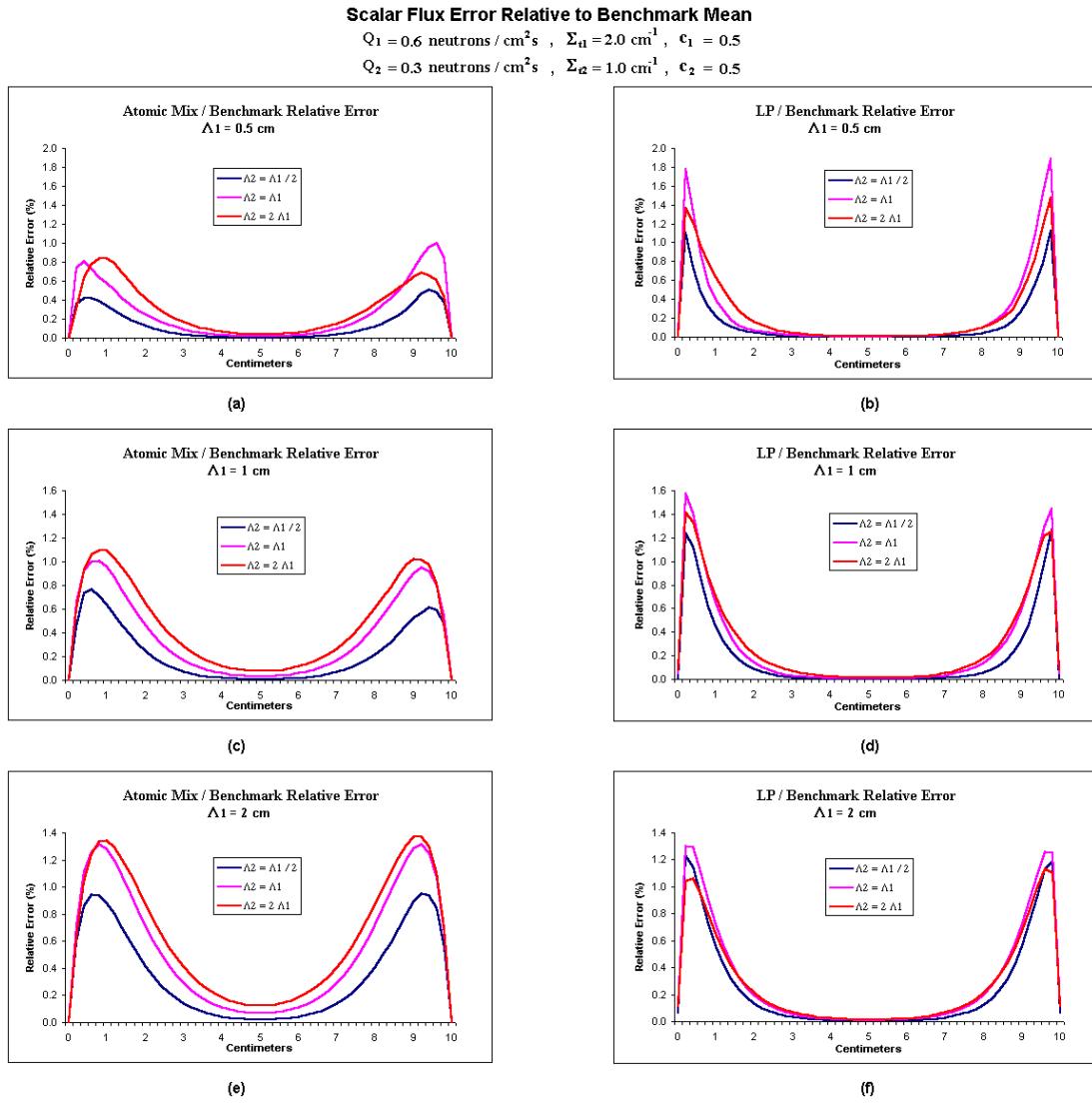
Figure 5.20: Relative errors of the atomic mix and Levermore-Pomraning methods ($\pm 1\%$ with 95% confidence) - Set 2.2
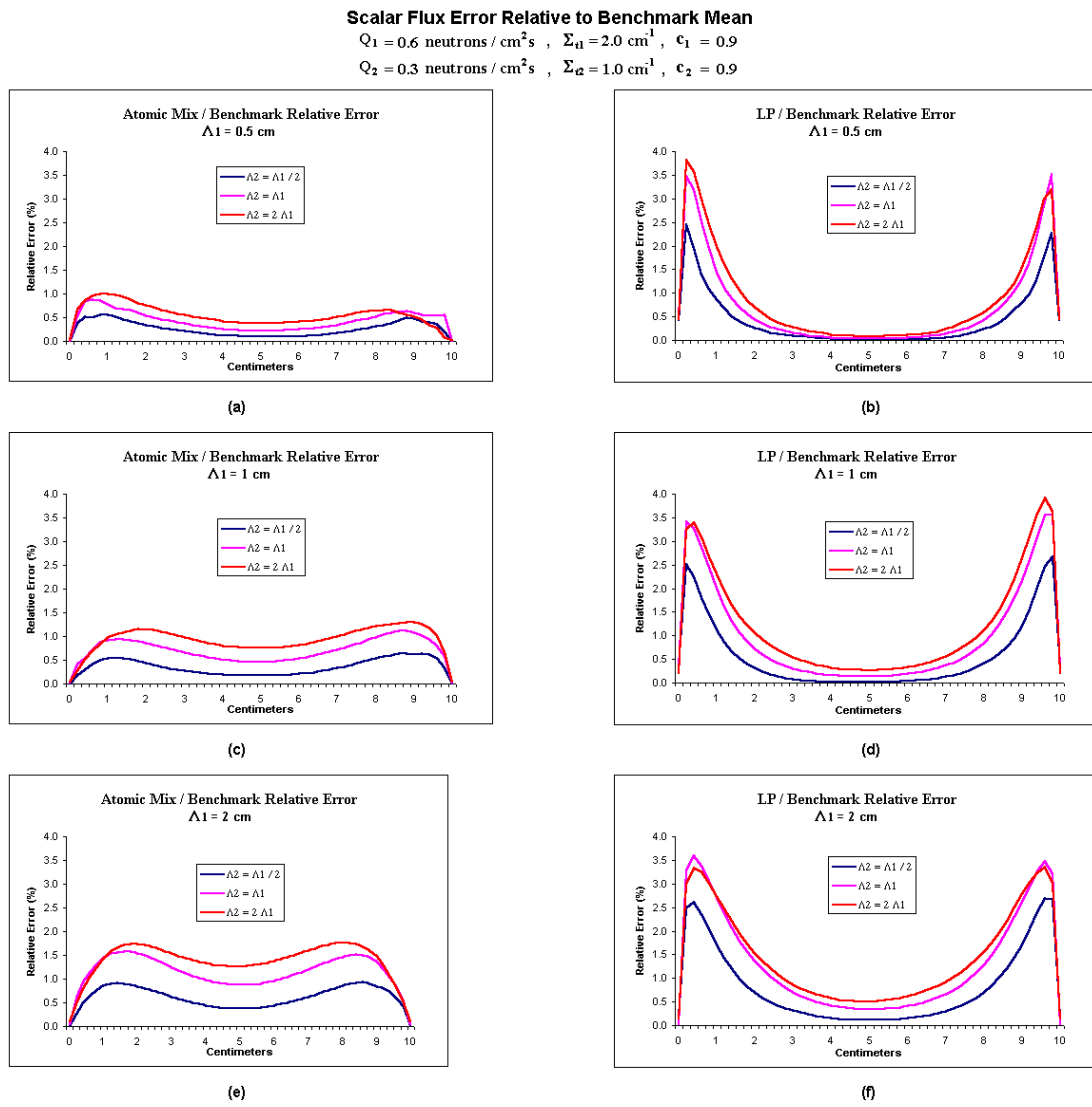
Figure 5.21: Relative errors of the atomic mix and Levermore-Pomraning methods ($\pm 1\%$ with 95% confidence) - Set 2.3

6 CONCLUSIONS

6.1 English Version

In this work we have presented a review of particle transport theory in a binary stochastic medium. The reader may have noticed that the statistics of the mixture was often assumed to be Markovian; this reflects the emphasis on Markov mixing statistics encountered in the literature. For this special class of statistics, many relatively simple results can be obtained. On the other hand, the use of renewal theory to describe particle transport in a binary stochastic medium, first suggested by Vanderhaegen [87], has provided important contributions in both Markovian and non-Markovian mixing problems [16, 26, 48, 50, 63, 71, 78, 94]. This theory uses the integral equation as the underlying description of particle transport, rather than the integro-differential equation.

It is important to emphasize that the prediction of the variance (and the standard deviation) of these systems are as important as the prediction of the ensemble-averaged solution. The variance gives an indication of the magnitude of the spread of the stochastic solution about the mean. A large variance implies a large spread, and in this case a knowledge of the the mean solution alone is not enough to fully understand what is going on within the system. The atomic mix and Levermore-Pomraning models do not provide an estimate of the variance. As far as we know, very little work has been done towards this particular objective [43, 61]; nevertheless, the interest in improving the existent models to predict the variance of such problems has increased over the last years [2, 21, 22]. The development of error estimates and convergence analysis for these problems is also a relevant feature of this research line. Some recent work has been done in this sense [14, 38, 39] (especially in regards to homogenization techniques), but there is still much to be done. We hope to contemplate this work in the future.

Analysing the results reported in Chapter 5, we conclude that, in general, if a single model must be chosen, then the Levermore-Pomraning equations should be used to model this class of transport problems. The Levermore-Pomraning model is always an improvement over the atomic mix model in low and moderately diffusive systems. For highly diffusive systems with small mean chord lengths, the atomic mix prediction is more accurate than the Levermore-Pomraning prediction. However, for such systems, when the chord lengths become sufficiently large, the atomic mix and Levermore-Pomraning results become comparable in accuracy. These trends were already observed by Davis, Palmer and Larsen [12], where problems in "Solid-Void" mixtures were examined, and by Vasques et al. [90], where a 50-point Gauss-Legendre quadrature was used in the discrete ordinates angular approximation.

Moreover, analysing the power demonstrated by the LTS_N method in the numerical calculations, and bearing in mind the proved convergence of the LTS_N approach [42], we are confident to stress that this method is robust (under the computational point of view) to calculate benchmark results, as well as the atomic mix and Levermore-Pomraning predictions. This paves the road to the generation of extremely accurate benchmark solutions, which can be calculated using higher-order Gauss-Legendre quadratures. Furthermore, recalling the equivalence between the S_{2N} and the A_N approximations shown by Coppa et al. [11], we intend to develop an algorithm to calculate benchmark results using the LTA_N method [6, 7]. We also want to apply this new algorithm to the generation of numerical results for the idea proposed in section 4.2, as well as to work on the improvement of this idea.

6.2   Portuguese Version

Neste trabalho foi apresentada uma revisão da teoria do transporte de partículas em um meio estocástico binário. Pode-se notar que a estatística da mistura foi frequentemente assumida como sendo Markoviana; isto reflete a

ênfase em estatística Markoviana encontrada na literatura. Para esta classe especial de estatística muitos resultados relativamente simples podem ser obtidos. Por outro lado, o uso de "renewal theory" para descrever o transporte de partículas em um meio estocástico binário, primeiramente sugerido por Vanderhaegen [87], tem fornecido importantes contribuições para problemas Markovianos e não-Markovianos [16, 26, 48, 50, 63, 71, 78, 94]. Esta teoria usa a equação integral como descrição do transporte de partículas, ao invés da equação íntegro-diferencial.

É importante enfatizar que a predição da variância e do desvio-padrão destes sistemas é tão importante quanto a predição da solução média. A variância fornece uma indicação da magnitude da variação da solução estocástica ao redor da média. Uma grande variância implica uma grande variação, e neste caso um conhecimento da solução média por si só não é suficiente para um completo entendimento do comportamento do sistema. Os modelos de mistura atômica e de Levermore-Pomraning não fornecem um estimativa da variância. Até onde sabemos, muito pouco foi feito no que se refere a este objetivo em particular [43, 61]; mesmo assim, o interesse em aperfeiçoar os modelos existentes para a predição da variância de tais problemas tem crescido nos últimos anos [2, 21, 22]. O desenvolvimento de estimativas de erro e análise de convergência para estes problemas também é uma característica relevante desta linha de pesquisa. Trabalhos recentes têm sido realizados neste sentido [14, 38, 39] (especialmente no que se refere a técnicas de homogeneização), mas ainda há muito a ser feito. Esperamos contemplar este trabalho no futuro.

Analisando os resultados apresentados no Capítulo 5 concluímos que, se um modelo deve ser escolhido, então as equações de Levermore-Pomraning devem ser em geral preferidas para modelar esta classe de problemas de transporte. O modelo de Levermore-Pomraning é sempre um progresso quando comparado com o modelo de mistura atômica em sistemas com difusividade baixa e moderada. Para problemas altamente difusivos com pequenos comprimentos de corda médios, a predição do modelo de mistura atômica é mais precisa que a predição do modelo

de Levermore-Pomraning. Entretanto, para tais sistemas, quando os comprimentos de corda médios se tornam grandes o suficiente, os resultados de ambos os modelos se tornam comparáveis em precisão. Estes comportamentos já foram previamente observados por Davis, Palmer e Larsen [12], onde problemas em misturas "Sólido-Vácuo" foram examinados, e por Vasques et al. [90], onde uma quadratura de Gauss-Legendre de 50 pontos foi usada na aproximação angular das ordenadas discretas.

Além disso, analisando o poder demonstrado pelo método LTS_N nos cálculos numéricos e tendo em mente a demonstrada convergência da abordagem LTS_N [42], estamos confiantes em afirmar que este método é robusto (sob o ponto de vista computacional) para calcular resultados de benchmark, assim como as predições dos modelos de mistura atômica e de Levermore-Pomraning. Isto abre caminho para a geração de soluções de benchmark extremamente precisas, que podem ser calculadas usando quadraturas de Gauss-Legendre de ordens mais altas. Ainda, recordando a equivalência entre as aproximações S_{2N} e A_N mostradas por Coppa et al. [11], pretendemos desenvolver um algoritmo para calcular resultados de benchmark usando o método LTA_N [6, 7]. Queremos também aplicar este novo algoritmo na geração de resultados numéricos para a idéia proposta na seção 4.2, assim como trabalhar no aperfeiçoamento desta idéia.

BIBLIOGRAPHY

[1] ADAMS, M. L., LARSEN, E. W., AND POMRANING, G. C. "Benchmark Results for Particle Transport in a Binary Markov Statistical Medium", *J. Quant. Spectrosc. Radiat. Transfer* **42** (1989), 253.

[2] AKCASU, A. Z. AND LARSEN, E. W. "A Model of the Scalar Flux Variance for Random Media Transport Problems", *Trans. Am. Nucl. Soc.* **89** (2003), 298.

[3] AUDIC, S. AND FRISCH, H. "Monte Carlo Simulation of a Radiative Transfer Problem in a Random Medium - Application to a Binary Mixture", *J. Quant. Spectrosc. Radiat. Transfer* **50** (1993), 127.

[4] BOISSE, P. "Radiative Transfer Inside Clumpy Media - The Penetration of UV Photons Inside Molecular Clouds", *Astronomy & Astrophysics* **228** (1990), 483.

[5] BOLTZMANN, L. "Weitere Studien über Wärmegleichgewicht unter Gasmolekülen", *Wiener Berichte* **66** (1872), 275.

[6] CARDONA, A. V. AND VILHENA, M. T. "Analytical Solution for the A_N Approximation", *Ann. Nucl. Energy* **24** (1997), 495.

[7] CARDONA, A. V., VILHENA, M. T., DE OLIVEIRA, J. V. P., AND VASQUES, R. "The One-Dimensional LTA_N Solution in a Slab with High Order of Quadrature", in *Proc. 18th International Conference on Transport Theory,* Rio de Janeiro (2003), 260.

[8] CASE, K. M., DEHOFFMANN, F., AND PLACZEK, G. *Introduction to the Theory of Neutron Diffusion.* U.S. Government Printing Office, Washington, 1953.

[9]   CASE, K. M. AND ZWEIFEL, P. F. *Linear Tranport Theory.* Addison-Wesley, Massachusetts, 1967.

[10]   CECCHI-PESTELLINI, C., BARLETTI, L., BELLINI-MORANTE, A., AND AIELLO, S. "Radiative Transfer in the Stochastic Interstellar Medium", *Transport Th. Statist. Phys.* **28** (1999), 199.

[11]   COPPA, G., RAVETTO, P., AND SUMINI, M. "Numerical Performance of the A_N Method and Comparisons with S_N Calculations", *Atomkernenergie Kerntechnik* **42** (1983), 107.

[12]   DAVIS, I. M., PALMER, T. S., AND LARSEN, E. W. "A Comparison of Binary Stochastic Media Transport Models in "Solid-Void" Mixtures", *PHYSOR 2004 - The Physics of Fuel Cycles and Advance Nuclear Systems: Global Developments*, Chicago (2004), on CD-ROM.

[13]   DUDERSTADT, J. J. AND MARTIN, W. R. *Transport Theory.* Wiley-Interscience, New York, 1979.

[14]   DUMAS, L. AND GOLSE, F. "Homogenization of Transport Equations", *SIAM J. Appl. Math.* **60** (2000), 1447.

[15]   FRISCH, U. "Wave Propagation in Random Media", in *Probabilistic Methods in Applied Mathematics* **Vol. 1**, Academic Press, New York (1968), 75.

[16]   FRISCH, H., POMRANING, G. C., AND ZWEIFEL, P. F. "An Exact Analytical Solution of a Radiative Transfer Problem in a Binary Mixture" *J. Quant. Spectrosc. Radiat. Transfer* **43** (1990), 271.

[17]   KELLER, J. B. "Effective Behavior of Heterogeneous Media", in *Statistical Mechanics and Statistical Methods in Theory and Application*, Plenum Press, New York (1977), 631.

[18]   KUBO, R. "Stochastic Liouville Equations", *J. Math. Phys.* **4** (1963), 174.

[19]   LAMARSH, J. R. *Introduction to Nuclear Reactor Theory.* Addison-Wesley, Massachusetts, 1966.

[20]   LARSEN, E. W. "Comments on the Pomraning Mix Model", *Unpublished notes*, 2002.

[21]   LARSEN, E. W. "Asymptotic Derivation of the Atomic Mix Diffusion Model for 1-D Random Media", *Trans. Am. Nucl. Soc.* **89** (2003), 296.

[22]   LARSEN, E. W. "Asymptotic Derivation of the Atomic-Mix Diffusion Model for 1-D Random Diffusive Media", in *Proc.* 18th *International Conference on Transport Theory,* Rio de Janeiro (2003), 129.

[23]   LARSEN, E. W. "Asymptotic Derivation of a 3-D Diffusion Approximation for a 1-D Random Diffusive Medium", *seminar given at Universidade Federal do Rio Grande do Sul,* Porto Alegre (2003).

[24]   LARSEN, E. W. "Comments on the Pomraning Mix Model (2)", *Unpublished notes*, 2004.

[25]   LEVERMORE, C. D., POMRANING, G. C., SANZO, D. L., AND WONG, J. "Linear Transport Theory in a Random Medium", *J. Math. Phys.* **27** (1986), 2526.

[26]   LEVERMORE, C. D., POMRANING, G. C., AND WONG, J. "Renewal Theory for Transport Processes in Binary Statistical Mixtures", *J. Math. Phys.* **29** (1988), 995.

[27]   MALVAGI, F. AND POMRANING, G. C. "A Class of Transport Problems in Statistical Mixtures with Scattering", *Journal de Physique (Colloque C7)* **49** (1988), 321.

[28]   MALVAGI, F., LEVERMORE, C. D., AND POMRANING, G. C. "Asymptotic Limits of a Statistical Transport Description", *Transport Th. Statist. Phys.* **18** (1989), 287.

[29]   MALVAGI, F. AND POMRANING, G. C. "Renormalized Equations for Linear Transport in Stochastic Media", *J. Math. Phys.* **31** (1990), 892.

[30]   MALVAGI, F. AND POMRANING, G. C. "Comparison of Models for Particle Transport Through Stochastic Mixtures", *Nucl. Sci. Eng.* **111** (1992), 215.

[31]   MALVAGI, F., POMRANING, G. C., AND SAMMARTINO, M. "Asymptotic Diffusive Limits for Particle Transport in Markovian Mixtures", *Nucl. Sci. Eng.* **112** (1992), 199.

[32]   MALVAGI, F., BYRNE, R. N., POMRANING, G. C., AND SOMERVILLE, R. C. J. "Stochastic Radiative Transfer in a Partially Cloudy Atmosphere" *J. Atmos. Sci* **50** (1993), 2126.

[33]   MALVAGI, F. AND POMRANING, G. C. "Stochastic Atmospheric Radiative Transfer" *Atmos. Ocean Optics* **6** (1993), 610.

[34]   MAXWELL, J. C. "Illustrations of the Dynamical Theory of Gases", *Phil. Mag.* [**4**] (1860): **19**, 19 and **20**, 21.

[35]   MEYER, P. L. *Introductory Probability and Statistical Applications.* Addison-Wesley, Massachusetts, 1965.

[36]   MILLER, D. S. "A Stochastic Method for Brownian-like Optical Transport Calculations in Anisotropic Biosuspensions and Blood", *J. Math. Phys.* **39** (1998), 1534.

[37]   MILLER, D. S. "A Convergence Analysis of Source Iteration for
         the Solution of Coupled Transport Equations in Stochastic Me-
         dia", *Lawrence Livermore National Laboratory report* **UCRL-
         JC-141985** (2001).

[38]   MILLER, D. S., GRAZIANI, F., AND RODRIGUE, G. "Benchmark
         and Models for Time-Dependent Grey Radiation Transport with
         Material Temperature in Binary Stochastic Media", *J. Quant.
         Spectrosc. Radiat. Transfer* **70** (2001), 115.

[39]   MOKHTAR-KHARROUBI, M. "Homogenization of Boundary Value
         Problems and Spectral Problems for Neutron Transport in Locally
         Periodic Media", *Mathematical Models and Methods in Applied
         Sciences* **[14]** (2004), 47.

[40]   MORRISON, J. A. "Moments and Correlation-Functions of Solu-
         tions of Some Stochastic Matrix Differential Equations" *J. Math.
         Phys.* **13** (1972), 299.

[41]   PARZAN, E. *Stochastic Processes.* Wiley, New York, 1962.

[42]   PAZOS, R. P., THOMPSON, M., AND VILHENA, M. T. "Error
         Bounds for Spectral Collocation Method for the Linear Boltz-
         mann Equation", *Int. J. Comp. Num. Anal. Appl.* **1** (2002), 237.

[43]   POMRANING, G. C. *Linear Kinetic Theory and Particle Transport
         in Stochastic Mixtures.* World Scientific Press, Singapore, 1991.

[44]   POMRANING, G. C. "Transport and Diffusion in a Statistical
         Medium", *Transport Th. Statist. Phys.* **15** (1986), 773.

[45]   POMRANING, G. C. "Radiative Transfer in Random Media with
         Scattering", *J. Quant. Spectrosc. Radiat. Transfer* **40** (1988), 479.

[46] POMRANING, G. C. "Classic Transport Problems in Binary Homogeneous Markov Statistical Mixtures" *Transport Th. Statist. Phys.* **17** (1988), 595.

[47] POMRANING, G. C. "The Milne Problem in a Statistical Medium", *J. Quant. Spectrosc. Radiat. Transfer* **41** (1989), 103.

[48] POMRANING, G. C. "Statistics, Renewal Theory, and Particle Transport", *J. Quant. Spectrosc. Radiat. Transfer* **42** (1989), 279.

[49] POMRANING, G. C., LEVERMORE, C. D., AND WONG, J. "Transport Theory in Binary Statistical Mixtures", in *Lecture Notes in Pure and Applied Mathematics* **Vol. 115**, Marcel Decker, New York (1989), 1.

[50] POMRANING, G. C. AND SANCHEZ, R. "The Use of Renewal Theory for Stochastic Transport", *J. Quant. Spectrosc. Radiat. Transfer* **43** (1990), 267.

[51] POMRANING, G. C. "A Model for Interface Intensities in Stochastic Particle Transport", *J. Quant. Spectrosc. Radiat. Transfer* **46** (1991), 221.

[52] POMRANING, G. C. "The Effect of Random Material Density on Reactor Criticality", *Nucl. Sci. Eng.* **108** (1991), 325.

[53] POMRANING, G. C. "Transport Theory in Stochastic Mixtures", *Trans. Am. Nucl. Soc.* **64** (1991), 286.

[54] POMRANING, G. C. "Diffusive Transport in Binary Anisotropic Stochastic Mixtures", *Ann. Nucl. Energy* **19** (1992), 737.

[55] POMRANING, G. C. "Simple Balance Methods for Transport in Stochastic Mixtures", in *Proc. Workshop on Nonlinear Kinetic Theory and Mathematical Aspects of Hyperbolic Systems*, World Scientific Press, Singapore (1992), 204.

[56]   POMRANING, G. C. "Flux-Limiting in Three-Dimensional Stochastic Radiative Transfer", *J. Quant. Spectrosc. Radiat. Transfer* **54** (1995), 637.

[57]   POMRANING, G. C. AND PRINJA, A. K. "On the Propagation of a Charged Particle Beam in a Random Medium. II: Discrete Binary Statistics", *Transport Th. Statist. Phys.* **24** (1995), 565.

[58]   POMRANING, G. C. "Small Correlation Length Solutions for Planar Symmetry Beam Transport in a Stochastic Medium", *Ann. Nucl. Energy* **23** (1996), 843.

[59]   POMRANING, G. C. "Effective Radiative Transfer Properties for Partially Cloudy Atmospheres", *Atmos. Ocean Optics* **9** (1996), 7.

[60]   POMRANING, G. C. "The Planar Symmetry Beam Problem in Stochastic Media", *J. Quant. Spectrosc. Radiat. Transfer* **55** (1996), 771.

[61]   POMRANING, G. C. "The Variance in Stochastic Transport Problems with Markovian Mixing", *J. Quant. Spectrosc. Radiat. Transfer* **56** (1996), 629.

[62]   POMRANING, G. C. "Transport Theory in Discrete Stochastic Mixtures", in *Advances in Nuclear Science and Technology* **24**, Plenum Press, New York (1996), 47.

[63]   POMRANING, G. C. "Renewal Analysis for Higher Moments in Stochastic Transport", *J. Quant. Spectrosc. Radiat. Transfer* **57** (1997), 295.

[64]   POMRANING, G. C. "Transport in Discrete Stochastic Mixtures", *Transport Th. Statist. Phys.* **27** (1998), 405.

[65]   POMRANING, G. C "A Stochastic Eigenvalue Problem", *Ann. Nucl. Energy* **26** (1999), 217.

[66]   PRINJA, A. K. "Pencil Beam Transport in a Random Medium Using the Fermi Transport Equation", *Transport Th. Statist. Phys.* **27** (1998), 667.

[67]   SAHNI, D. C. "An Application of Reactor Noise Techniques to Neutron Transport Problems in a Random Medium", *Ann. Nucl. Energy* **16** (1989), 397.

[68]   SAHNI, D. C. "Equivalence of Generic Equation Method and the Phenomenological Model for Linear Transport Problems in a 2-State Random Scattering Medium", *J. Math. Phys.* **30** (1989), 1554.

[69]   SAMMARTINO, M. AND POMRANING, G. C. "Flux-Limiting in Stochastic Transport", *J. Quant. Spectrosc. Radiat. Transfer* **46** (1991), 237.

[70]   SAMMARTINO, M., MALVAGI, F., AND POMRANING, G. C. "Diffusive Limits for Particle Transport in Stochastic Mixtures", *J. Math. Phys.* **33** (1992), 1480.

[71]   SANCHEZ, R. "Linear Kinetic Theory in Stochastic Media", *J. Math. Phys.* **30** (1989), 2498.

[72]   SANCHEZ, R. AND POMRANING, G. C. "A Statistical Analysis of the Double Heterogeneity Problem" *Ann. Nucl. Energy* **18** (1991), 371.

[73]   SEGATTO, C. F., VILHENA, M. T., AND GOMES, M. G. "The One-Dimensional LTS$_N$ Solution in a Slab with High Degree of Quadrature", *Ann. Nucl. Energy* **26** (1999), 925.

[74]   SEGATTO, C. F. AND VILHENA, M. T. "The State of Art of the LTS$_N$ Method", in *Proc. ANS Topical Meeting: Mathematics and Computation, Reactor Physics and Environmental Analysis in Nuclear Applications,* Madrid (1999), 1618.

[75]   SEGATTO, C. F., VILHENA, M. T., AND TAVARES, L. S. S. "The Determination of Radiant Parameters by the LTS$_N$ Method", *J. Quant. Spectrosc. Radiat. Transfer* **70** (2001), 227.

[76]   SELIM, M. M., ABDEL KRIM, M. S., ATTIA, M. T., AND EL WAKIL, S. A. "Stochastic Radiative Transfer in a Finite Plane with Anisotropic Scattering in a Binary Markovian Mixture", *Waves Random Media* **9** (1999), 327.

[77]   STEPHENS, G. L., GABRIEL, P. M., AND TSAY, S-C. "Statistical Radiative Transport in One-Dimensional Media and its Application to the Terrestrial Atmosphere", *Transport Th. Statist. Phys.* **20** (1991), 139.

[78]   SU, B. AND POMRANING, G. C. "Benchmark Results for Particle Transport in Binary Non-Markovian Mixtures", *J. Quant. Spectrosc. Radiat. Transfer* **50** (1993), 211.

[79]   SU, B. AND POMRANING, G. C. "A Stochastic Description of a Broken Cloud Field", *J. Atmos. Sci* **51** (1994), 1969.

[80]   SU, B. AND POMRANING, G. C. "Limiting Correlation Length Solutions in Stochastic Radiative Transfer", *J. Quant. Spectrosc. Radiat. Transfer* **51** (1994), 893.

[81]   SU, B. AND POMRANING, G. C. "Modification to a Previous High Order Model for Particle Transport in Binary Stochastic Media" *J. Quant. Spectrosc. Radiat. Transfer* **54** (1995), 779.

[82]   SU, B. AND POMRANING, G. C. "P_1, P_2 and Asymptotic Approximations for Stochastic Transport", *Nucl. Sci. Eng.* **120** (1995), 75.

[83]   SU, B. AND POMRANING, G. C. "The Fermi-Eyges Beam Analysis for a Heterogeneous Absorbing Stochastic Medium" *Ann. Nucl. Energy* **23** (1996), 1153.

[84]   TITOV, G. A. "Statistical Description of Radiation Transfer in Clouds", *J. Atmos. Sci.* **47** (1990), 24.

[85]   VALENTYUK, A. N. AND TSYMBAREVICH, E. G. "Stochastic Propagation of Radiation in the Atmosphere and Ocean", *Atmospheric & Oceanic Phys.* **35** (1999), 52.

[86]   VANDERHAEGEN, D. "Radiative Transfer in Statistically Heterogeneous Mixtures", *J. Quant. Spectrosc. Radiat. Transfer* **36** (1986), 557.

[87]   VANDERHAEGEN, D. "Impact of a Mixing Structure on Radiative Transfer in Random Media", *J. Quant. Spectrosc. Radiat. Transfer* **39** (1988), 333.

[88]   VANDERHAEGEN, D. AND DEUTSCH, C. "Linear Radiation Transport in Randomly Distributed Binary Mixtures: a One-Dimensional and Exact Treatment for the Scattering Case", *J. Statist. Phys.* **54** (1989), 331.

[89]   VAN KAMPEN, N. G. *Stochastic Processes in Physics and Chemistry.* North Holland, Amsterdam, 1981.

[90]   VASQUES, R., VILHENA, M. T., THOMPSON, M., AND LARSEN, E. W. "State of Art of Particle Transport Theory in Stochastic Media", in *Proc. XXV Iberian Latin American Congress on Computational Methods in Engineering*, Recife (2004), on CD-ROM.

[91]   WILLIAMS, M. M. R. "The Effect of Random Geometry on the
        Criticality of a Multiplying System", *Ann. Nucl. Energy* **27**
        (2000), 143.

[92]   WILLIAMS, M. M. R. "The Effect of Random Geometry on the
        Criticality of a Multiplying System II: Extension to Resonance
        Absorption", *Ann. Nucl. Energy* **27** (2000), 517.

[93]   WILLIAMS, M. M. R. AND LARSEN, E. W. "Neutron Transport in
        Spatially Random Media: Eigenvalue Problems", *Nucl. Sci. Eng.*
        139 (2001), 66.

[94]   ZUCHUAT, O., SANCHEZ, R., ZMIJAREVIC, I., AND MALVAGI,
        F. "Transport in Renewal Statistical Media: Benchmarking and
        Comparisons with Models", *J. Quant. Spectrosc. Radiat. Transfer*
        51 (1994), 689.

[95]   ZUEV, V. E. AND TITOV, G. A. "Radiative Transfer in Cloud
        Fields with Random Geometry", *J. Atmos. Sci.* **52** (1995), 176.

Livros Grátis

(http://www.livrosgratis.com.br)

Milhares de Livros para Download:

Baixar livros de Administração
Baixar livros de Agronomia
Baixar livros de Arquitetura
Baixar livros de Artes
Baixar livros de Astronomia
Baixar livros de Biologia Geral
Baixar livros de Ciência da Computação
Baixar livros de Ciência da Informação
Baixar livros de Ciência Política
Baixar livros de Ciências da Saúde
Baixar livros de Comunicação
Baixar livros do Conselho Nacional de Educação - CNE
Baixar livros de Defesa civil
Baixar livros de Direito
Baixar livros de Direitos humanos
Baixar livros de Economia
Baixar livros de Economia Doméstica
Baixar livros de Educação
Baixar livros de Educação - Trânsito
Baixar livros de Educação Física
Baixar livros de Engenharia Aeroespacial
Baixar livros de Farmácia
Baixar livros de Filosofia
Baixar livros de Física
Baixar livros de Geociências
Baixar livros de Geografia
Baixar livros de História
Baixar livros de Línguas